CLIMATE SENSITIVE DESIGN APPROACH TO REDUCE THE URBAN HEAT ISLAND EFFECT: CASE OF POLIGON STREAM AND ITS SURROUNDINGS, IZMIR

A Thesis Submitted to
the Graduate School of Engineering and Sciences of
Izmir Institute of Technology
in Partial Fulfillment of the Requirements for the Degree of

MASTER OF SCIENCE

in Urban Design

by
Leyla Nur TUNÇBİLEK

December 2023
İZMİR

We approve the thesis of **Leyla Nur TUNÇBİLEK**

Examining Committee Members:

Asst. Prof. Dr. Nicel SAYGIN
Department of City and Regional Planning, Izmir Institute of Technology

Prof. Dr. Koray VELİBEYOĞLU
Department of City and Regional Planning, Izmir Institute of Technology

Prof. Dr. Şebnem GÖKÇEN
Department of City and Regional Planning, Dokuz Eylül University

5 December 2023

Asst. Prof. Dr. Nicel SAYGIN
Supervisor, Department of City and Regional Planning
Izmir Institute of Technology

Prof. Dr. Koray VELİBEYOĞLU
Head of The Department of
City and Regional Planning

Prof. Dr. Mehtap EANES
Dean of the Graduate School of
Engineering and Sciences

ACKNOWLEDGMENTS

First, I would like to thank Asst. Prof. Dr. Nicel SAYGIN, who contributed significantly to the preparation of my master's thesis, thanks to her valuable thoughts, suggestions, and support.

I would also like to thank Prof. Dr. Şebnem GÖKÇEN and Prof. Dr. Koray VELİBEYOĞLU, for their valuable contributions to the final version of the thesis.

I would like to wholeheartedly thank TÜBİTAK Scientist Support Programs Directorate (BİDEP) for providing scholarship support within the scope of the 2211-Domestic Graduate Scholarship Program during my graduate education.

I am deeply grateful to my beloved mother, Gülseren GÖRBAŞ, and my dear father, İrfan GÖRBAŞ, whose presence has been a source of strength throughout my life, providing unwavering support both materially and spiritually.

I owe a debt of gratitude to my dear husband, Eren TUNÇBİLEK, who has consistently offered support, love, and kindness during the challenging times of my master's thesis process, just as they have throughout various stages of my life.

I want to express my heartfelt thanks to all of them.

ABSTRACT

CLIMATE SENSITIVE DESIGN APPROACH TO REDUCE THE URBAN HEAT ISLAND EFFECT: CASE OF POLIGON STREAM AND ITS SURROUNDINGS, IZMIR

Climate change, destruction of the natural environment, high-rise buildings, intense urbanization, and high energy consumption are increasingly making urban living challenging. Climate change triggers this situation, creating an increased urban heat island effect. Outdoor thermal comfort is crucial for pedestrian health in urban areas. The growing heat island effect due to climate change leads to thermal comfort issues in cities, negatively affecting urban life. Different urban forms within cities provide different microclimatic comfort zones for pedestrians. We must adapt urban planning to climate conditions from macro to micro scales with a holistic perspective. This study examines how the heat island effect in the Poligon Stream, and its surrounding area can be reduced using a climate-sensitive design approach. The main purpose of this study is to enhance the urban microclimate around the Poligon Stream by proposing design solutions at various scales to mitigate the urban heat island effect. To calculate land surface temperature and the heat island effect, satellite data from the hottest day of the year 2022 was utilized. Wind and thermal comfort models were developed using meteorological data such as air temperature, global radiation, wind speed, and relative humidity. The morphological structure of the study area, along with the analysis results of meteorological parameters and land surface temperature, indicates that the cooling capacity in the district is considerably low. Due to the heat island effect, urban life reaches levels that adversely affect living conditions in the summer months. Resulting in substantial, sustainable urban design proposals, focusing on ecological, nature-based, and climate-sensitive approach, were developed, resulting in a 13% reduction in the urban heat island effect.

Keywords: *Climate sensitive design, outdoor thermal comfort, urban heat island effect*

ÖZET

KENTSEL ISI ADASI ETKİSİNİ AZALTMAK İÇİN İKLİM DUYARLI TASARIM YAKLAŞIMI: POLİGON DERESİ VE ÇEVRESİ, İZMİR ÖRNEĞİ

İklim değişikliği, doğal çevrenin tahribi, yüksek binalar ve yoğun kentleşme, yüksek enerji tüketimi gibi faktörlerden kaynaklanan bir sorun olarak giderek şehir içerisinde yaşamayı zorlaştırmaktadır. Bu durum, kentsel ısı adası etkisi oluşturarak iklim değişikliği tarafından tetiklenmektedir. Kentlerde açık hava termal konforu, kentsel alanlarda yaya sağlığı için önemlidir. İklim değişikliği nedeniyle artan kentsel ısı adası etkisi, kentlerde termal konfor sorunlarına yol açarak şehir hayatını olumsuz etkilemektedir. Şehirler içinde farklı kentsel formlar, yaya için farklı mikroklimatik konfor bölgeleri sunar. Şehir planlaması, iklim koşullarına makrodan mikro ölçeklere kadar bütünsel bir bakış açısıyla uyarlanmalıdır. Bu çalışma, Poligon Deresi ve yakın çevresindeki alanda iklime duyarlı tasarım yaklaşımı kullanılarak ısı adası etkisinin nasıl azaltılabileceğini incelemektedir. Bu çalışmanın temel amacı, Poligon deresi ve çevresindeki kentsel mikro iklimleri iyileştirmek, farklı ölçeklerde analizler oluşturularak iklime duyarlı kentsel tasarım önerisi sunmak ve kentsel ısı adası etkisini azaltmaktır. 2022 yılının en sıcak gününe ait uydu verisi üzerinden yer yüzey sıcaklığı ve ısı adası etkisi hesaplanmıştır. Hava sıcaklığı, küresel radyasyon, rüzgâr hızı ve bağıl nem verileri gibi meteorolojik veriler kullanılarak rüzgâr ve termal konfor modeli oluşturulmuştur. Çalışma alanının morfolojik yapısı, meteorolojik parametreler ve yer yüzey sıcaklığı analizi, ısı adası etkisi, termal konfor analizi ve rüzgâr analizi sonuçları, bölgenin soğutma kapasitesinin çok düşük olduğunu ve ısı adası etkisinin yaz aylarında şehir hayatını olumsuz etkileyecek düzeylere ulaştığını göstermektedir. Sürdürülebilir, ekolojik, doğa temelli ve mikro-iklim duyarlı kentsel tasarım önerileri geliştirilmiştir. Bu öneriler sonucunda ısı adası etkisi %13 oranında azaltılmıştır.

Anahtar Kelimeler: *İklime duyarlı tasarım, açık hava termal konforu, kentsel ısı adası etkisi*

ABBREVIATIONS

LST: Land Surface Temperature

UHI: Urban Heat Island

DEM: Digital Elevation Model

DSM: Digital Surface Model

SVF: Sky View Factor

NDVI: Normalized Difference Vegetation Index

UTFVI: Urban Thermal Field Variance Index

IPCC: Intergovernmental Panel on Climate Change

UCCRN: Urban Climate Change Research Network

WHO: World Health Organization

UMEP: Urban Multi-scale Environmental Predictor

PET: Physiological Equivalent Temperature

TABLE OF CONTENTS

LIST OF FIGURES

Figure **Page**

Figure **Page**

Figure **Page**

LIST OF TABLES

CHAPTER 1

INTRODUCTION

When evaluated globally, it has been indicated that the temperature in the Mediterranean region has increased by 20% faster from the Industrial Revolution to the present day (Mediterranean Experts on Climate and Environmental Change 2019). Industrialization, urbanization, and the destruction of the natural environment contribute to more adverse temperature effects daily. These triggering factors of climate change negatively affect the lives of people living in cities. IPCC highlighted in its 4th assessment report in 2007 that average summer temperatures gradually increase in some geographies, increasing local climate-related problems. According to the 2nd assessment report of the Urban Climate Change Research Network (UCCRN) in 2018, the rising trend in carbon emissions emphasizes that providing thermal comfort is becoming increasingly challenging in different regions of the world. Extreme weather events, which we are already experiencing today, are expected to become more widespread due to climate change, leading to severe problems, especially in cities where high temperatures are observed. In addition to heat waves, the frequency of natural disasters such as intense rainfall and sudden floods is expected to increase in urban areas where impermeable surfaces continue to rise.

Cities are approximately 3 °C warmer at night than rural areas due to increased exposure to urban heating throughout the day (Voogt 2004). The urban heat island is the phenomenon of cities having higher temperatures than the surrounding rural environments (Oke 1982, Gerçek and Bayraktar 2014). Impermeable surfaces absorb solar radiation during the day, particularly raising the nighttime air temperature, and due to their inability to release the absorbed heat, these surfaces remain warm. The light energy from the sun reaching the Earth’s surface is converted into heat energy on the materials used in urban structures, as these materials cannot reflect this heat energy. The surface temperature increases.

This situation contributes to the amplification of the urban heat island effect by increasing the storage of energy affecting the Earth's surface (Parker and Warner, 1973; Zhang et al. 2006; Li et al. 2013, Ndossi and Avdan 2016, Yıldız et al. 2017). The regional temperature increase is attributed to global climate change and factors such as rapid urbanization, vegetation destruction, and land cover changes (Wong and Yu 2005; Leconte et al. 2015; Liu et al. 2017).

Among the methods used to understand the urban heat island effect in urban areas, one fundamental parameter that can be calculated using the remote sensing method is land surface temperature. Land surface temperature is related to the radiation value between the surface and the atmosphere, the exchange of heat flux at all scales, surface energy, and water balance (Anderson et al. 2008; Brunsell and Gillies 2003; Karnieli et al. 2010; Kustas and Anderson 2009; Zhang et al. 2008). Land surface temperature can also be considered a parameter for local climate change and microclimate conditions within built environments in cities (Li et al. 2013; Rasul et al. 2017; Voogt and Oke 2003; Weng et al. 2011).

The increasing urban heat island effect prevents the achievement of outdoor thermal comfort in cities. Cities need to be resilient to the anticipated rise in average temperatures. In this regard, cities must be made resilient to extreme weather events. In recent years, the prioritization of criteria necessary for people to choose their living environment has changed. Outdoor comfort has become a more crucial factor in people's choice of location. Climate is the most significant factor influencing outdoor comfort (Çalışkan and Türkoğlu 2012). The foundation for individuals to feel psychologically and physically healthy is based on their relationship with climatic conditions. In this context, bioclimatic comfort is defined as the adaptation of individuals to their living environment with minimal energy expenditure (Özyavuz 2017). Meteorological parameters such as temperature, wind, and humidity are crucial in determining bioclimatic comfort conditions (Topay and Yılmaz 2004). The urban microclimate is a significant factor in urban design practices. Almost all designers know enclosed glass boxes cannot be designed without considering local climate conditions (Ribeiro et al. 2008). Climate-sensitive design includes design strategies to create outdoor spaces in green infrastructure and urban built environments that encourage people to go and spend time outdoors, capture and absorb rainwater, and provide conditions for human comfort.

1.1. Problem Definition

Global warming and climate change are among today's most critical environmental and social issues. Rapid urbanization since the Industrial Revolution has led to the depletion of natural assets due to many factors, such as the destruction of the natural environment, the increasing consumption of fossil fuels, and industrialization. As a result, we face serious problems such as increasing average temperatures, decreasing drinking water resources, air, and water pollution problems, increasing greenhouse gas emissions, and disruption of the natural ecosystem cycle (Yüceer 2015). The increase in average temperatures and the urban built environment absorbing sunlight, causing surface materials to be hot at all hours of the day, directly impact cities and people. The rise in average temperatures leads to an increase in temperature-related illnesses and, consequently, health problems. A heatwave in Central and Southern Europe in 2003, for example, resulted in the death of 35,000 people (WHO 2005). During extreme heatwaves, diseases and mortality rates caused by air pollution tend to increase (Harlan et al. 2006).

Urban built-up areas tend to be warmer than the surrounding natural areas. The scarcity of natural areas within the city, building materials used, dark and impermeable surfaces, and high-density construction contribute to the urban heat island effect. Therefore, the urban heat island effect is a significant problem in cities. The urban heat island effect adversely affects the daily activities and comfort conditions of people living in urban spaces with high-density construction. There needs to be more tree and vegetation coverage, increasing impermeable surfaces, and construction conditions disrupting natural ventilation, leading to serious city problems. The conversion of upper catchment areas of streams within the city for construction, the encasement of streams in concrete channels and their detachment from the urban environment, and the narrow sections of the channels increase the risk of flooding. These problems that cities face today directly affect urban life. Changing climate conditions and the urban heat island effect increase air temperatures and negatively affect the bioclimatic conditions of urban areas.

1.2. Aim and Scope of the Study

This study aims to redesign existing urban fabrics using a climate-sensitive design approach, focusing on the relationship between microclimates and settlement areas. The goal is to address issues in residential areas by leveraging their specific climates and, consequently, implement interventions that improve bioclimatic comfort conditions for people while reducing the urban heat island effect.

The scope of this research is, first and foremost, to conduct a detailed analysis of land surface temperature, green areas, and permeable surfaces in an area covering the central districts of Izmir and the basins of streams within these districts. Secondly, the Poligon Stream basin has been examined. Subsequently, due to the crucial importance of accurately and site-specifically identifying local climate conditions, residential areas around meteorological stations within the city center have been thoroughly investigated. In this context, the area around the Güzelyalı meteorological station, particularly the Poligon Stream and its surroundings, has been selected as the study area. The primary objective of this study is to enhance urban microclimates, thereby mitigating the urban heat island effect and improving people's bioclimatic comfort conditions. The aim is to provide nature-based, sustainable, and climate-sensitive design solutions at different scales.

The questions this study investigates and tries to answer are:

Q 1: To what extent does the use of climate-sensitive design principles in dense residential areas affect the urban heat island effect?

Q2: How is the urban heat island effect measured, and what measures can be taken to reduce its impact?

Q3: What are the principles of climate-sensitive design?

1.3. Methodology

The following methods were employed to address the research questions specified in the aim section. The proposed method begins with a literature review, examining all

publications related to climate-sensitive design and urban heat island effects. Following content analysis, the best practices from around the world and in Türkiye were researched.Among these best practices, projects in countries located in the Mediterranean climate zone have been particularly taken into consideration Subsequently, numerous analyses were conducted in the Poligon Stream area, located in the city center of Izmir, where dense construction areas surround it, after being chosen as the study area. Based on these analyses, an urban design project was proposed using climate-sensitive design principles. Since designing urban structures independently is not feasible, a comprehensive top-down analysis and design method have been developed. In this context, a four-stage analysis method categorizing these steps into city, basin, neighborhood, and street has been established. This scalable approach plays a crucial role in addressing the study comprehensively.

To calculate surface temperatures, Landsat 8 images corresponding to July 24, 2022, representing the day with the highest average temperature and least cloud cover during the summer months of 2022 in Izmir city center, were used. Two methods were employed to calculate the urban heat island effect. The first method utilized formulas specified in the literature applied to surface temperature maps. After calculating the urban heat island effect, evaluations were made according to the Urban Thermal Footprint Vulnerability Index (UTFVI). The second method involved calculating the maximum urban heat island effect using meteorological data, SVF, and vegetation indices.

The data obtained in the study include local climate characteristics such as wind speed, air temperature, global solar radiation, and relative humidity. These data were collected through a secondary data collection method, with meteorological data obtained from the Güzelyalı Meteorology Station.

Some data were collected through on-site observations. These observations include surface material properties (grass, soil, asphalt, and concrete), building heights in the vicinity, vegetation cover, land use, and climate data. Analyses of surface properties and vegetation at the street scale were prepared using the data collected through on-site observations.

Another tool used in the research is software. Thermal comfort analysis at the street scale was calculated using the SOLWEIG tool to create a thermal comfort map. DEM data used in the thermal comfort analysis model were obtained from ALOS PALSAR high-resolution satellite data. DSM data were downloaded from Open Topography as part of the ALOS World 3D dataset. When determining bioclimatic

comfort zones in the study area, the Physiological Equivalent Temperature (PET) index, considering human physiological characteristics, was used.

Wind analysis using software is another analysis to be conducted at the street scale. In this analysis, buildings were modeled to create a three-dimensional wind simulation at the street scale. Within the scope of the study, a climate-sensitive urban design plan was proposed, incorporating climate-sensitive design principles obtained from content analysis. Additionally, intervention methods recommended to reduce the urban heat island effect, obtained through literature review, were integrated into the design plan. Comparisons were made between the proposed plan and existing conditions. Subsequently, the extent of improvements on the land surface and the degree to which the urban heat island effect was reduced were calculated.

1.4. Structure of the Study

After a brief introduction in the first section, the text covers the problem definition, information about the scope and study area, the methodology of the designed study, data collection methods, and the software used.

The second section provides definitions from the literature regarding the approach of climate-sensitive design, the urban heat island effect, and outdoor thermal comfort concepts, along with information about the criteria related to these concepts. The concept of climate-sensitive design, the design principles of this concept, and the important points are emphasized, and the points that need to be considered are explained.

The third part is divided into two parts: research and design examples. The current research section includes various studies from around the world and from Türkiye. In the design examples section, global and national-scale projects are presented using the same approach.

The fourth section aims to examine the morphological structure and climatic measurements of the developed areas around Poligon Stream. The provided analyses are explained through maps, photographs, and graphs. Subsequently, design proposals and strategies are developed after evaluating the research area in terms of climate sensitivity

and urban heat island effect. The results section explains the changes brought about by the interventions.

In conclusion, after reviewing all the findings obtained from the study, the importance of climate sensitivity has been emphasized. The improvements in the study area with the developed design methods have been discussed. Suggestions have been provided for interventions to reduce the urban heat island effect. The possibilities of nature-based solutions at different scales and the development of strategies have been addressed. Additionally, the changes in land cover and the extent to which the urban heat island effect has been reduced in the proposed design have been calculated. The final section presents recommendations on what can be done to bridge the gap between current urban design practices and microclimatic conditions.

CHAPTER 2

LITERATURE REVIEW

Within the scope of this study, three main topics have been examined. Climate-sensitive design, the urban heat island effect, and outdoor thermal comfort concepts were investigated through a literature review of studies in urban planning, urban design, architecture, civil engineering, landscape architecture, environmental engineering, and geography.

2.1. Climate Sensitive Design

The climate-sensitive design approach, according to Emanuel (2005), is an approach that refers to the issue of sustainable development. Approaches such as sustainability, energy efficiency, green architecture, and ecology have gained importance since the late 1960s. Climate-sensitive design, which encompasses these approaches, is an essential tool for producing nature-based solutions suitable for different climate types. Each climate has its specific design criteria (Oktay 2001). When examining past settlement examples, the design of the Harran houses served as a protective shell from the heat. At the same time, the Eskimos lived in igloos that protected against the cold (Demirbilek 2001, quoted by Yüceer 2015). Microclimate is greatly influenced by urban settlement and design criteria (Eliasson and Svensson 2002; Giridharan et al. 2004-2005; Gomez et al. 2004; Johansson 2006; Eliasson 1996; Johansson and Emmanuel 2006).

The climate-sensitive design approach includes many design principles. In urban environments, wind circulations are also emphasized in climate-sensitive design guidelines. Since buildings act as obstacles to the wind, open spaces in the city vary depending on the wind conditions (Givoni 1998). Buildings affect the heat balance, wind,

and temperature conditions near the ground (Givoni 1998). Urban density can also have an impact on local wind conditions. In general, the average height of buildings and the distance between them should be considered. However, differences in height between deattach buildings will have the greatest local impact. A high-rise building will locally create strong air currents (Givoni 1998).

The relationship between wind and the built environment has a significant impact on urban quality of life. Due to its effects on human health, indoor and outdoor comfort, and its inhibitory effects on the formation of urban heat islands effect, urban air currents should be taken into account. The H/W ratio is a design element that determines these circulations in three different ways, as seen in Figure 2.1.

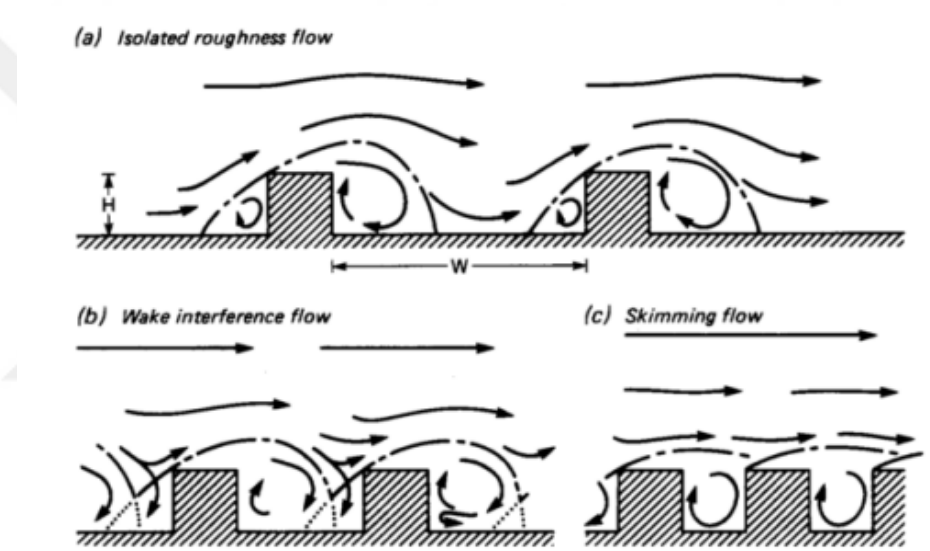

Figure 2.1. Air Flow Regimes for Increasing H/W Ratios

(Source: Oke 1988)

Street orientation and design can influence the microclimate of a street due to their ability to either accelerate or decelerate wind circulation. Straight and parallel streets encourage air circulation within urban environments, while narrow and winding streets reduce wind speeds (Kim and MacDonald 2015, Shishegar 2013). The absence of vegetation in straight streets can affect the occurrence of severe hot or cold weather, as wind can move unobstructed along the streets (Givoni 1998). Friction between building walls and other surfaces (trees, furniture, signs, etc.) can also delay the approaching wind flow (Ahmad, Khare, and Chaudhry 2005, Jamei et al. 2016).

Building heights are also seen as an important tool in directing air flows. Milosovicova (2010) and Shishegar (2013) have mentioned that several tall structures can increase the flow speed if their orientation is parallel or perpendicular to the street's wind direction. The positioning of high rise buildings on the terrain can also cause temperature increases or decreases. Designing streets parallel to the dominant wind direction in urban environments can enhance air movements, while designing narrow and winding streets can slow down wind movements in the opposite scenario.

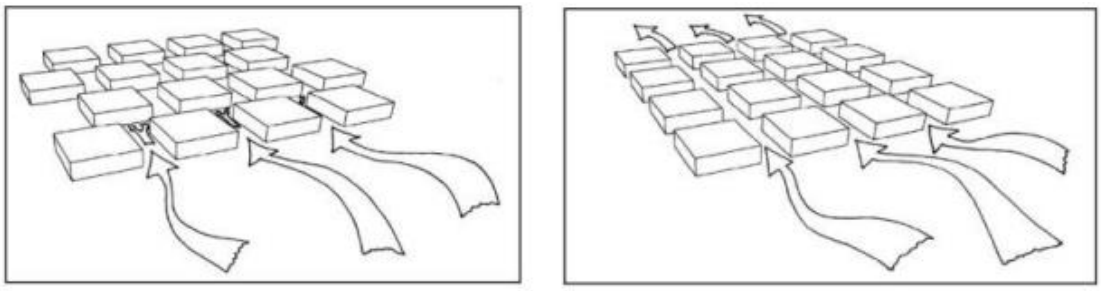

Figure 2.2. Curved And Broken Streets Slow Winds, While Straight Streets Conduct Winds Easily

(Source: Shishegar 2013)

Landscape is one of the tools used to alter local microclimate conditions. Thurow (1983) mentions the potential benefits of vegetation for wind protection in the case of Dayton. Deciduous trees with bare trunks can be employed to provide wind protection at various heights (Morrison, Hershfield, Theakston, and Rowan 1979). Coniferous trees can be utilized to intervene in wind speed throughout the year.

In urban areas, aside from developed regions, significant land uses include parks and green spaces. The positive effects of such areas on urban climate and air quality are clearly stated (Barış 2005, Koç et al. 2016, Özyavuz 2016, Şimşek and Şengezer 2012, Şimşek 2016). Green spaces stand out as areas that facilitate drainage of rainwater, provide shading, filter radiation, and offer natural ventilation (Milosovicova 2010).

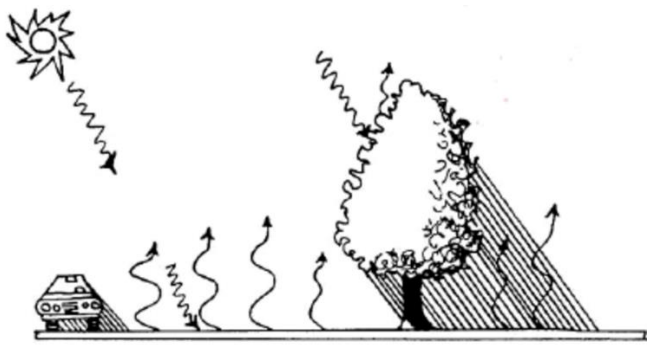

Figure 2.3. Trees Shade And Filter Radiation

(Source: Brown and Gillespie 1995)

Urban geometry is one of the most determining factors for urban climate and outdoor comfort. The ratio between building height and street width, as well as the sky view factor, are crucial indicators in terms of climate-sensitive design. These indicators define the sunlight exposure and ventilation opportunities in the city, serving as important criteria. Factors influencing climatic conditions perceived at the pedestrian level in the streets should be considered in the design process (Milosovicova 2010). A high building-to-street (H/W) ratio restricts the heat dissipation from urban areas to the atmosphere and slows down nighttime cooling (Milosovicova 2010, Shishegar 2013). The concept of canyon geometry, used in the literature concerning street designs, also contributes significantly to climate-sensitive designs and is determined by the H/W ratio. The horizontal and vertical surfaces in canyons constitute design elements that impact the quality of life.

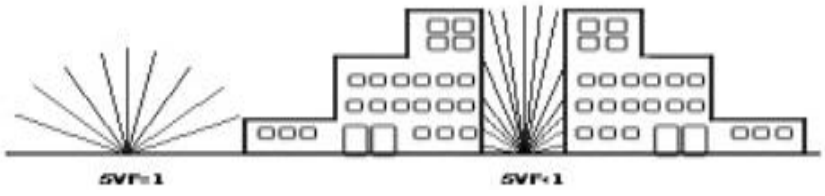

Figure 2.4. If the SVF Value Is 1, The Case on the Left; If It Is Less Than 1, The Case on the Right

(Source: Milosovicova, 2010)

Parameters such as temperature, humidity, and wind affect the urban landscape. The effect of the urban landscape on urban space, such as solar exposure and wind, artificial structures, architectural form, and water surfaces, is quite significant.

Effective parameters can be examined in two categories in the climate-sensitive design approach. Parameters can be divided into physical and environmental parameters. In this context, physical parameters (e.g., urban form and the ratio of width/height, building characteristics) and environmental parameters (e.g., temperature, wind speed, humidity) have been studied in detail.

2.1.2. Physical Parameters

Different urban forms perform differently in terms of climate type. In this respect, the form can positively affect ambient temperature by influencing the microclimate of the settlement area, thus increasing bioclimatic comfort levels (Golany 1996). In addition, Johansson (2006) states that urban geometry, such as the distance between buildings, average building height, and building configuration, directly affects local climate conditions. Bosselmann and Arens (2005) argue that the position of buildings and the size of streets affect the urban climate, indicating an essential relationship between urban form and climate. The climate-sensitive design approach implements design interventions considering physical parameters. All physical interventions carried out at the urban or building scale result in significant changes in the local climate.

Physical parameters are grouped into the following three categories:

• Urban configuration: location, urban pattern, urban density, street width and direction, nature of ground surface.

• Landscape elements: sidewalk materials and colors, vegetation and green areas, pools, fountains, fixed or operable shading devices, and other design elements.

• Building configuration: distance between buildings, average building height, H/W ratio, surface materials, facade features, and other design settings and building services.

2.1.3. Environmental Parameters

In many studies conducted on settlement areas, environmental parameters are always taken into consideration (Giridharan et al. 2004, 2005; Johansson 2006; Bosselmann and Arens 2005; Nikolopoulou et al. 2001; Nikolopoulou and Lykoudis 2006; Walton et al. 2007; Gomez et al. 2004; Johansson and Emmanuel 2006; Thorsson et al. 2007; Manioğlu and Yılmaz 2008; Yılmaz 2007). The following environmental parameters are the most used in these studies:

- Ta - Air temperature (°C-Celsius, °F-Fahrenheit, °K-Kelvin)
- RH - Relative humidity (%)
- W - Wind speed (m/s, km/h, knots, mph)
- SRD - Solar radiation (MJ/m2)

2.1.4. Scale Approach

Climate-sensitive design is not an approach that can work independently of each other at different scales. In this approach, it is necessary to evaluate all scales from top to bottom together and consider their differences. In this approach, a comprehensive study must be carried out at the scale of the city, street, and building.

On the urban scale, the form of the city has a significant impact on climate change. According to studies in literature, the effect of the form of the city on the formation of urban heat islands is second (Zhou 2017). On the urban scale, city form, land-use balance, and green spaces are essential variables in the bioclimatic approach.

Studies carried out at the street scale mainly emphasize three main variables: street layout, sky view factor, and shading variables. Street layout has a wide range of effects on average temperatures, ground surface temperatures in the city, as well as the width and height of the street (Bourbia and Boucheriba 2010).

On the building scale, the three main variables that affect the amount of energy consumed are the orientation of the building, the form of the building, and the construction materials. A building's orientation about the movement of the sun and the

prevailing wind conditions affects the energy required for cooling and heating activities inside the building (Sarte 2010). The correct position and orientation of a building can protect it from unwanted sun rays or wind or benefit from natural air circulation (Gut and Ackerknecht 2003).

In conclusion, ensuring thermal comfort in urban life is related to building and indoor spaces, the formation of streets and urban fabrics, and the levels of outdoor comfort provided by these fabrics. The table summarizes the variables that can be considered in climate-sensitive design.

Table 2.1. Climate Sensitive Design Variables at Building, Street and City Scales

Scales	**Climate sensitive design variables**	**Reference**
Building	(1) Orientation of the building (2) Building form (3) Construction materials	Cofaigh et al. (1998) Gut ve Ackernecht (2003) Jeanjean et al. (2013)
Street	(1) Street layout (2) Sky view factor (3) Shading	Cofaigh vd. (1998) Gut and Ackernecht (2003) Watson and Johnson (1987) Golany (1996)
Urban	(1) Urban form (2) Solid-void balance (3) Green field	Goulding et al. (1993) Yasin et al. (2020) Zhou et al. (2017)

2.2. Urban Heat Island Effect

Most people living in the world live in urban settlements. While migration from rural areas to cities continues rapidly, the migration movement is expected to continue, and the number of people living in cities will increase daily. Urbanization affects the destruction of the natural land surface, the increase in pollution, and the change in the physical and chemical properties of the atmosphere with the release of greenhouse gases. In densely populated areas, the impact of urbanization is observed to be higher in terms

of temperature compared to rural and natural areas. Cities are more exposed to urban heat islands than rural areas; therefore, they are 3°C hotter at night than rural areas (Voogt 2004).

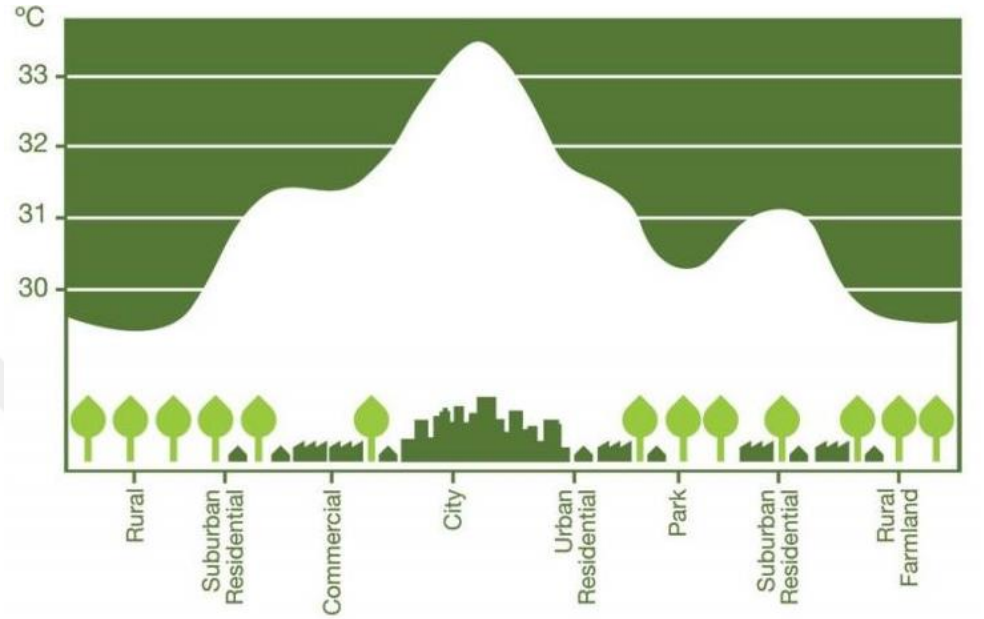

Figure 2.5. Cities and Heat Islands Effect

(Source: Öztürk 2021)

Building materials such as roofs, asphalt, concrete, and sidewalks absorb more heat energy from the sun than other natural surfaces. This energy is also spread as heat and increases even more at night. This phenomenon of increased heat in urban areas compared to surrounding rural areas is called the Urban Heat Island (UHI) effect (Oke 1982).

According to Givoni (1998), when observed daily, the average temperature in urban environments is higher than in rural areas. Higher temperature differences can be observed, especially at night. When built environments and natural areas are compared, temperature differences of 3-5 °C are observed, and in some regions, this difference can reach up to 8-10°C, causing profound temperature differences. This temperature difference between urban residential and surrounding natural areas is called the Urban Heat Island (UHI) effect (Givoni 1998).

The UHI effect is influenced by two types of factors: environmental and physical. The first is related to environmental factors such as wind speed and humidity. The second can strongly affect the size of the UHI effect, such as the size of the city and the density of the settlement area. The UHI effect can cause the formation of an air dome resembling a canopy shape over the settlement area and its surroundings (Rosenlund 2000), as shown in Figure 2.6.

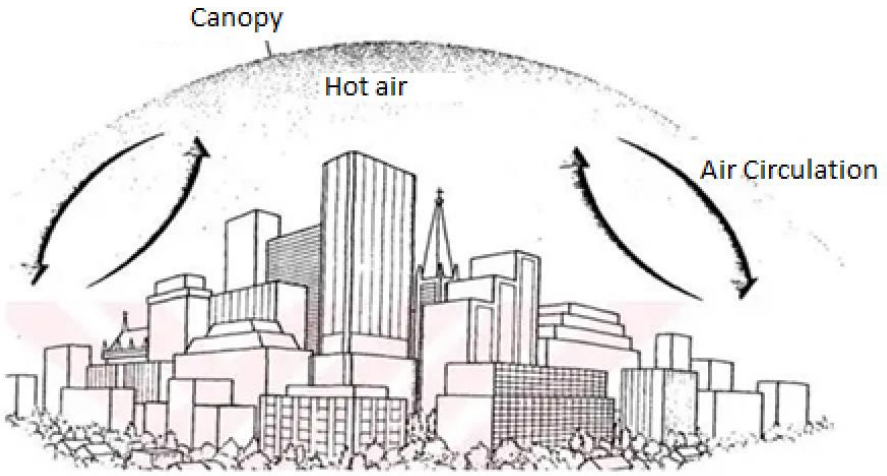

Figure 2.6. Urban Heat Island Effects

(Source: Çağlar 2021)

Additionally, impermeable urban surfaces cause rapid water drainage and reduce overall evaporation (Kim 1992, Owen et al. 1998). This contributes to forming an Urban Heat Island because it prevents heat loss (Oke 1987). In addition, human-related activities such as vehicle exhaust, heat emission from cooling, urban form, urban texture, building materials, and thermal properties are important factors affecting the formation of the urban heat island (Taha 1992; Yamamoto 2006). The urban heat island effect can reach levels that exceed the comfort threshold for people living in hot climate regions during specific periods of the year. This can indirectly result in negative impacts such as health problems, air pollution, and water scarcity and even cause regional-scale climate changes (Yang et al. 2011).

There are fundamental strategies for reducing the urban heat island effect. It is necessary to use roofing materials with a high albedo value in buildings, and using light-colored roofing materials minimizes the urban heat island effect as they do not absorb

heat (Akbari et al. 2001). In addition to high albedo roofs, using surface coatings with a high albedo value also helps reduce the urban heat island effect. Increasing green vegetation is essential for regulating urban microclimates (Wilmers 1988; Dimoudi and Nikolopoulou 2003; Synnefa et al. 2008; Takebayashi and Moriyama 2009; Xu et al. 2010). Tree shading provides a cool environment for pedestrians in public areas during hot weather (Sailor 2006). Additionally, approximately 200,000 shade trees have been planted annually in the United States to reduce the urban heat island effect (Scott et al. 1999).

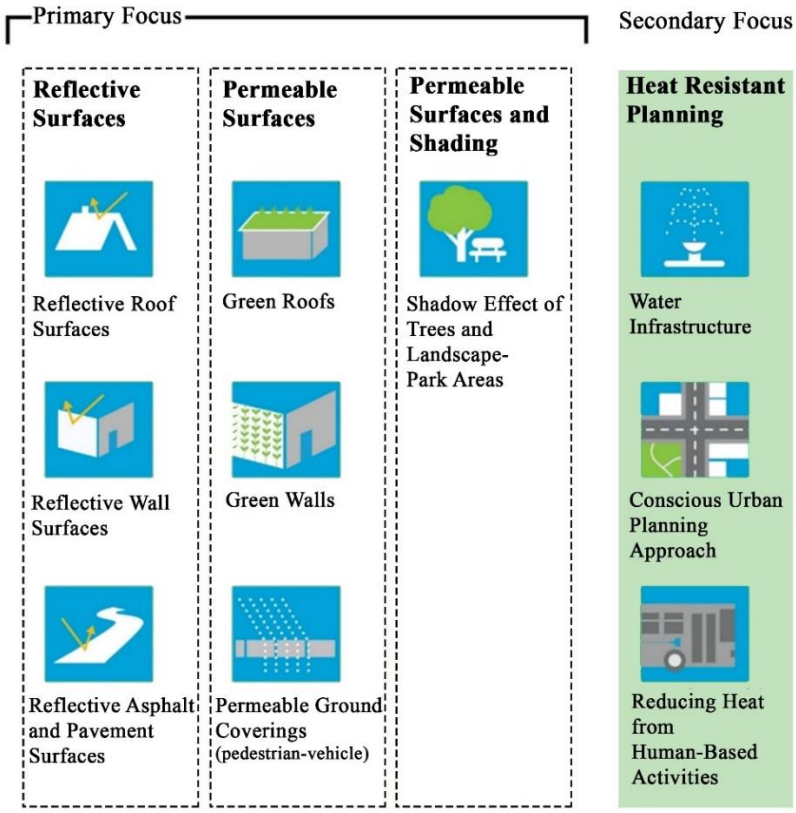

Figure 2.7. Sustainable Cooling Approach for Urban Areas

(Source: ESMAP 2020)

Increasing the number of permeable surfaces is an essential strategy. Permeable surfaces increase cooling capacity by absorbing water (Sailor 2006). Along with wind, the presence of water masses through evaporation increases cooling capacity and reduces the temperature effect (Robitu et al. 2006). Yamamoto (2006) argued that proper planning strategies could reduce the urban heat island effect in a settlement located along a stream.

He suggested planning buildings perpendicular to the stream to avoid disrupting the airflow from the stream to the city. According to Wong (2005), widespread implementation of green roof practices significantly reduces the urban heat island effect. The widespread adoption of green roof practices has a considerable impact in urban areas with numerous buildings.

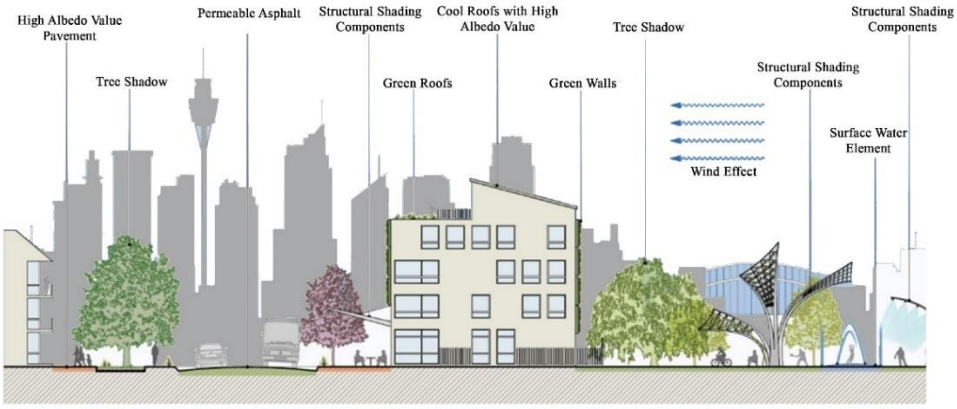

Figure 2.8. Sustainable Cooling Steps in an Urban Section

(Source: Osmond and Sharifi 2017)

2.3. Outdoor Thermal Comfort

The outdoor thermal environment is greatly influenced by the built environment, e.g., anthropogenic heat, evaporation, and evapotranspiration of plants, shading by trees and man-made objects, and ground surface cover such as natural grass and artificial paving, etc. Outdoor spaces provide a pleasurable thermal comfort experience for people and effectively improve the quality of urban living. People experience different thermal sensations while carrying out outdoor activities in streets, plazas, playgrounds, urban parks, etc. Thermal Comfort is the condition of mind that expresses satisfaction with the thermal environment and is assessed by subjective evaluation (ANSI/ASHRAE Standard 55 2004).

Humans have been searching for ways to cope with the negativity of the environment for a long time. Throughout history, all societies have tried to protect

themselves from climatic negativity. They have built shelters and created living areas to protect or benefit from the sun's rays (Yüceer 2015).

The foundation of people feeling physically and mentally healthy is based on their relationship with the climate conditions. Therefore, bioclimatic comfort is defined as the ability of humans to adapt to their environment while expending a minimum amount of energy (Özyavuz 2017). Temperature, wind, and humidity are essential in determining bioclimatic comfort conditions (Topay and Yılmaz 2004).

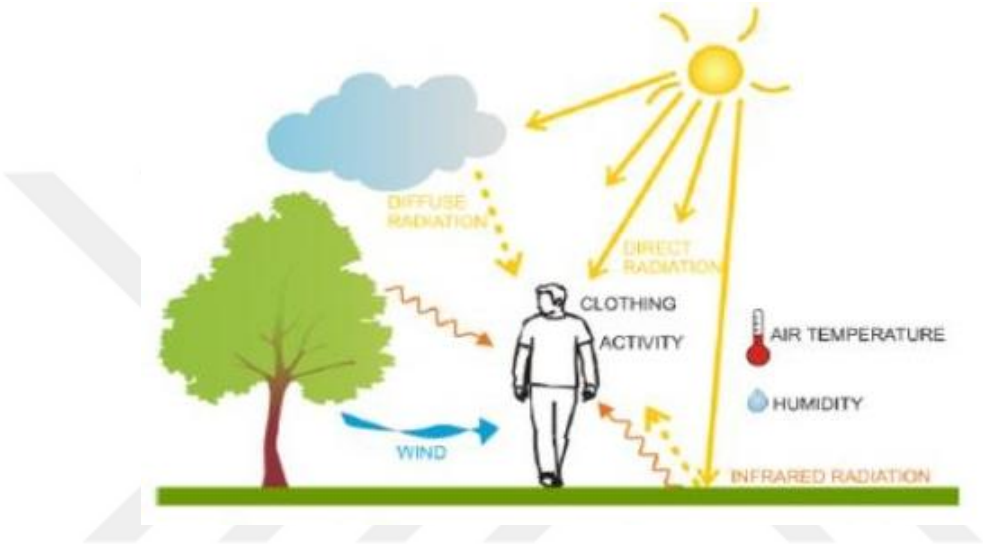

Figure 2.9. Outdoor Thermal Comfort

(Source: Perrineau 2013)

According to the literature on thermal comfort, outdoor comfort conditions affect the quality of life, and the amount of energy consumed to provide indoor comfort also affects it (Deb and Ramachandraiah 2011). The role of the city form in daylight, natural ventilation, and sun exposure is particularly determinant in energy consumption (Yao et al. 2012). A literature review shows climate-sensitive design principles can ensure comfort conditions with less energy consumption in indoor and outdoor environments. The climate-sensitive areas in the components of the city and the spatial scales must be determined to provide thermal comfort in urban environments. Therefore, designing the city's future with a holistic approach between different scales is essential (Peker 2020).

The Perceived Temperature (PT) is an equivalent temperature based on the "Klima-Michel-Model," which is an energy balance model for humans (Jendritzky et al. 1990) (Staiger et al. 2012). It is designed for people in the open air. It is defined as "the

temperature of the air in a reference environment that is expected to be the same as thermal perception in the actual environment" (Staiger et al. 2012).

Table 2.2. The Thermo-Physiological Meaning of PT Results for Central Europe (Source: VDI 2008 and Stagier et al. 2012)

PT (°C)	Thermal Perception	Thermo-physiological stress
≥ +38	Very hot	Extreme heat stress
+32 — +38	Hot	Great heat stress
+26 — +32	Warm	Moderate heat stress
+20 — +26	Slightly warm	Slight heat stress
0 — +20	Comfortable	Comfort possible
-13 — 0	Slightly cool	Slight cold stress
-26 — -13	Cool	Moderate cold stress
-39 — -26	cold	Great cold stress
< -39	Very cold	Extreme cold stress

Outdoor thermal comfort parameters are divided into two categories. These are divided into objective and subjective. Air temperature, wind, humidity, radiation, metabolic temperature, and clothing insulation constitute objective parameters.

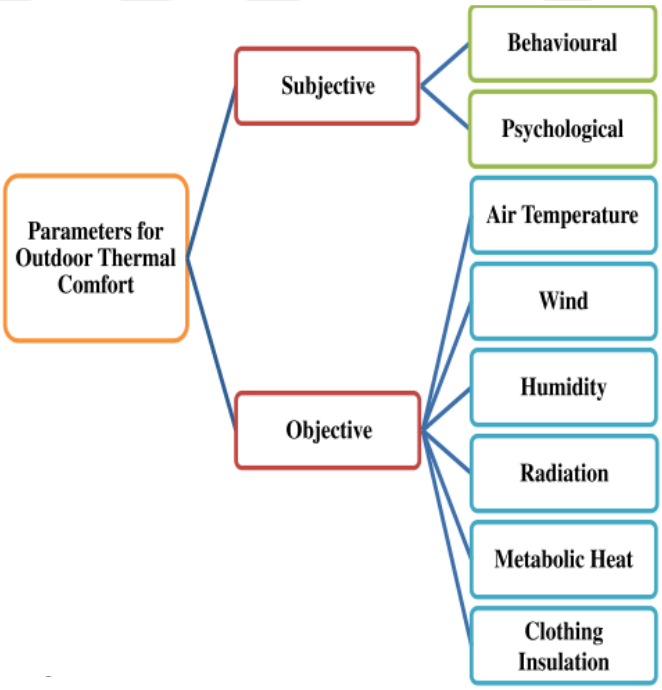

Figure 2.10. Outdoor Thermal Comfort Parameters

(Source: Mukherjee and Mahanta 2014)

2.4. Evaluation

The literature review has been conducted under three separate headings. The principles of climate-sensitive design were investigated, and these principles were implemented in the proposed urban design plan. The foundation of the current research emphasizes environmental and physical parameters. A portion of this study was conducted based on these parameters. The analysis of the spatial characteristics of the site was explored based on physical parameters, while data from the meteorological station were selected according to environmental parameters. In the method of scale approach, analyses and evaluations were integrated into this study at different scales. The design was oriented parallel to the prevailing wind direction. Climate-sensitive design principles were taken into account in the orientation of streets and the design of green spaces. The second concept in the literature review is the urban heat island effect. Factors causing the urban heat island effect and solutions to reduce this effect were utilized in the study area. Methods obtained from the literature for reducing the heat island effect include increasing permeable and reflective surfaces, implementing green walls, green roofs, shading, and water elements. The third concept involves evaluations in the study area based on outdoor thermal comfort parameters and the PET index. Outdoor comfort for pedestrians is crucial. Therefore, in this study, tree canopies were recommended to protect pedestrians from the adverse effects of hot weather during the summer months. This increased the shading elements in the study area. Additionally, the continuous circulation of the prevailing wind within the study area is important for enhancing pedestrian comfort. All information obtained from the literature review demonstrates how outdoor climate conditions are directed through design concerning physical parameters.

CHAPTER 3

RECENT RESEARCH, MODELS AND DESIGN EXAMPLES

This section discusses research projects that have implemented climate-sensitive design approaches to reduce the urban heat island effect. These projects exemplify the models and methods used in such research. In addition, detailed explanations of the projects planned with a climate-sensitive design approach around the world and in Türkiye were included.

3.1. Research and Models Related to Climate-Sensitive Design

In recent years, many models and methods have been used for climate simulations in the world and in Türkiye. These simulations enable us to obtain scientific data regarding urban spaces. Research projects that have examined models featuring microclimatic analyses and the methods used according to these models within the scope of this work are reviewed. Among the projects examined, 6 projects were selected in line with the determined criteria. The selection criteria are shown in Table 3.1.

Table 3.1. Recent Research Projects Selection Criteria

	Climate Simulations	Climate Sensitive Design	Heat Island Effect	Meteorological Data
Holland -Delft	■	■		■
Austria-Tyrol	■	■		■
England- West Midlands	■		■	■
Erzurum- Yıldızkent	■	■		■
Ankara- City Center	■	■		■
Izmir- City Center			■	■

3.1.2. Research from Around the World on Climate-Sensitive Design

When we examine examples from around the world, within the scope of this study, the latest research and models conducted in the Netherlands city of Delft, Tyrol in Western Austria, and the West Midlands region of England were examined.

3.1.2.1.Holland -Delft

Firstly, a research study conducted in the city of Netherlands, Holland, will be described. In their study, **Taleghani, Kleerekoper, Tenpierik, and Dobbelsteen (2014)** investigated different typologies based on the hottest day recorded in Holland until the day of their study. On June 19, 2000, the maximum temperature measured in Holland was 33°C. These typologies constitute single, linear, and courtyard forms. Figure 3.1 shows these study areas. Different urban forms provide different microclimates for the users of space.

Figure 3.1. Urban Forms Selected in the City of Delft

(Source: Taleghani, Kleerekoper, Tenpierik and Dobbelsteen 2014)

In this study, the ENVI-met and RayMan simulation programs were used. Five different urban forms have been identified to investigate thermal comfort in the temperate climate of the city of Delft. Measurements at a height of 1.40 m were conducted at selected points in the center of the defined urban forms. The ENVI-met simulation program simulated air temperature, relative humidity, and mean radiant temperature. The physiological equivalent temperature was also calculated, and outdoor thermal comfort

was assessed using the RayMan program. Outputs of the simulations were compared among the different urban forms. As a result, it was determined that in the temperate climate conditions of the city of Delft, singular-form buildings provided prolonged solar radiation. At the same time, urban blocks in courtyard form offered less solar radiation during the summer, leading to more comfortable microclimatic conditions. Since the urban heat island effect tends to increase due to climate change and urbanization, the problem is becoming increasingly severe. In this direction, if urban planning is done correctly, more fabulous urban spaces can be created (Taleghani, Kleerekoper, Tenpierik, and Dobbelsteen 2014).

3.1.2.2.Austria-Tyrol

Secondly, in a study conducted in Austria, **Back, Bach, Jasper-Tönnies, Rauch, and Kleidorfer (2021)** carried out spatial modeling related to the thermal climate index, surface temperature, and mean radiant temperature. For the simulation, six different urban sections were selected in the mountain city of Innsbruck. As shown in Figure 3.2, they are divided into six categories: industrial, administrative, and commercial areas, city center mixed-use, social facilities, multi-story residential areas, and residential areas. On an urban scale, vegetated and impermeable surfaces directly affect the surface temperature model. Meteorological data were obtained from two different stations in the city, one at the University of Innsbruck and the other at Innsbruck airport. The urban sections closest to one of the stations used the data from that station. Local authorities provided DEM data and building vector layers.

Figure 3.2. Selected Study Areas in The Tyrol Region

(Source: Back, Bach, Jasper-Tönnies, Rauch and Kleidorfer 2021)

This study presents a three-scale approach. As seen in Figure 3.3, it is divided into three categories: regional scale, local scale, and micro scale. A three-scale approach has been adopted to model LST, UTCI, and MRT values. This approach is a useful method for determining priority areas at different scales throughout the city. As a result, it was observed that surfaces with high albedo values reduce land surface temperature while increasing the apparent temperature, directly affecting thermal comfort. Additionally, the sky view factor is identified as having a significant impact on bioclimatic conditions in the study (Back, Bach, Jasper-Tönnies, Rauch, and Kleidorfer 2021).

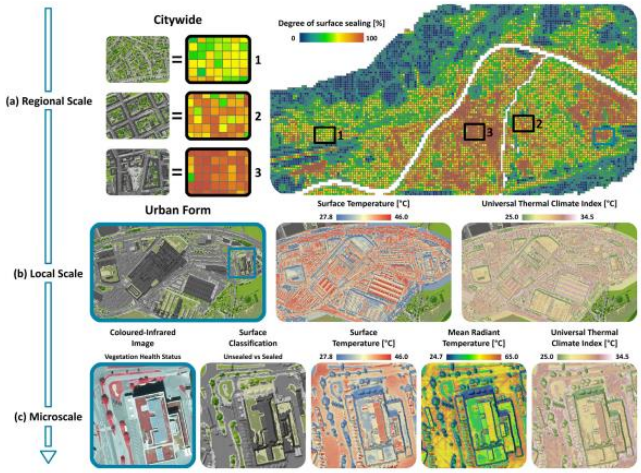

Figure 3.3. The Scale Approach in the Study

(Source: Back, Bach, Jasper-Tönnies, Rauch and Kleidorfer 2021)

3.1.2.3.England- West Midlands

Thirdly, a study conducted in the West Midlands region of England has been examined. **Bradley, Thornes, Chapman, Unwin, and Roy (2002)** analyzed physical variables such as slope, sky view factor, surface roughness, emission, and albedo using a Geographic Information System (GIS) program. Figure 3.4 shows the analyses conducted in this context.

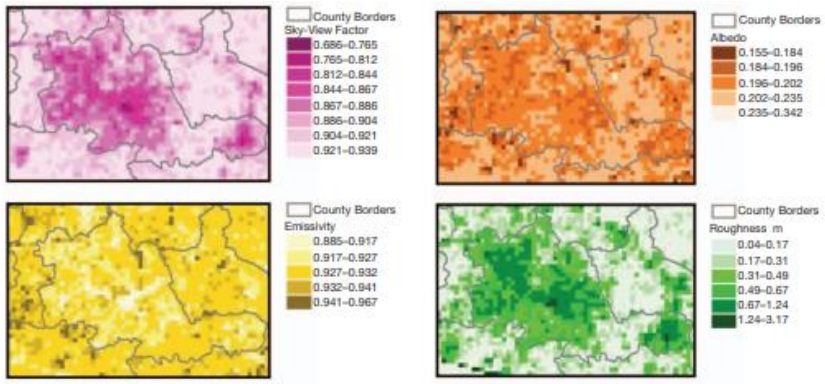

Figure 3.4. Analyzes Obtained in the West Midlands Region

(Source: Bradley, Thornes, Chapman, Unwin, and Roy 2002)

The model used meteorological data such as Radiant Surface Temperature (RST), wind speed, cloud type, relative humidity, air temperature, and cloud cover. These measured values were calibrated to be consistent with Met Office Operational Radiance (OR) forecasts. A model defined by Outcalt (1971) has been used to calculate RSTs at locations in the study area. The modeled urban heat island is more sensitive to the sky view factor values used than in rural areas. The intensity of the urban heat island in West Midlands is 4.7°C. The effect of the urban heat island has been examined over 24 hours. As shown in the 05:00 timeframe in Figure 3.5, the city center is observed to be 1.5°C warmer, while rural areas are between 0 to 1°C cooler. Rural areas tend to cool down quickly. City centers remain warm (Bradley, Thornes, Chapman, Unwin, and Roy 2002).

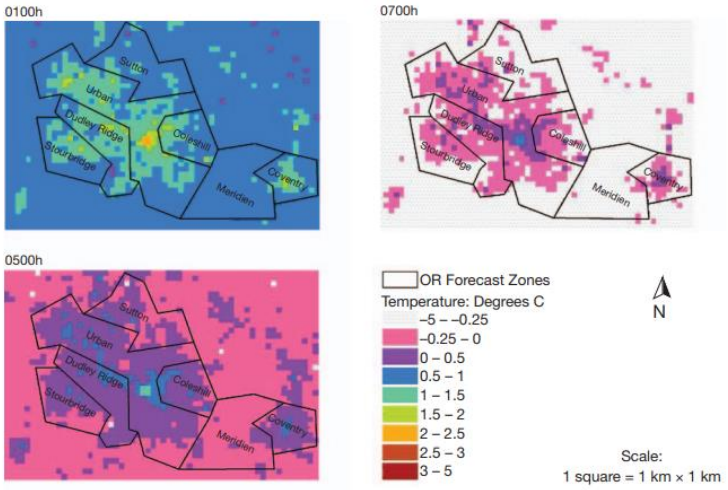

Figure 3.5. The Urban Heat Island Effect in the West Midlands Region

(Source: Bradley, Thornes, Chapman, Unwin, and Roy 2002)

3.1.3. Research from Türkiye on Climate-Sensitive Design

Studies and modeling work related to climate-sensitive design and the urban heat island effect carried out in the cities of Erzurum, Ankara, and Izmir in Türkiye have been reviewed.

3.1.3.1.Erzurum- Yıldızkent

In their study, **Yavaş and Sevgi (2020)** state that the selection of the city of Erzurum is significant due to its location in a cold climate zone. The study describes how urban planning directly affects microclimates. Between 2018 and 2019, 32 climate simulations were performed, and the measurements from these simulations were obtained from the FINEST-345 model device, which measures at a height of 2 meters in the city center. Meteorological data for the same days were taken from Erzurum Regional Directorate of Meteorology. The ENVI-met simulation program was used to create the

model. Eight different variations were created within the Yıldızkent district. One of these variations is shown in Figure 3.6. The calculated data is the average reflected temperature, wind speed, air temperature, surface temperatures, relative humidity, sky view factor, and cloudiness. When the study outputs are examined, it has been revealed that when climate-sensitive design principles are explicitly applied to space, the thermal comfort value can be increased by up to 2.0°C in the winter months (Yavaş and Sevgi 2020).

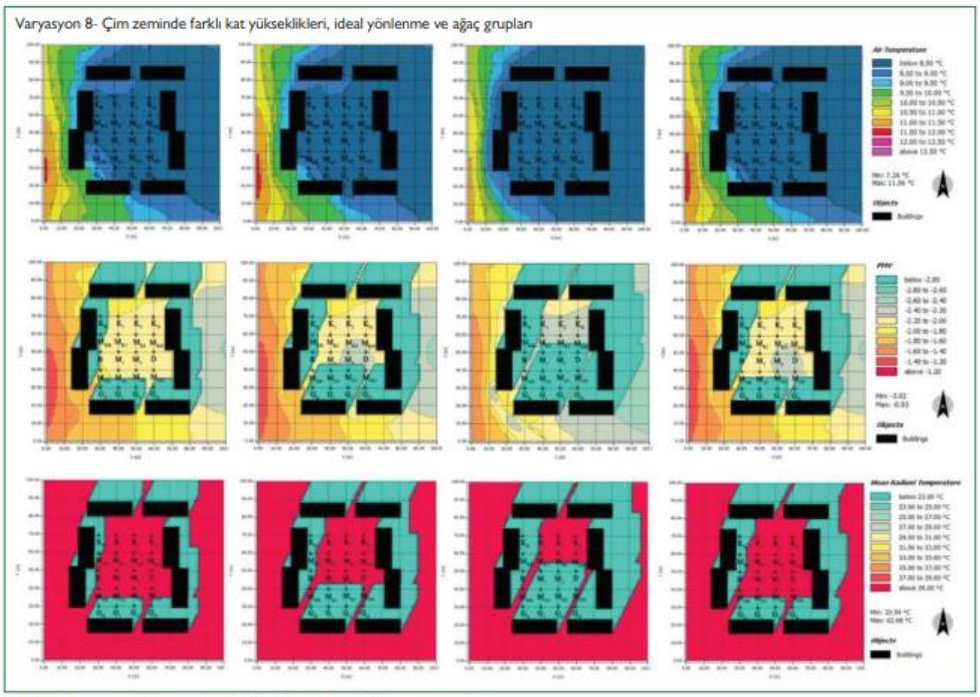

Şekil 13. Varyasyon-8 hava sıcaklığı, PMV, T_{MRT} değeri simülasyon sonuçları.

Figure 3.6. Simulation Results in Yıldızkent

(Source: Yavaş and Sevgi 2020)

3.1.3.2.Ankara- City Center

In the study by Yüksel and Yılmaz (2008) aimed at measuring the urban heat island effect in the city of Ankara, Landsat-5 TM (thermal band) images for 1985 and 1995, and Landsat-7 ETM images for 2002, as well as aerial photographs of Ankara, were utilized. Three temperature and humidity data loggers were placed in different land covers within the city to take measurements. These areas were determined as Migros station,

Bahçelievler station, and Anıtkabir station. The collected data were spatialized in Erdas Imagine 8.5 and Arc GIS 9.0 software. Surface temperatures were examined using the sixth band of the Landsat satellite data for 1985, 1995, and 2002, and comparisons were made between these years. Land cover and vegetation analyses were also calculated and compared for these three years. As a result, Ankara's morphological and topographical structure, remaining within a geomorphological basin, is an essential factor that increases the urban heat island effect. Additionally, rapid and irregular urbanization and the lack of vegetation cover in Ankara also play a role in intensifying the urban heat island effect. The proportion of residential areas in Ankara city has increased from 1985 to 2002. The urban heat island effect is observed in Ankara during summer (Yüksel and Yılmaz 2008).

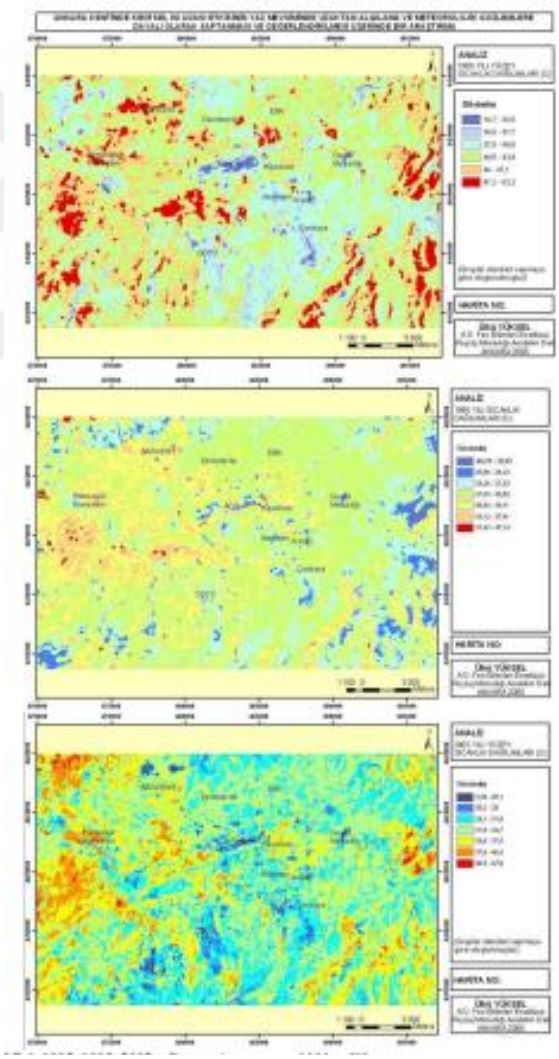

Figure 3.7. Surface Temperatures for the Years 1985, 1995, and 2002 in Ankara (Source: Yüksel and Yılmaz 2008)

3.1.3.3.Izmir- City Center

Şentürk and Çubukçu (2023) aimed to identify areas clustered with low temperatures in their study. The study area includes the central districts of Menemen, Çiğli, Karşıyaka, Bayraklı, Bornova, Konak, Karabağlar, Buca, Balçova, Narlıdere, and Gaziemir. Thermal bands from Landsat OLI 8 satellite images, specifically Bands 10 and 11, were utilized in the study. Analyses were conducted using satellite data from August 5, 2020. Surface temperature and NDVI were calculated. Anselin Local Moran's I, one of the spatial autocorrelation methods, was employed to identify clusters of excellent areas. The obtained data were spatialized using ArcGIS Pro software. Consequently, urban cool areas with relatively low surface temperature values are in certain residential areas in the inner parts of the city and along the coast in the central districts of Izmir. However, an increase in surface temperature values is observed in industrial zones. Urban cool islands are primarily located in areas with dense green spaces, including Kültürpark, Inciraltı City Forest, Ege University, Air Training Command, Manavkuyu, Evka 3, and Narlıdere residential areas. The size of the urban cool islands identified in the study has been measured as 5 hectares (Şentürk and Çubukçu 2023).

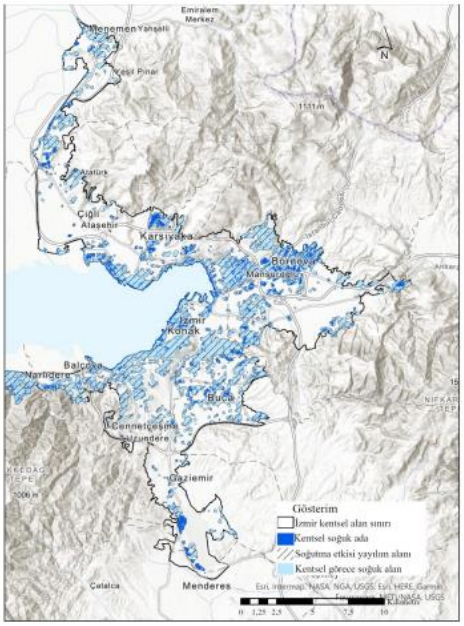

Figure 3.8. Spatial Pattern of Surface Temperature in Izmir

(Source: Şentürk and Çubukçu 2023)

3.2. Climate-Sensitive Design and Projects

Design examples that are climate-sensitive and reduce the urban heat island effect will be examined in two parts: projects from around the world and from different cities in Türkiye. Among the projects examined, 10 projects were selected in line with the determined criteria. The selection criteria are shown in Table 3.2.

Table 3.2. Design Projects Selection Criteria

	Green Elements	Permeable Surface	Wind Direction	Water Management	Nature-Based Solutions	Energy Efficiency
Eco-Viikki- Helsinki	■	■	■	■	■	■
St. Stephen's Green - Dublin	■	■			■	
Christie Walk- Adelaide	■	■	■	■	■	■
The Sustainable Urban District of Vauban - Freiburg	■	■			■	■
Ex-Isotta Fraschini Area Urban Reform-Saronno	■	■			■	
Climate Islands - Barcelona	■	■	■	■	■	■
Gebze Eco-City - Kocaeli	■	■		■	■	■
5 Ocak Park and Its Surroundings - Adana	■	■	■		■	■
Kükürtlü Climate Street - Bursa	■	■		■	■	
Sasalı Climate-Sensitive Research Institute - Izmir	■	■		■	■	■

3.2.2. Exemplary Practices and Projects Across the World

Projects designed in the cities of Helsinki, Dublin, Adelaide, Freiburg, Saronno and Barcelona have been examined in detail as they offer solutions that are sensitive to climate and mitigate the urban heat island effect.

3.2.2.1.Eco-Viikki - Helsinki

The Eco-Viikki project is located 5 kilometers from the city center of Helsinki. This project aims to reduce energy consumption, manage stormwater, and reduce water pollution to preserve natural life. It is a mixed-housing type project (URL 1 2023).

Figure 3.9. Residential Areas of the Eco-Viikki Project

(Source: Hakaste, Jalkanen, Korpivaara, Rinne, Siiskonen 2005)

The project features green fingers permeating the residential areas, as demonstrated in Figure 3.10. The area has a green design with low-density housing. The housing types include row houses and duplexes. Building heights increase from the edges towards the center. The orientation of the housing areas is toward the south. (Hakaste et al. 2005).

Figure 3.10. Ecological Plan of the Eco-Viikki Project

(Source: Hakaste, Jalkanen, Korpivaara, Rinne, Siiskonen 2005)

A vital feature of this project is the intermingling of natural and built environments, as seen in Figure 3.11. The green fingers, composed of trees and shrubs, also play a significant role in stormwater collection, directing it to a stream at the perimeter of the project area. The dominant wind direction in this study area is southwest. Dense vegetation has been planted along the southern edge as a windbreak. This is advantageous for fields and is also essential for reducing windiness to lower energy consumption and improve living comfort (City of Helsinki City Planning Department 2010).

Figure 3.11. Eko-Viikki Master Plan

(Source: City of Helsinki City Planning Department 2010)

3.2.2.2.St. Stephen's Green - Dublin

St. Stephen's Green in Dublin, Ireland, is a public park dating back to the Victorian era. The park was in a marshland on the outskirts of the city and used for grazing. The Dublin authorities later decided to create a park on this site. Today, the park features colorful flower gardens and tree-lined walking paths (URL 2 2023).

It is a 9-hectare green park in the city center with many features that can alter the microclimate of the surrounding neighborhood. Permeable grass surfaces, diversity of trees, shading

Figure 3.12. A View from St. Stephen's Green

(Source: URL 3 2023)

3.2.2.3.Christie Walk - Adelaide

In Adelaide, Australia, the goal was to create a livable and sustainable urban environment that supports eco-sensitive economic development. The Christie Walk project is an experiment in forming a small community of 27 residences and gardens. It includes three-story residences oriented according to the sun's position (URL 4 2023).

The city of Adelaide experiences the characteristics of the Mediterranean climate, where temperatures rise in the summer months and are cool in the winter months, requiring cooling in summer and heating in winter. The urban heat island effect is

intensely present in Australian city centers. For this reason, the Christie Walk project has been designed as an ecological project (URL 5 2023).

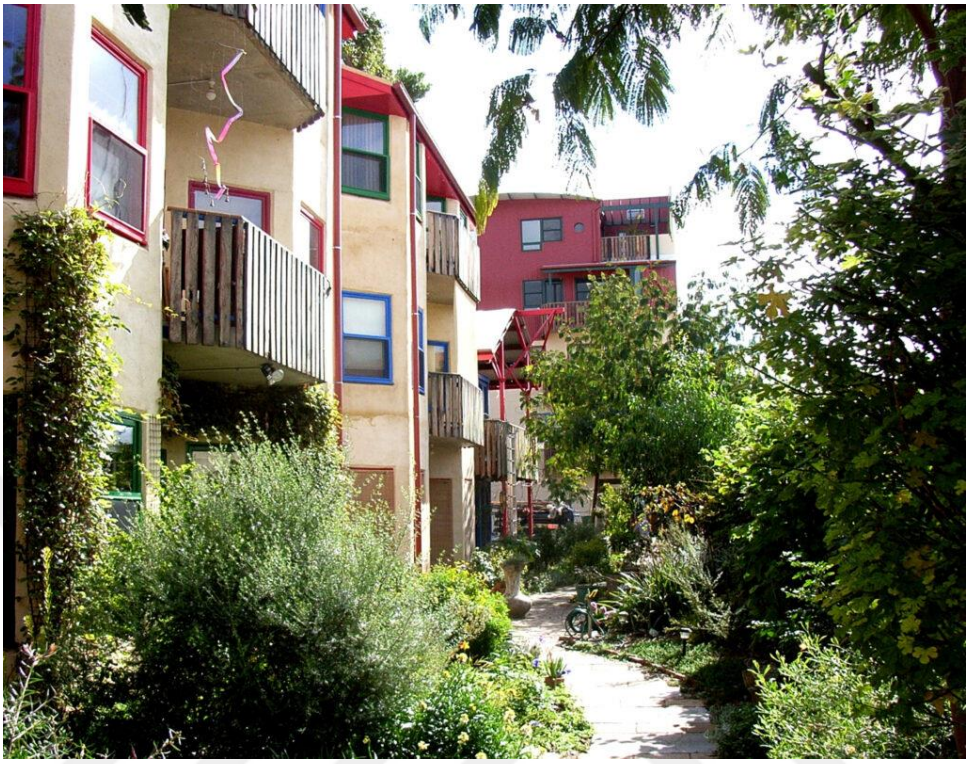

Figure 3.13. Christie Walk Residential Area

(Source: URL 4 2023)

The Christie Walk project aims to utilize energy efficiency at the highest level. It maximizes the use of solar energy. This pedestrian and plant-friendly project includes extensive roof gardens and pathways. The roof gardens facilitate the collection of rainwater. To regulate temperatures, walls have been constructed from fly ash concrete, and all project stages have utilized natural and recycled materials. The east-west orientation of the buildings helps insulate the interiors from heat and cold. The landscaping designed on the north side of the project enhances natural ventilation. Efficiency forms the foundation of the project. All these features in the project constitute climate-sensitive design tools (URL 6 2023).

Figure 3.14. Christie Walk Sketch Plan

(Source: URL 6 2023)

3.2.2.4.The Sustainable Urban District of Vauban – Freiburg

Freiburg ranks among the top green cities in Europe. The German city of Freiburg boasts excellent quality of life with its parks, public transportation, and clean air. In the Vauban district of Freiburg, rows of houses equipped with solar panels can be found. Thanks to these panels, more energy is produced than consumed in the neighborhood. Additionally, buildings in the area feature green roofs that collect rainwater. Despite continuous growth in population and economy, Freiburg has been reducing its CO2 emissions for over a decade.

After more than a decade of effort, Freiburg has finally convinced its manufacturing sector to go green, marking a significant step in environmental conservation. Solar panels are used on roofs and open spaces, and combined heat and power technology is employed to capture the heat that will warm thousands of homes. The city's comprehensive plan covers various aspects, including mobility, energy management, efficiency, and renewable energies (URL 7 2023).

Figure 3.15. Freiburg is a Neighborhood with Solar Panels

(Source: URL 7 2023)

3.2.2.5.Ex-Isotta Fraschini Area Urban Reform-Saronno

The abandoned industrial area of the former Isotta Fraschini represents a break in the southwest sector physically hindering the connection with the historical center, symbolizing a rupture in the city. The transformation proposal aims to restore this break functionally, morphologically, and environmentally. The goal is not only to design a livable place but also to make it a memorable one in order to shape the future of Saronno. The former Isotta Fraschini Area presents an extraordinary opportunity to restore some parts of the city, offering a chance to continuously engage with the spirit of the past while building bridges to the present world.

One of the key development objectives offered by the project is the environmentally sustainable redevelopment of forest and tree species, increasing green surfaces, and preserving existing green areas. The plan includes the creation of a university center with educational rooms and exhibition spaces, as well as the

construction of multifunctional buildings. The project holds significant importance in achieving the sustainable development goals of the European Union (URL 8 2023).

Figure 3.16. Ex-Isotta Fraschini Area Urban Reform Project

(Source: URL 8 2023)

3.2.2.6.Climate Islands – Barcelona

In this project, seven "Climate Islands" architectural-landscape interventions have been designed as a pioneering initiative to create green urban environments that can mitigate the effects of climate change. The project focuses on strategic locations and proximity to the urban context in the area closest to the sea around Port Vell. It strategically addresses and responds to citizens' needs. Intervention points are defined by combining elements such as the continuation of street texture, integrated planting, and suitable climate conditions. The project includes components of ecological significance,

enhancing urban biological diversity while providing meeting, resting, and recreational points.

Special technical solutions, such as planting vegetation obtained from Mediterranean climates and the use of water vapor systems, are implemented. The installation of low thermal index coatings that can reduce ambient temperature during intense heat periods is planned. Plants from various Mediterranean climates have been used, as these plants are adapted to saline environments and are resilient. The ultimate goal of these interventions is to enhance the quality of life for individuals by improving social interaction in public spaces, considering that such interaction is crucial for the development of the human species (URL 9 2023).

Figure 3.17. Climate Islands Project

(Source: URL 9 2023)

3.2.3. Design Project Examples from Türkiye

Projects from the cities of Kocaeli, Adana, Bursa, and Izmir have been examined in detail regarding climate-sensitive design projects in Türkiye.

3.2.3.1.Gebze Eco-City – Kocaeli

The Gebze Eco City project is in the Mollafenari village, within the sub-region of the Istanbul Metropolitan Area and the boundaries of the Kocaeli Metropolitan Municipality. Positioned within the Ballıkayalar basin, the project's approach aims to achieve a sustainable living environment. The eco-city project area is bounded by the valley edge to the south. The vision of the eco-city prioritizes street life and features neighborhood units that are harmonious with nature. To the north of the project area are forest villages, and to the south are neighboring settlements. This project, providing economic, social, and environmental well-being, encompasses walking paths, open spaces, shops, and cafes, thus representing a comprehensive urban design. The ecological and sustainable project, with its approach to environmental conservation, open spaces, and green surfaces, is in harmony with nature and represents a climate-sensitive design (URL 10 2023).

Figure 3.18. The Gebze Eco-City Project

(Source: URL 10 2023)

3.2.3.2.5 Ocak Park and Its Surroundings – Adana

The city of Adana experiences very high temperatures during the summer months. Although the Mediterranean climate is predominant, the heat felt in the summer can be highly intense. High humidity levels and the impact of temperature directly affect pedestrian comfort. Therefore, in this city, it is essential to apply climate-sensitive design principal decisions in urban designs. 5 Ocak Park and its surroundings are located near the city's northern edge. The prevailing wind direction during summer is from the south-southwest. One of the project's main goals is to bring this prevailing wind into the project area. To this end, an orange spine has been designed. This spine brings the wind into the project area and features broad-trunked trees with high shading capacity along the created pedestrian axes. The spine is also significant in connecting the disjointed and irregular parcels within the project area and creating a sense of unity. Street widths have been designed not to interrupt the airflow and to plan for new axes that can disperse the wind flow. Bioclimatic hubs, supported by planting work, have been designed to reduce the impact of extreme heat and humidity. A stream in the project area has been uncovered and naturalized. This design decision is essential for recreational activities and increasing cooling capacity. Another project goal is to capture rainwater and direct it to the stream. The design approaches used in this project serve as an excellent example of incorporating all climate-sensitive approaches (URL 11 2023).

Figure 3.19. 5 Ocak Park and Its Surroundings Urban Design Project

(Source: URL 11 2023)

3.2.3.3.Kükürtlü Climate Street – Bursa

With climate change, especially in city centers, numerous problems arise, becoming a severe crisis. Therefore, the Bursa Metropolitan Municipality has initiated a pilot project and launched a climate street project on Kükürtlü Street in the city center. Project proposals offer solutions that will increase the efficient use of energy by reducing carbon emissions released into the atmosphere and the urban heat island effect. As part of this, numerous interventions have been designed along the street. Solutions such as pocket parks, green tunnels, rain gardens, parklets, solar panel bus stops, increased vegetation, and permeable paving have been created. These solution proposals can be seen in detail in Figure 3.20. All these design decisions include nature-based solutions. Nature-based solutions are essential in combating significant problems such as climate change and the urban heat island effect. All details and strategies within the project will be determined in workshops to be conducted with the participation of stakeholders (URL 12 2023).

Figure 3.20. Bursa Climate Street Project

(Source: URL 12 2023)

3.2.3.4.Sasalı Climate-Sensitive Agriculture Education and Research Institute – İzmir

Many reports on climate change mention that in the coming years, scenarios include heatwaves and long periods of drought. To take precautions against these adversities, it is aimed to design a resilient institute. In the Çiğli district of İzmir, in Sasalı, the Sasalı Climate-Sensitive Agriculture Education and Research Institute project plans for a significant focus on production and education. Greenhouses applied agriculture areas, and laboratories comprise the project's parts. The units are designed linearly. Bioswales serving as connectors between these units create an integral axis. Entry is from the northern axis, with users experiencing the units on the linear axis. The design is completed with intelligent soil applications at the area's southern end. Essential strategies of the project include sustainable rainwater management, storing and reusing water from roofs, creating a backbone connecting units with a bio boulevard using nature-based solutions, and the use of natural materials (URL 13 2023).

Figure 3.21. Sasalı Climate-Sensitive Agriculture Education and Research Institute (Source: URL 13 2023)

3.3. Evaluation

Research projects examined from around the world, including Türkiye, largely consist of urban-scale projects where climate simulations are created using software programs, primarily utilizing meteorological data. The data, software, and methodology used in these research projects are important examples from the perspective of this study. The meteorological data used in this study, including surface temperature and the calculation of the urban heat island effect, has been fundamentally adopted from recent research projects that employ a macro-to-micro scale approach. Furthermore, principles used in design projects examined from around the world, including Türkiye, have also been utilized within the scope of this study. Among the examined sample projects, there are design projects from countries in different climate zones, including those in the Mediterranean climate zone. The design principles used in these projects consist of criteria related to climate sensitivity, sustainability, ecology, nature-based solutions, and criteria aimed at reducing the urban heat island effect. In this context, approaches have been taken from the examined projects that integrate wind flow and direction into the design, use green elements, manage water, reduce impermeable surface areas, and integrate nature-based solutions.

Within the framework of recent developments in climate, this study demonstrates the current situation globally and in Türkiye. This situation helps define the need for research in climate-sensitive areas and guides how research projects specific to Türkiye's urban structure and climate conditions can be conducted. Research and design projects play a crucial role in determining data collection techniques and the methodology of this study. Additionally, design projects have been compiled as the best examples of the practical application of climate sensitivity principles."

CHAPTER 4

CASE STUDY: POLIGON STREAM AND ITS SURROUNDINGS

In this section, the focus is on İzmir's Güzelyalı neighborhood and the Poligon Stream and its surroundings in this neighborhood. Spatial analysis has been categorized into four scales. Detailed analyses have been conducted within this scope at the city, basin, neighborhood, and street scales. Figure 4.1 illustrates these scales and their scopes.

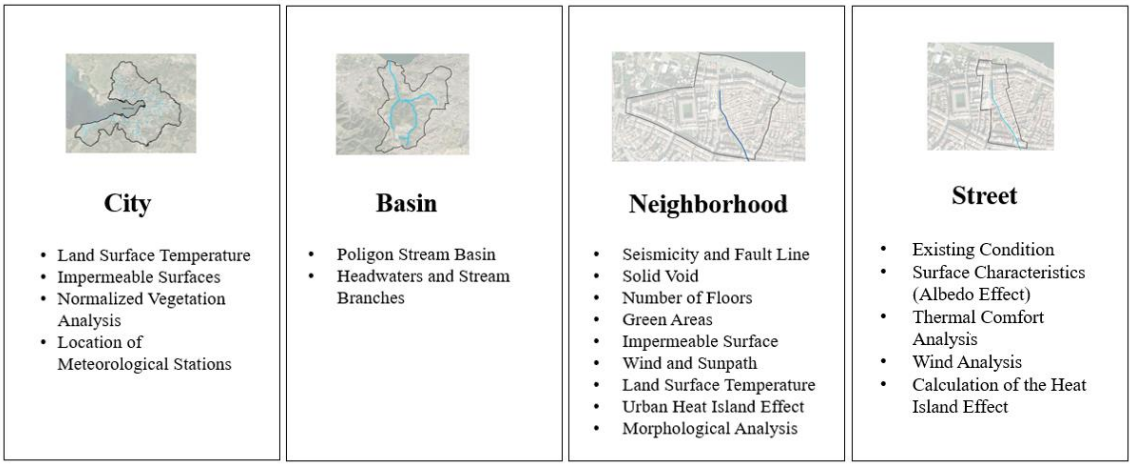

Figure 4.1. Scale Approach Determined in the Study

Güzelyalı is a neighborhood located on the western coastline of İzmir within the boundaries of Konak district. It is the most populous neighborhood in the Konak district and has a population of 17,512 people, according to the 2022 data. The neighborhood has changed names, including Reşadiye, Mirkati, and Kokaryalı.

According to the Güzelyalı meteorological station data, the long-term average temperature of the study area is 17.9°C, showing a temperature increase trend. The highest daily maximum temperature recorded to date was 43.0°C in 2002. The average wind speed recorded for many years around Güzelyalı neighborhood is 3.0 m/s, and the

highest wind speed recorded was 42.2 m/s (151.9 km/h) in 1962 (Güzelyalı Meteorological Station).

4.1. Analyzes at City Scale

Analyses and evaluations have been carried out starting from the city scale, considering the overall situation and hierarchy between scales without abstracting the study area from the city. The study area boundary at the city scale was determined by overlapping the watershed boundaries of the streams in the central district of İzmir. This approach was followed to not only evaluate the city within administrative boundaries but also to consider natural boundaries.

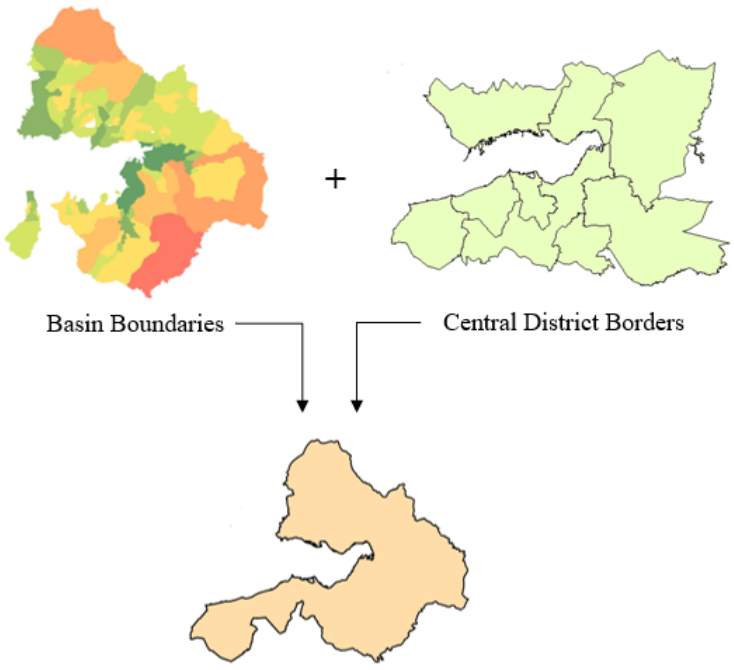

Figure 4.2. Determination of Area Boundaries at City Scale

4.1.2. Land Surface Temperature

Landsat 8 (OLI/TIR) remote sensing satellite data were initially utilized to calculate this analysis. The average temperature of July 24, 2022, the hottest and cloudless summer day in İzmir, was used. Images with a resolution of approximately 30 m per arc second produced by the SRTM global mission and Digital Elevation Model (DEM) data were also used. Thermal (bands 10 and 11) and visible (bands 4 and 5) bands of Landsat 8 images taken in the summer of 2022 were used. After processing these data in ArcGIS 10.8 software, land surface temperature analysis was obtained at the city scale. Figure 4.3 provides a detailed overview of the stages of the analysis.

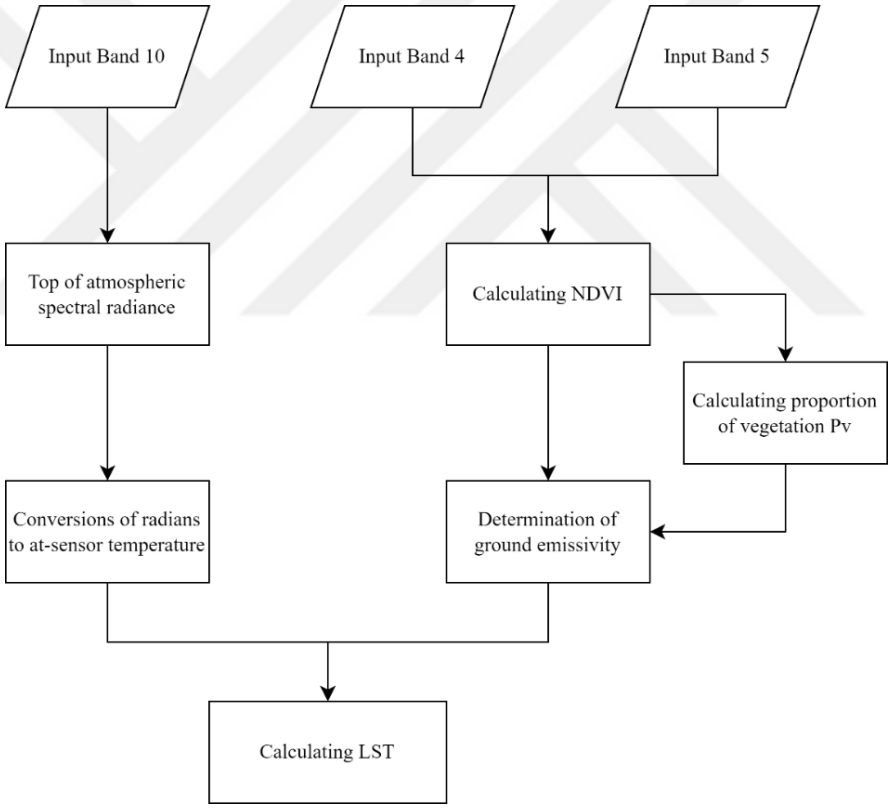

Figure 4.3. Land Surface Temperature Calculation Stages

The calculation stage of the surface temperature map was created using the formulas described in the literature and the specified formulas (Akyürek 2020; Kumar et al. 2022).

In the first stage, the following formula was used to convert the pixel value to the spectral brightness value for band 10:

$$TOA = ML \times Qcal + AL \quad (1)$$

Here, TOA represents the spectral brightness value, and ML represents the specific scaling factor for band 10.

In the second stage, the following formula was used to convert the radiance value to the brightness temperature:

$$BT = K2/ \ln (K1/L) + 1)) - 273{,}15 \quad (2)$$

K1 and K2 contain thermal conversion constant values, and BT represents the brightness temperature.

In the third stage, the Normalized Difference Vegetation Index (NDVI) was calculated using band 5 and band 4 obtained from satellite data. The NDVI analysis, measuring the vegetation cover ratio on the land, was calculated using the following formula:

$$NDVI = (Band5 - Band4)/(Band5 + Band4) \quad (3)$$

The vegetation cover ratio (Pv) closely related to NDVI was calculated using the formula:

$$((NDVI - NDVImin)/(NDVImax - NDVImin))^{2} \quad (4)$$

The surface emission ratio (ε) related to Pv was calculated as the fifth step:

$$Ɛ = 0{,}004 \times Pv + 0{,}986 \quad (5)$$

In the final stage, using the data calculated in the other steps, the land surface temperature (LST) was computed with the formula:

$$LST = (BT / (1 + (0{,}00115 \times BT / 1{,}4388) \times \ln(Ɛ))) \quad (6)$$

All these calculations were performed using ArcGIS 10.8 software. Applying these formulas, the surface temperature map for the city of Izmir on July 24, 2022, was obtained from the resulting data.

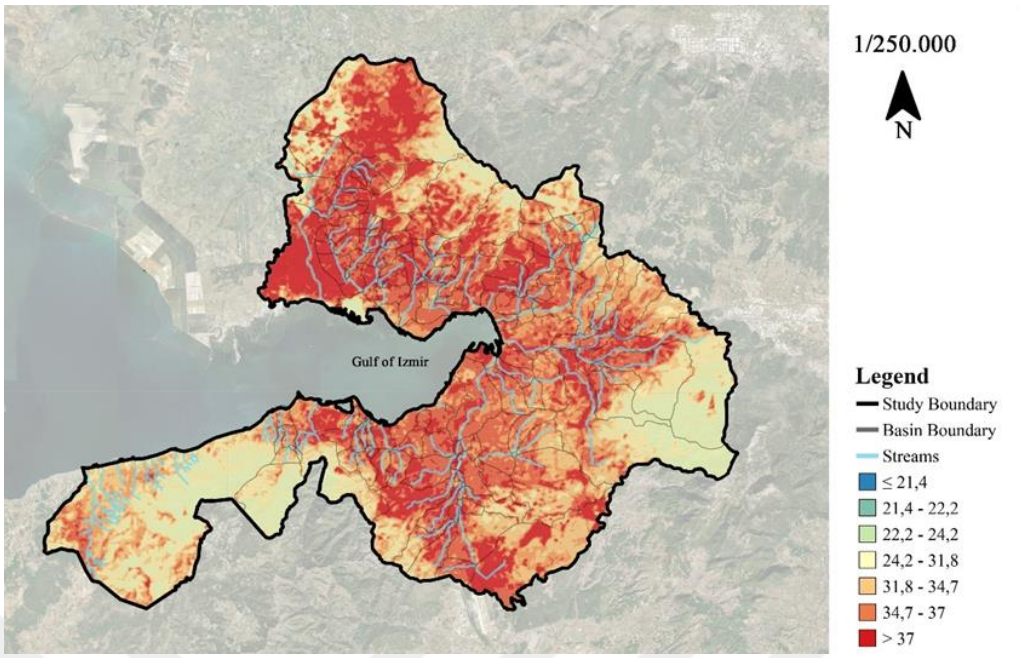

Figure 4.4. City-Scale Land Surface Temperature

(Source: Based on Landsat 8 (OLI/TIR) remote sensing satellite data)

When examining the land surface temperature, it is observed that temperatures in the city center are higher than 34.7°C. Upon analyzing the data within the study area boundary, it has been calculated that 22.75% of the area has a land surface temperature value exceeding 37°C, while 20.83% has a temperature lower than 30°C.

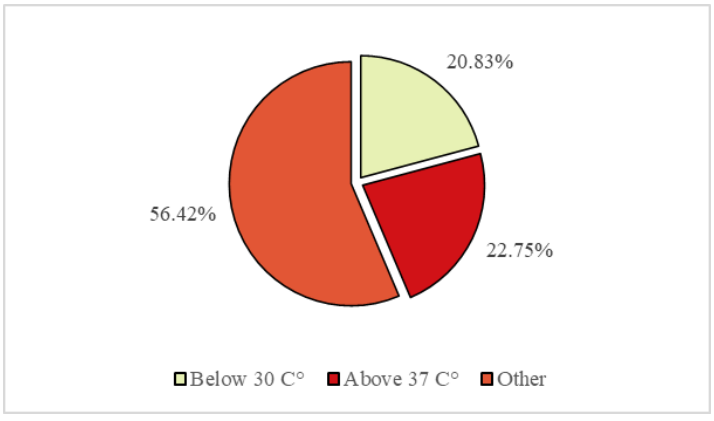

Figure 4.5. Distribution Graph of Urban-Scale Land Surface Temperature

4.1.3. Normalized Vegetation Index (NDVI)

It was calculated using Band 4 and Band 5 from Landsat 8 (OLI/TIR) satellite imagery. Detailed calculations have been explained in the previous section. NDVI analysis is an index that helps us understand whether the vegetation within the study area is healthy or unhealthy. NDVI analysis values range from +1 to -1. Areas with dense and healthy vegetation approach +1, while areas with unhealthy or insufficient vegetation approach -1. Intermediate values represent shrubs and grasslands.

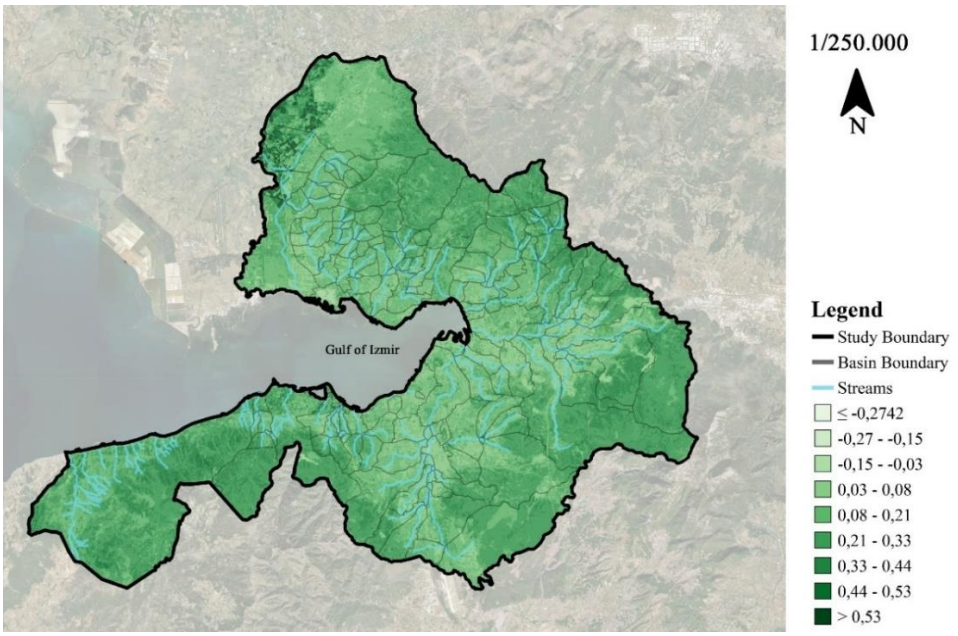

Figure 4.6. City-Scale NDVI Analysis

(Source: Based on Landsat 8 (OLI/TIR) remote sensing satellite data)

When examining our urban-scale study area, the areas with the unhealthiest and most insufficient vegetation make up 9.17% of the study area.

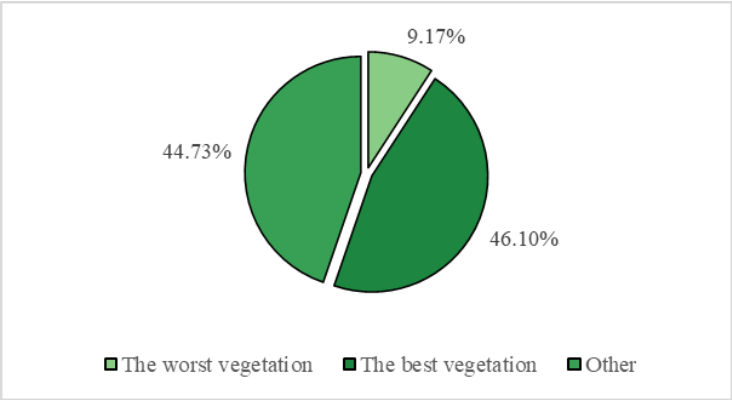

Figure 4.7. Vegetation Distribution Graph at City Scale

4.1.4. Impervious Surfaces

Impermeable surfaces are an essential indicator of change in urban settlement areas over time. (Wang et al. 2015). They are not only a measure of urbanization degree but also important indicators of environmental quality and ecological structure due to their impact on environmental and ecological change (Chen et al. 2019; Weng 2012). Surfaces such as roads, buildings, parking lots, asphalt, concrete, and bricks are defined as impervious. The increase in impervious surfaces increases surface runoff and increases flood frequency (Weng 2012). The increase in impervious surfaces also contributes to the urban heat island effect, microclimate changes, and drought (Chen et al. 2020; Hidayati and Suharyadi 2019; Wang et al. 2015).

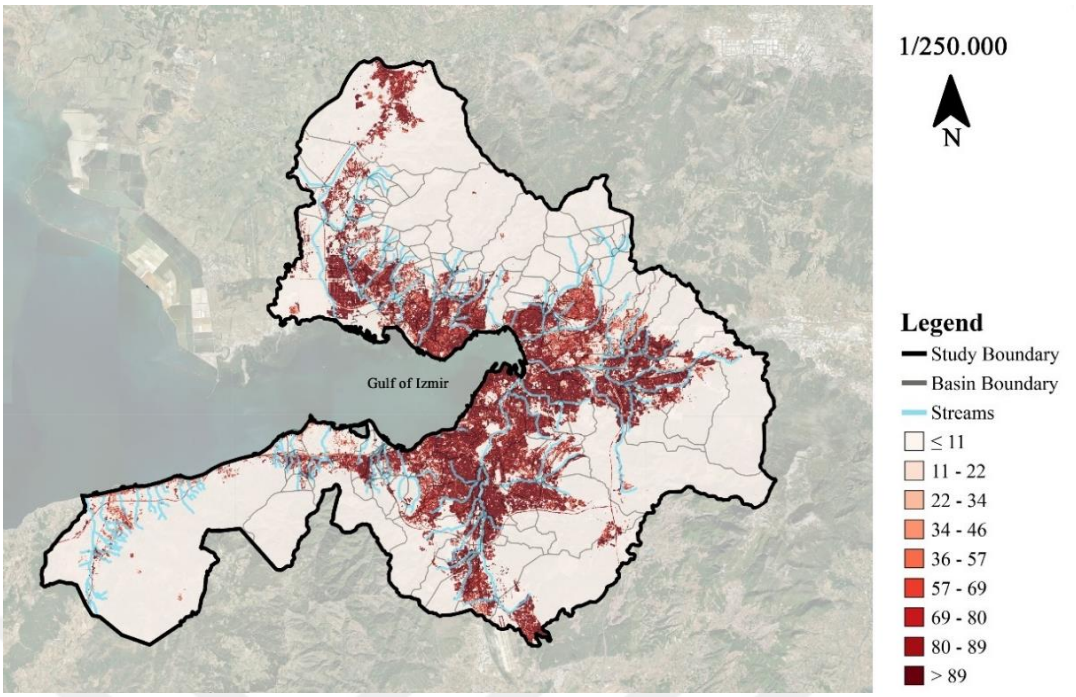

Figure 4.8. Impermeable Surfaces at City Scale

At the urban scale, the least permeable surfaces at the boundary of the study area constitute 10.29% of the area. At this scale, the proportion of impermeable surfaces is 29.11%. Focusing on the city center, the ratio of impermeable surfaces increases.

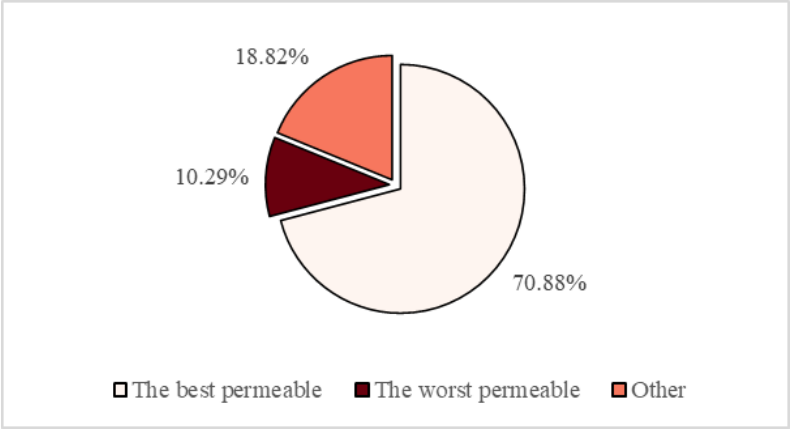

Figure 4.9. Impermeable Surfaces Distribution Graph at City Scale

4.1.5. Meteorological Station Locations

At the urban scale, there are 12 meteorological stations. The data and locations measured by these stations have been thoroughly examined. As a result, it has been determined that the Güzelyalı Meteorology Station measurements are the most detailed in İzmir province. The measurement sensors at Güzelyalı meteorology station are 29 meters above the ground.

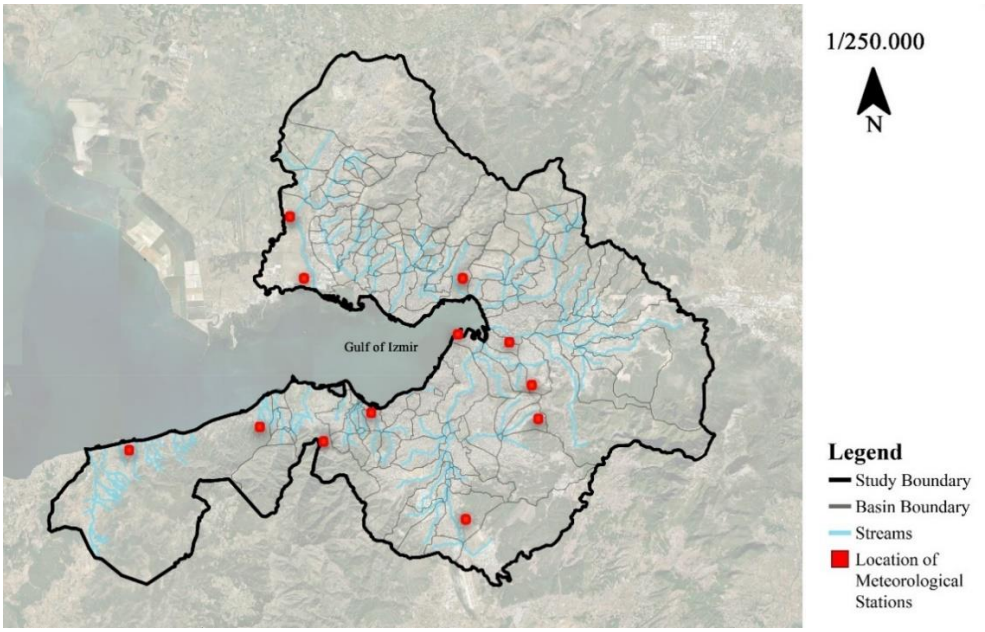

Figure 4.10. Meteorology Station Locations at City Scale

(Source: 2nd Regional Directorate of Meteorology)

4.2. Analyses at the Basin Scale

Secondly, after the city scale, the situation of the Poligon Stream within the basin area in the study area was examined.

4.2.1. Poligon Stream Basin

The Poligon Stream starts west of the Ahmet Adnan Saygun Art Center and flows into the Poligon Valley. It then branches into several arms, one of which flows towards Limontepe, while the others extend around the valley to reach the Olympic Village. Floods occur in the Poligon stream on days with increased rainfall. Due to the insufficient cross-sectional area of each stream crossing structure, the water level rises upstream.

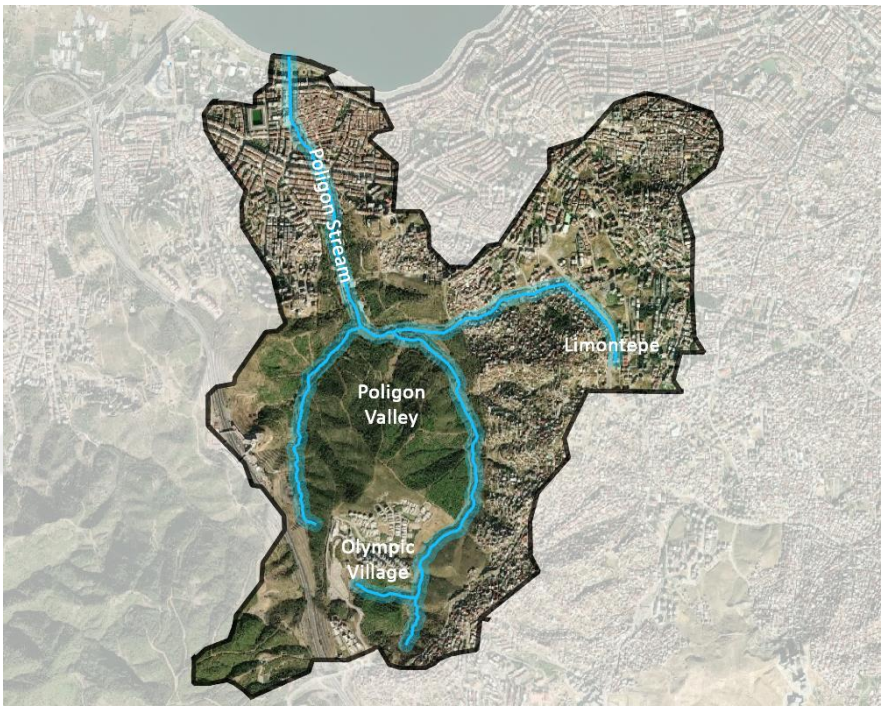

Figure 4.11. Poligon Stream Basin

(Source: Google Earth Pro)

4.2.2. Headwaters and Stream Branches

When examining the headwaters of the Poligon Stream's branches, the Olympic Village, located in the stream's headwaters, stands out. Urban development in this area directly affects the Poligon Stream. Another branch of the stream reaches the Limontepe

area, and due to the concentration of urban development in this area, water drainage into the stream's headwaters becomes challenging, thereby increasing the risk of flooding in the stream.

Figure 4.12. Poligon Stream Basin 3D View

(Source: Google Earth Pro)

4.3. Neighborhood Scale Analyzes

The third section we will examine is at the neighborhood scale. At the neighborhood scale, a portion of the Güzelyalı neighborhood to the west of the Poligon Stream and a portion of the Mehmet Ali Akman neighborhood to the east are studied.

4.3.1. Seismicity and Fault Line

The Güzelyalı neighborhood is in a high-risk earthquake zone. A live fault line runs through the study area, known as the Halosen fault. This fault is characterized by producing earthquakes resulting from surface ruptures. Additionally, when examining the

soil structure in the study area, it is found to be alluvial soil, which increases the risk of liquefaction of the ground.

Figure 4.13. Active Fault Line within the Study Area

(Source: URL 14 accessed date November 5, 2023)

4.3.2. Solid Void

The solid-void analysis is utilized as a significant tool for evaluating the space. Through this analysis, the building density condition in the field can be determined.When analyzing the solid void analysis, it is observed that in the Güzelyalı neighborhood, building footprint areas cover a significant portion of the parcels, with many places utilizing the entire parcel as a building footprint area. The Mehmet Ali Akman neighborhood has predominantly gardens and detached homes.

Figure 4.14. Solid and Void Analysis at Neighborhood Scale

Within the neighborhood-scale study area boundary, buildings comprise 39% of the study area. The Göztepe Gürsel Aksel Stadium and the Ahmet Adnan Saygun Art Center form large solid masses. Additionally, the buildings facing towards the north and the seaside are in a continuous layout and are multi-story, resulting in long blocks.

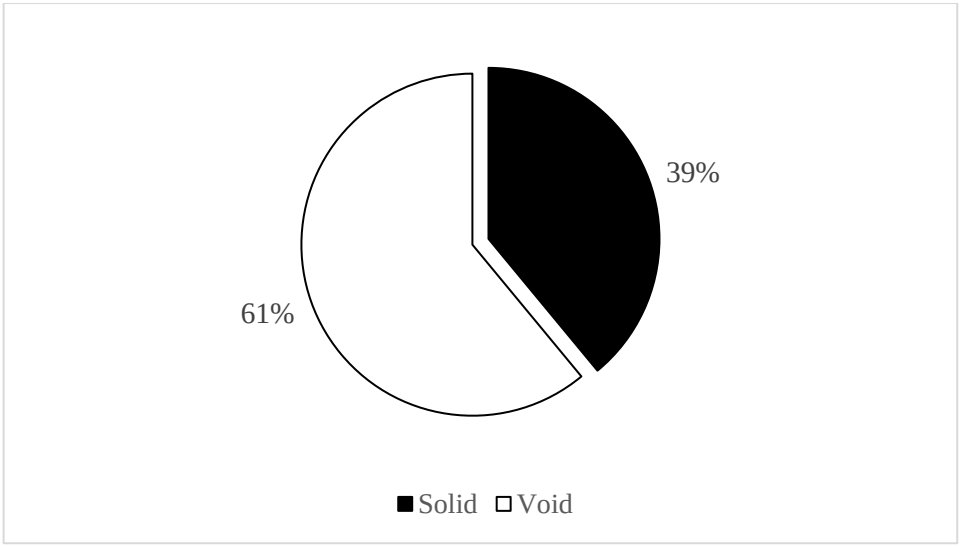

Figure 4.15. Solid and Void Distribution at Neighborhood Scale

4.3.3. Number of Floors

When examining the analysis of the number of floors, it is observed that the buildings within the study area have between 1 and 12 floors. The buildings on the periphery of the study area have seven floors and above, while most of the buildings in the inner areas are five stories tall.

Figure 4.16. Analysis of Floor Numbers at Neighborhood Scale

(Source: Izmir Metropolitan Municipality)

The analysis of floor numbers is crucial for understanding the structure of the study area. Additionally, building heights are a significant factor that influences wind speed and direction.The area covered by the buildings in the study area was calculated based on the number of floors. According to this calculation, most of the area is covered by 5-story buildings, accounting for 40%. The higher area coverage by 9-story buildings is due to the extensive layout of the Göztepe Gürsel Aksel Stadium.

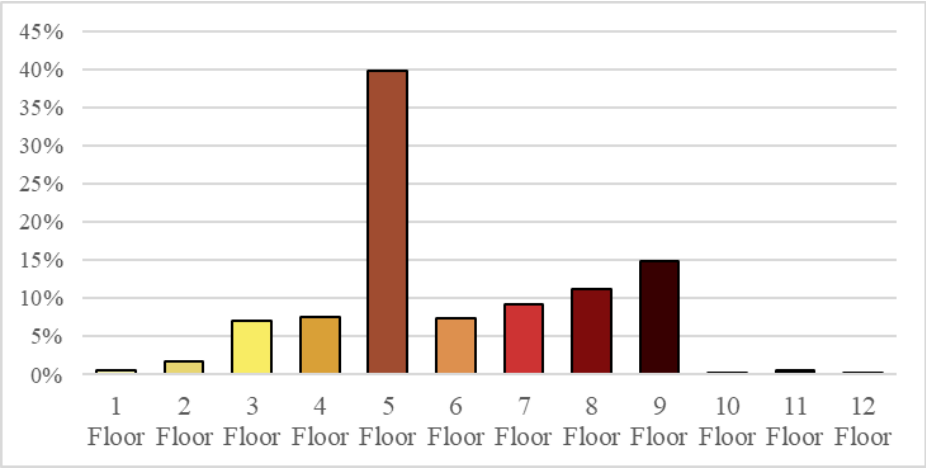

Figure 4.17. Distribution by Number of Building Floors at Neighborhood Scale

4.3.4. Green Areas

When examining the green area analysis, Ali Rıza Akıncı Park and Mehmet Ali Akman Park are in the easternmost part of the study area. There is also the 1st Çiçek Park south of the Gürsel Aksel Stadium. In the westernmost part of the study area, Güzelyalı Park is situated, and looking at the seaside area, Tarık Zafer Tunaya Park contributes to the green areas.

Figure 4.18. Green Spaces at Neighborhood Scale

Green areas in the study area make up 11.8% of the total area. It is observed that the green areas in Güzelyalı neighborhood in the western part of the area are insufficient. These proportions are depicted in Figure 4.19

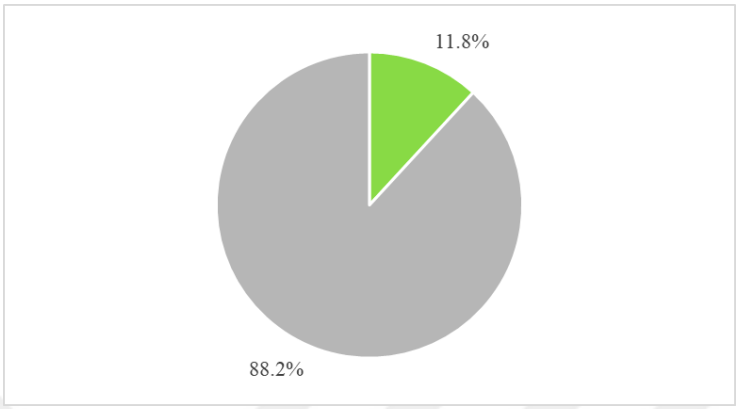

Figure 4.19. Distribution of Green Areas at Neighborhood Scale

A significant portion of the green areas in the area comprises the seaside section, with the seaside green areas accounting for 54% of all green areas. When looking at the entire study area, seaside green areas make up 6.3% of the total area. Parks constitute 3.8% of the green areas in the study area, with parks accounting for 32% of all green areas. The stadium covers 14% of the green areas, and the overall proportion of green areas in the study area is 1.7%.

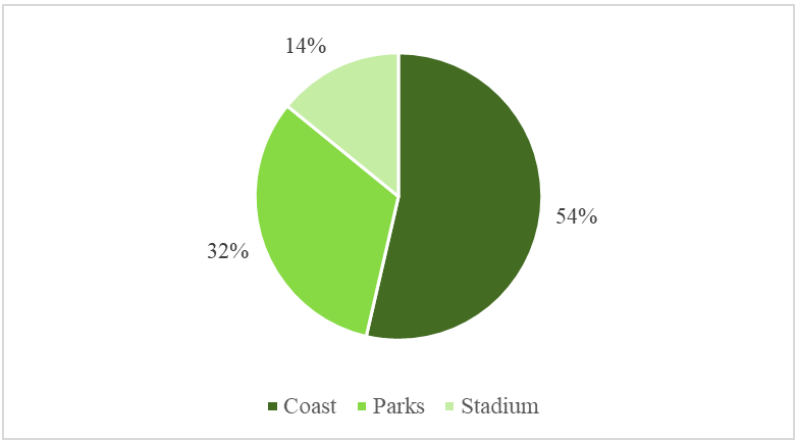

Figure 4.20. Distribution within Green Areas

4.3.5. Impermeable Surface

When we examine the impermeable surfaces in detail, it is seen that there are quite a lot of impervious surfaces in the Güzelyalı neighborhood in the west of the study area. The number of impermeable surfaces in this area is increasing due to reasons such as asphalt streets, concrete buildings that sit almost exactly on the parcel, and insufficient green areas.

Figure 4.21. Impermeable Surfaces at Neighborhood Scale

The highest proportion of impervious surface area in the study area is 55.91%. The permeable surface ratio in the study area is 13.57%. The proportional distribution of impermeability in the study area is shown in Figure 4.22

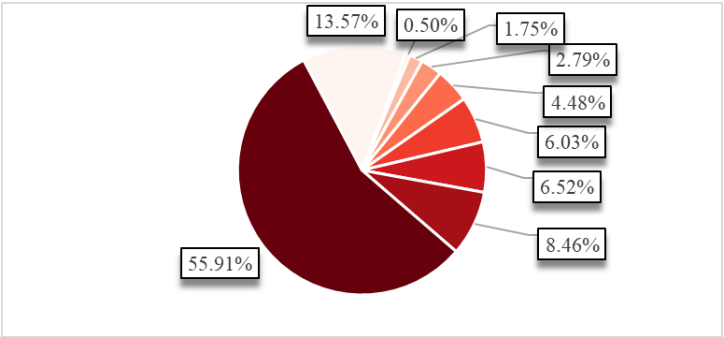

Figure 4.22. Distribution of Impervious Surfaces at Neighborhood Scale

4.3.6. Wind and Sunpath

According to İzmir Güzelyalı Meteorological Station data, the prevailing wind direction is South-Southeast, with the secondary prevailing wind direction being West-Northwest, depending on the seasonal conditions. The average wind speed in İzmir is 3.0 m/s.

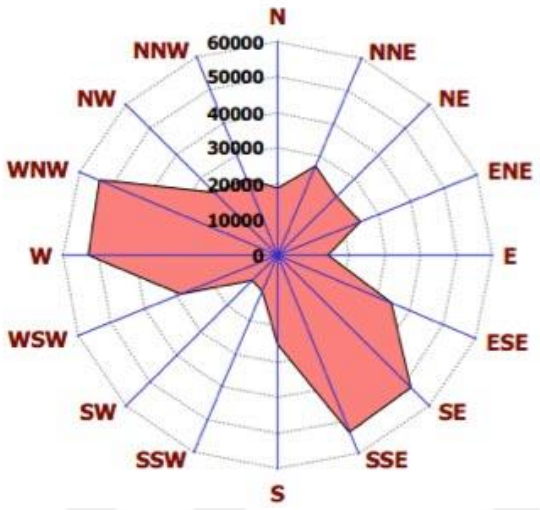

Figure 4.23. Güzelyalı Wind Rose Chart

(Source: Güzelyalı Meteorological Station)

Wind analysis and the prevalling wind direction are crucial in terms of climate-sensitive design principles. Therefore, in this study, both the primary and secondary wind directions have been taken into consideration.

Based on the wind direction in the study area, it is observed that high rise buildings on the periphery obstruct strong winds coming from the northwest and southeast and attach buildings within the area, preventing the entry of wind into the area. Additionally, the Göztepe Gürsel Aksel Stadium significantly blocks the west-northwest winds and hinders their passage to the western part of the study area.

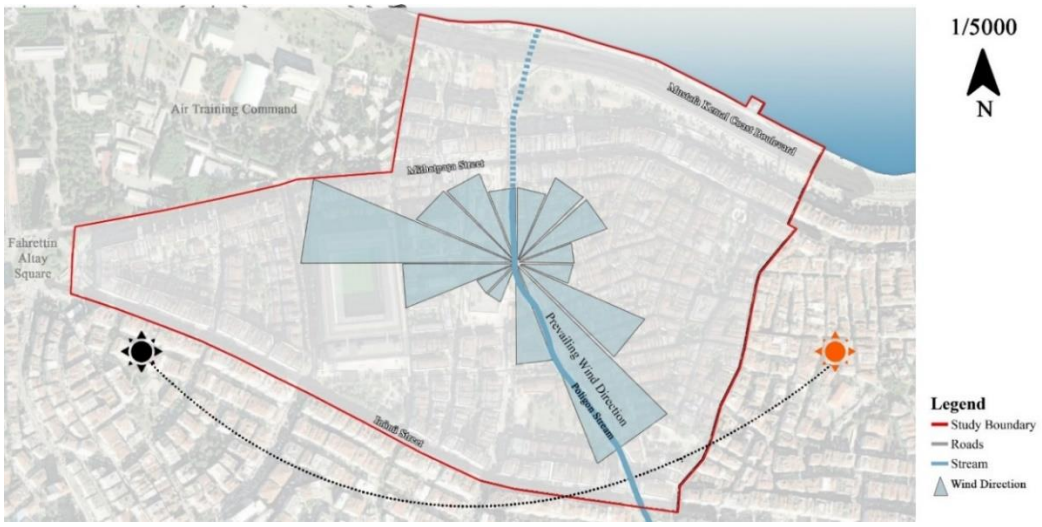

Figure 4.24. Wind Direction and Sunpath at the Neighborhood Scale

(Source: Güzelyalı Meteorological Station)

4.3.7. Land Surface Temperature

Land surface temperature analysis has also been examined at the neighborhood scale. The calculation method for this analysis was explained in detail in section 4.1.1.

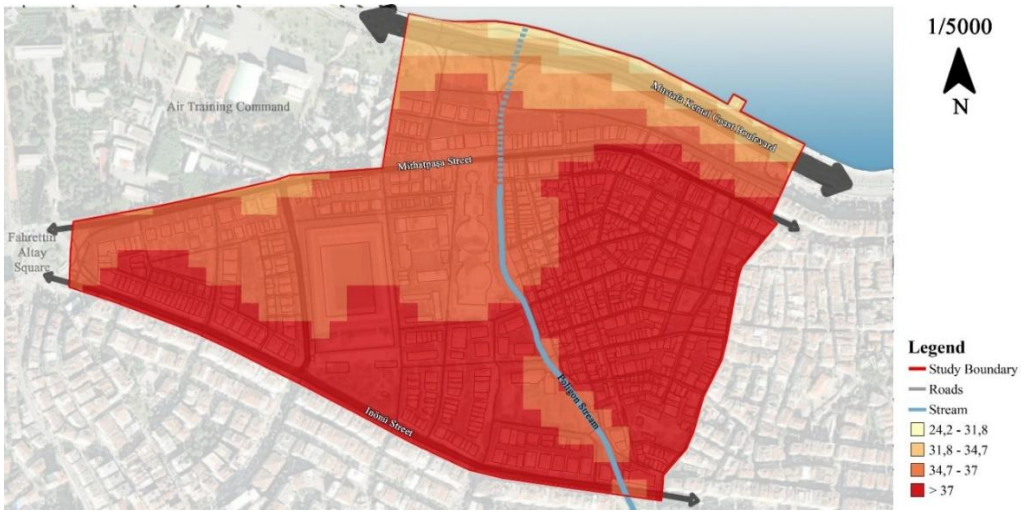

Figure 4.25. Land Surface Temperature at Neighborhood Scale

(Source: Based on Landsat 8 (OLI/TIR) remote sensing satellite data)

In our neighborhood-scale study area, areas with land surface temperatures of 37°C and above make up 49% of the study area. Areas with temperatures between 34.7°C and 37°C constitute 39% of the total area. Based on these values, it can be concluded that the land surface temperature in the study area is relatively high. It is also evident that these temperatures tend to decrease as you move towards the seaside.

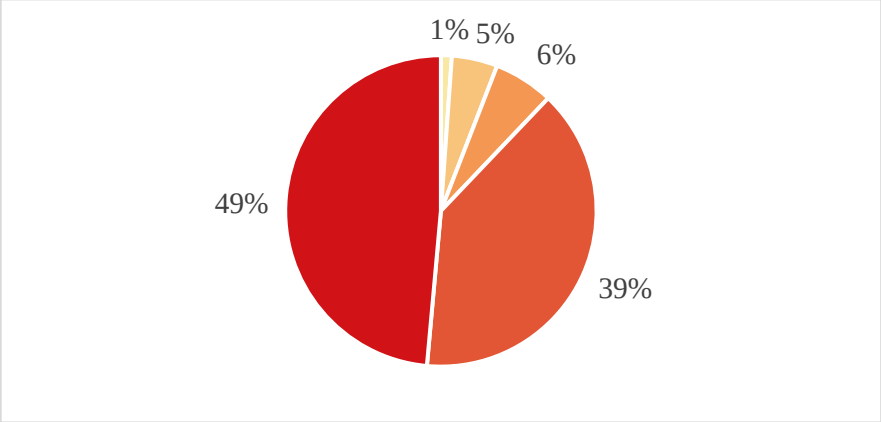

Figure 4.26. Land Surface Temperature Distribution at Neighborhood Scale

4.3.8. Urban Heat Island Effect

Land surface temperature analysis was utilized to measure the urban heat island effect. The following formula was used in ArcGIS 10.8 software to calculate the urban heat island effect: the average land surface temperature was subtracted from the land surface temperature map generated in the study area and then divided by the standard deviation. As a result, urban heat island values in the study area were calculated, ranging from a maximum of 32.45 to a minimum of 21.02 (Abutaleb et al. 2015).

$$UHI = \frac{LST - LST_{mean}}{STD} \quad (7)$$

Figure 4.27. Urban Heat Island Effect at Neighborhood Scale

(Source: Based on Landsat 8 (OLI/TIR) remote sensing satellite data)

To define the significance of the calculated urban heat island effect values, the Urban Thermal Fraction-Vegetation Index (UTFVI) was employed (Liu and Zhang 2011). After subtracting the average land surface temperature from the land surface temperature map, these values were divided by the values calculated in the land surface temperature map. This formula was used to calculate the UTFVI index values.

$$UTFVI = \frac{LST - LST_{mean}}{LST} \quad (8)$$

In their study, Zhang et al. (2006) defined six levels to evaluate this index. The calculation results indicate that the areas where the urban heat island effect is strongest are in the settlements south and west of the Poligon Stream.

Table 4.1. UTFVI Ecological Evaluation Index

(Source: Zhang et al. 2006)

UTFVI range	Urban Thermal Field Variance index (UTFVI)
0 <	None
0.000-0.005	Weak
0.005-0.010	Middle
0.010-0.015	Strong
0.015-0.020	Stronger
> 0.02	Strongest

Since the index values in the coastal area are negative, the urban heat island effect cannot be defined in this area. In the northeastern part of the stream, the urban heat island effect can be described as middle to strong.

Figure 4.28. UTFVI of Urban Heat Island Effect at Neighborhood Scale

4.3.9. Morphological Analysis

The morphological analysis selected six different zones from the study area. The building conditions in these zones are essential for understanding the morphology of the study area, as shown in detail below. The western part of the study area features continuous urbanization, while the eastern part has dispersed and block-type structures. The longest building block measures 127.5 meters. In the western part of the study area, buildings almost entirely cover their parcels. In the western part, residential areas with gardens can be observed.

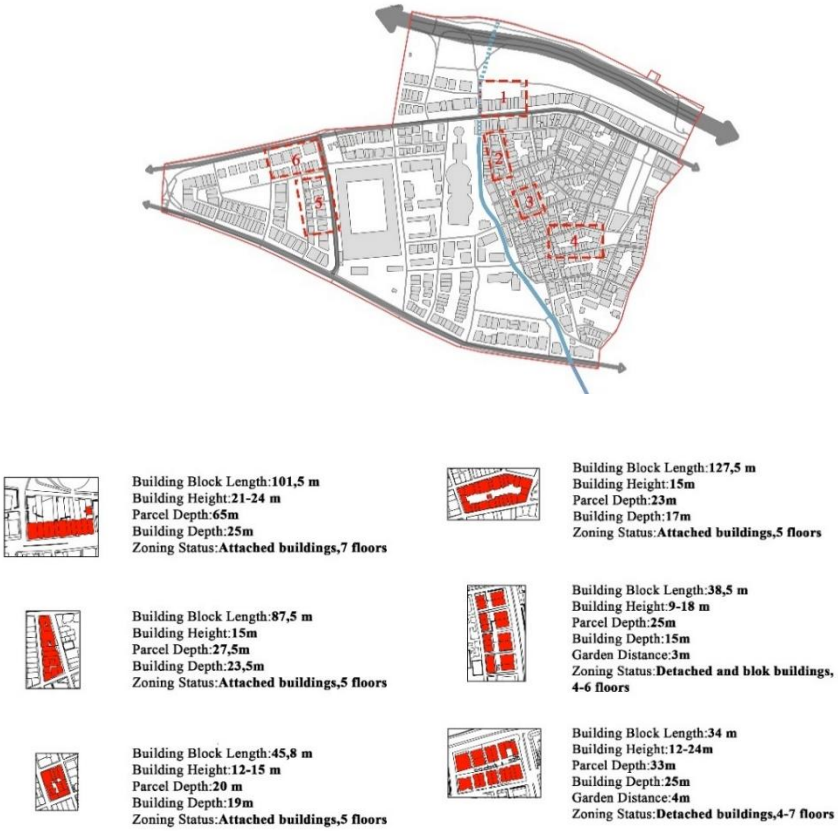

Figure 4.29. Morphological Analysis at Neighborhood Scale

4.3.10. Evaluation of Neighborhood Scale Analyzes

Figure 4.30. Evaluation of Neighborhood Scale Analyzes

P1: Constitutes the coastal area. Green areas and landscape design along the coast increase permeable surface area. It has the area's lowest land surface temperature and urban heat island temperature. The urban heat island effect cannot be defined in this area.

P2: Ahmet Adnan Saygun Art Center has significant potential due to its public nature. Poligon Stream is located west of this area.

P3: Poligon Stream presents the potential for intervention in the study area. However, because the stream has been a concrete channel, flood risk, bad smell, and pollution are significant problems.

P4: Güzelyalı Secondary School is a public space. The amount of permeable surface is quite dense in the parts of this region near the stream. The land surface temperature in this region is relatively lower than its surroundings.

P5: Two large green areas are in this region. The morphological structure of this area is quite suitable for the circulation of wind through the streets. Land surface temperature and urban heat island effect are calculated to be relatively lower in this area compared to the western part of the area.

N1: Building blocks in this area block the wind from the secondary prevailing wind direction, northwest, and create a barrier effect. The presence of seven floors and above buildings in this area also directly affects the inner parts.

N2: This area has the highest proportion of impervious surfaces. It is the region where the land surface temperature reaches its highest level, and the urban heat island effect is felt most strongly.

N3: There is a moderate urban heat island effect in this area. University buildings are in this area. In addition to high-rise buildings, there are also permeable surfaces.

N4: Göztepe Gürsel Aksel Stadium has a very large mass. This area acts as a barrier by blocking the wind. Additionally, due to its considerable height, it is a structure disconnected from the human scale and cannot integrate with its surroundings.

N5: The tall buildings in the southern part of this area do not allow the southeast wind to enter the area and obstruct it. Although the land surface temperature is 37°C and above in this area, a strong urban heat island effect has been calculated.

4.4. Street-Scale Analyses

A boundary has been established at the street scale, encompassing the islands east and west of the Poligon Stream. In determining this boundary, it has been designed at the street scale to include public areas to the east of the stream and residential areas to the west, intending not entirely to cover residential areas. Analyses conducted within the scope of this boundary include assessments of the current situation, surface characteristics (albedo effect), thermal comfort analysis, wind analysis, and urban heat island effect.

Figure 4.31. Determination of Area Boundaries at Street Scale

4.4.2. Existing Condition

The current conditions at the street scale were initially examined. Ratios of residential areas, public spaces, green areas, roads, and parking lots within the workspace were calculated. Understanding the existing conditions is crucial for comparing the potential changes that may occur in the field due to interventions.

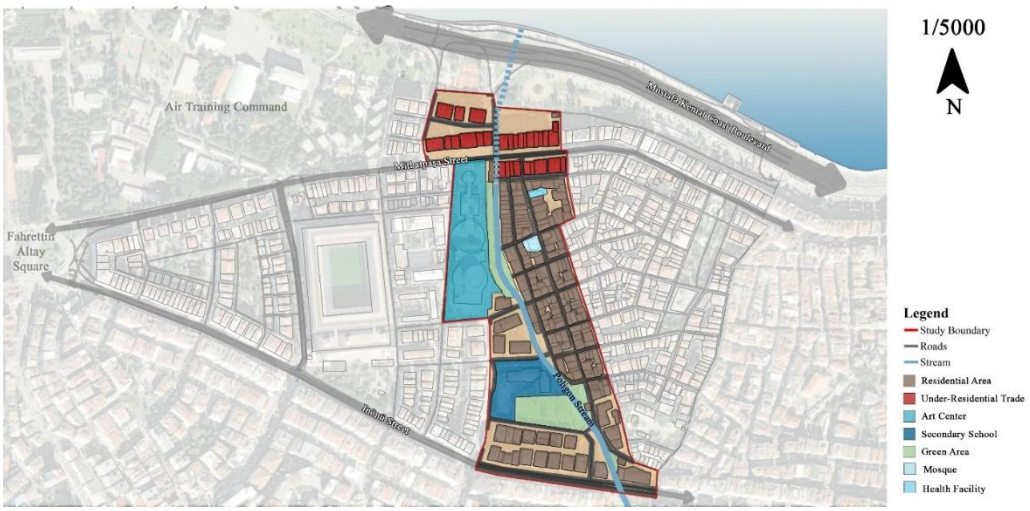

Figure 4.32. Current Situation Analysis at The Street Scale

(Source: Izmir Metropolitan Municipality)

As a result of these calculations, residential areas constitute 42.7%, public spaces 18.2%, and green areas comprise 6.2% of the workspace. The Poligon Stream accounts for 2.9%, while roads, parking lots, and parcel gaps outside buildings collectively comprise 30% of the workspace. The detailed calculations for these areas can be examined in Table 4.2

Table 4.2. Land Use Ratio at the Street Scale

The Current Situation	Area(m2)	Area / Total Area (%)
Residential Area	56451	42.70%
Secondary School	5667	4.20%
Art Center	18005	13.40%
Mosque	450	0.30%
Health Facility	360	0.30%
Stream	3890	2.90%
Green Area	9414	6.20%
Other (Roads, parking lots and gardens)	40463	30.00%

The analysis of the physical variables directly influencing the urban heat island effect has also been conducted in detail. Ratios of green areas developed spaces, and impermeable surfaces have been calculated.

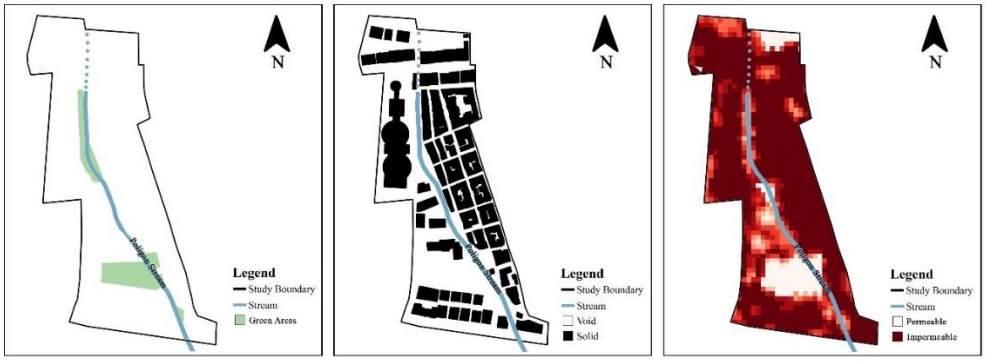

Figure 4.33. Analyses of the Built Environment at the Street Scale

The built environment constitutes 60.1% of the study area. The ratio of impermeable surfaces has been calculated as 91.7%. Green surfaces within the workspace cover an area of 6.20%.

Table 4.3. Proportional Distribution of Physical Parameters at the Street Scale

	Area(m2)	Area / Total Area (%)
Built up Area	80928	60.10%
Impermeability Rate	123519	91.7%
Green Space	9414	6.20%

4.4.3. Surface Characteristics (Albedo Effect)

Albedo is the reflectivity power of a surface, indicating how much electromagnetic energy can be reflected upon an object. Albedo values can vary depending on an object's color, texture, and area. Light-colored surfaces have a high albedo value compared to dark-colored surfaces. The closer a surface's albedo value is to

1, the higher its capacity to reflect light. As the albedo value approaches 0, the surface absorbs light without reflecting.

The albedo value is 1 for a perfectly reflective surface and 0 for an entirely dark surface. There is a direct relationship between the albedo effect and climate. Low albedo values on Earth's surfaces lead to more absorption of solar radiation. This situation implies an increasing trend in temperatures on Earth. (URL 15 2023).

Figure 4.34. Surface Characteristics at the Street Scale (Albedo Effect)

Surface materials in the study area have been categorized into four groups. Asphalt surfaces have the lowest albedo value, absorbing light without reflecting it. Secondly, buildings with tiled roofs were identified using Google Earth software. Buildings with concrete roofs were distinguished from those with tiled roofs. Concrete surfaces have a higher albedo value due to their light color. Green surfaces in the study area have the highest albedo value. The reflectance rate of these surfaces is the highest.

Table 4.4. Albedo Values of Surface Materials at the Street Scale
(Source: URL 16 2023)

Surface Materials	Albedo Value
Asphalt	0,05
Tile	0,10
Concrete	0,20
Green Surface	0,30

4.4.4. Thermal Comfort Analysis

UMEP (Urban Multi-scale Environmental Predictor) provides a city-based climate service by combining the tools and models necessary for climate simulations. UMEP encompasses various outdoor comfort, wind, and climate change mitigation models. The SOLWEIG model within the UMEP tools in the QGIS software was employed during thermal comfort analysis. The model utilizes meteorological data such as radiation, air temperature, and humidity. Additionally, urban geometry and geographic information are also incorporated. The schematic flow of the model is illustrated in Figure 4.35 below (URL 17 2023).

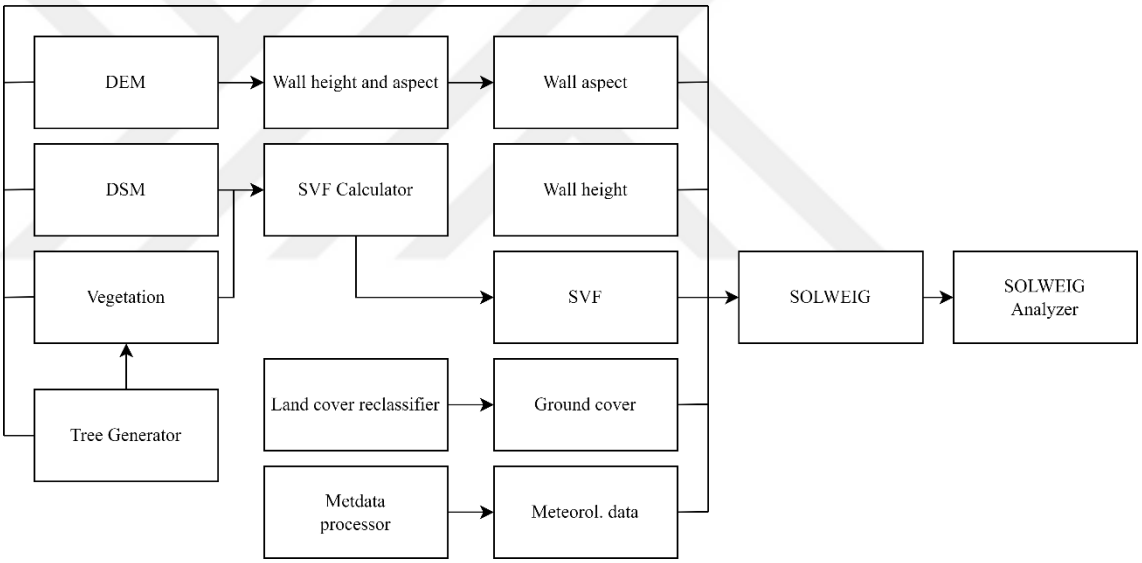

Figure 4.35. Stages of Thermal Comfort Analysis

(Source: URL 17 2023)

After downloading the UMEP tool in the QGIS software, the outdoor thermal comfort model has been selected from the processor section. Wall height and aspect are calculated based on the DEM data used in the model, while SVF data is calculated from DSM and vegetation data. It has been used in the model after converting meteorological data to the SOLWEIG format. The meteorological data includes hourly data for July in the year 2022.

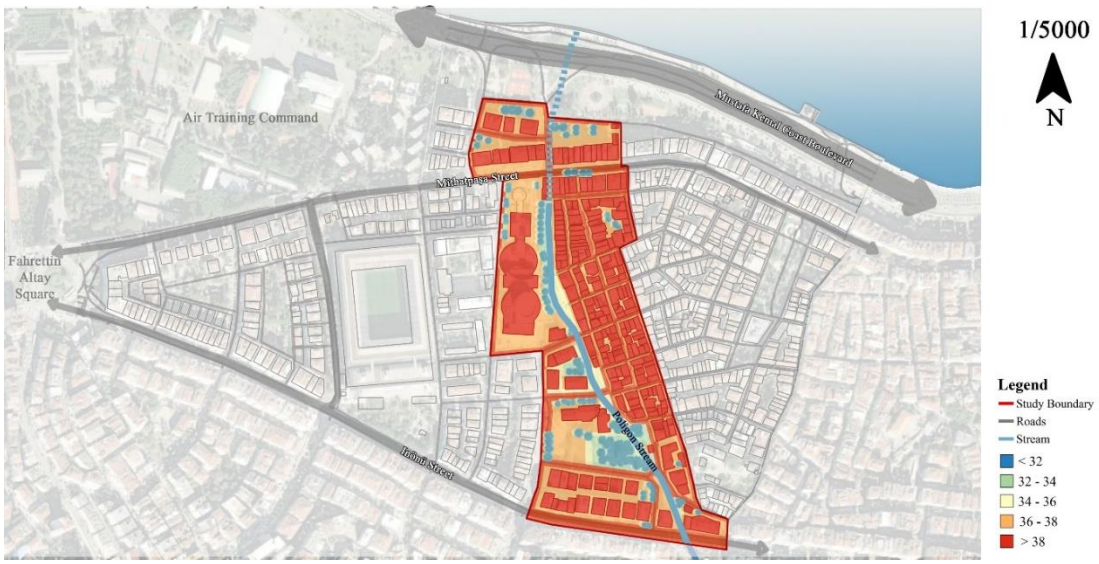

Figure 4.36. Thermal Comfort Analysis at the Street Scale

(Source: URL 18 2023 and URL 19 2023)

The DEM data used in the model was downloaded from ALOS PALSAR high-resolution satellite data. The DSM data was obtained from the ALOS World 3D dataset via Open Topography. According to the model results, the thermal comfort temperature of the buildings in the study area was calculated to be above 38 °C. The temperature in the streets and parcel gaps where the buildings are located varies between 36-38 °C. According to the PET index, these areas are under severe heat stress. Around the Poligon Stream, the thermal comfort temperature was calculated to be below 36 °C. In these areas, a moderate level of heat stress is observed according to the PET index.

4.4.5. Wind Analysis

Wind analysis holds a significant place in bioclimatic design. Wind direction and speed serve as a foundation for the design of the study area. The wind analysis at the street scale was executed in the simulation program through 7 steps, summarized below.

Step 1: A three-dimensional modeling process was completed using the SolidWorks program from a two-dimensional DXF file, with building heights set at 3m.

To expedite the analysis, complex building shapes in DXF were flattened, ensuring a more accurate mesh process in the subsequent step.

Step 2: The model to be analyzed was enclosed within a volume to determine wind input and output boundaries for wind analysis.

Step 3: The fully modeled three-dimensional design was saved. STEP format and transferred to the ANSYS Workbench environment.

Step 4: A CFD analysis was set up in the ANSYS Workbench environment.

Step 5: Since the finite element method was used for the analysis, the meshing process was conducted to break down all buildings into individual components.

Step 6: The wind direction was set to southeast, and the wind speed was set to 3.20 m/s.

Step 7: Wind input and output directions were defined, and the analysis was executed in the analysis environment.

Figure 4.37. Wind Analysis at the Street Scale

The analysis reveals that the wind from the southeast direction enters the study area at an average speed of 3.50 m/s. As one progresses northward, the wind speed gradually decreases within the built environment, falling below 1.75 m/s and diminishing to almost negligible levels. The wind diminishes further towards the inner areas and the circulation and impact of the wind decreases due to the tall buildings to the north. The three-dimensional visualization of the wind simulation in the study area is depicted in Figure 4.38.

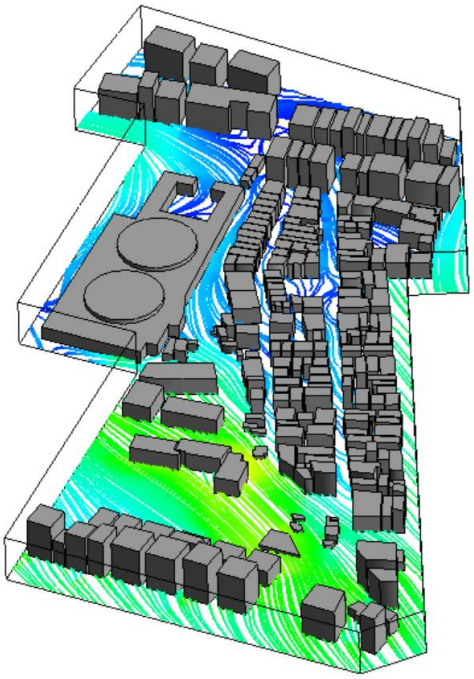

Figure 4.38. 3D Wind Simulation at the Street Scale

The (a) shape shown below indicates the wind input direction in the wind analysis, while the (b) shape illustrates the wind's output from the study area.

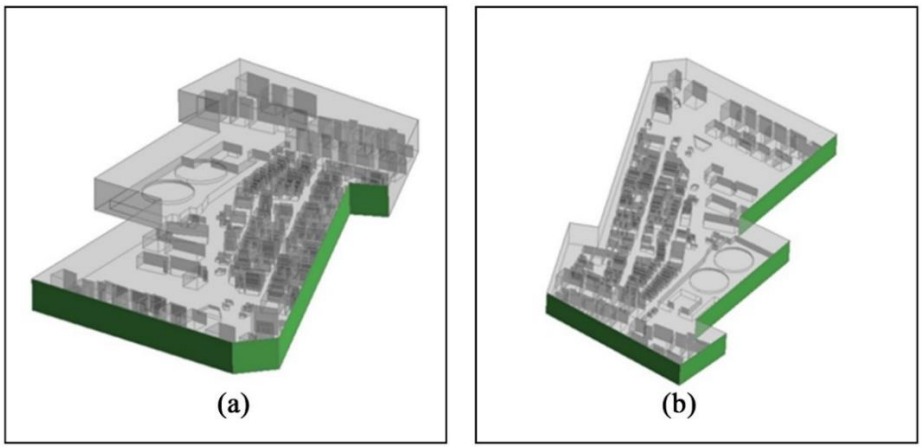

Figure 4.39. Wind Simulation Input-Output Directions

There are certain limitations within the scope of this study to run the simulation program. Walls have been defined around the study area boundary in the wind simulation conducted within the study area, as seen in Figure 4.40. These walls isolate the study area from its surroundings. Due to the insufficient technical equipment to include an area larger than this size in the simulation, running the software is only possible within a workspace of this magnitude. Therefore, the analysis only shows the wind distribution within its confines. Nevertheless, it is evident how the construction conditions in this study area affect the wind's impact and velocity reduction.

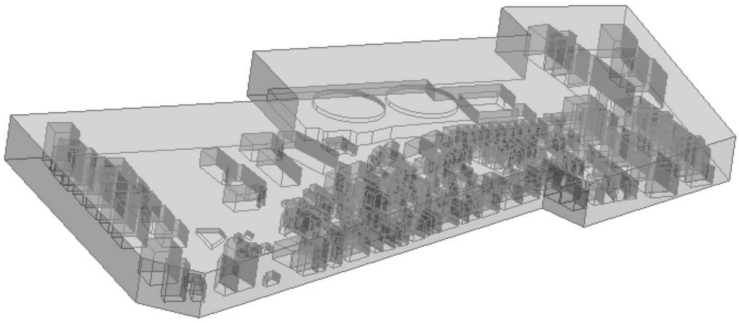

Figure 4.40. The Defined Walls Within the Study Area

4.4.6. Calculation of the Urban Heat Island Effect

An equation developed by Theeuwes et al. for calculating the maximum urban heat island effect obtained in Northwest Europe has been utilized to calculate the urban heat island effect at the street scale. This equation is employed by both Theeuwes et al. (2017) and Yang et al. (2019). The critical dimension analysis theorem derives the urban heat island equation using physically meaningful variables. The semi-empirical equation expressing UHImax about SVF is shown below (Koopmans et al. 2019).

$$UHI_{max} = M \,.\, (2 - Svf - Veg_f) \tag{9}$$

The variable M in this equation contains meteorological data. The part in parentheses of the equation consists of physical parameters. The formula used to calculate the M value is as follows:

$$M = \sqrt[4]{\frac{DTR^3.S}{U}} \tag{10}$$

In this formula, DTR is calculated as Tmax-Tmin. The S value represents the daily average radiation ratio, and the U value represents the hourly average wind speed. These values were calculated using temperature, wind, and radiation data from the Güzelyalı Meteorological Station on July 24, 2022.

The Sky View Factor (SVF) calculated during the thermal comfort analysis in Section 4.4.3 was initially used to calculate the physical variables. The SVF value calculated in this model was then utilized to measure the urban heat island effect at the street scale in this study section. In this context, the Sky View Factor extension in the SOLWEIG model was created using DSM data. Oke (1981) defines the Sky View Factor (SVF) as the ratio of the visible sky unobstructed by buildings and trees in viewable terrain. This parameter is crucial for climatic applications and takes values between 0 and 1. The closer the SVF value is to 1, the lower the radiation emitted from surfaces to the sky. The methodology used to calculate SVF in the model was developed by Lindberg and Grimmond (2010) (URL 20 2023).

As a result of the calculation, the SVF values in the study area are shown in Figure 4.41. Most of the study area has an average SVF value of 0.20. The proximity of this value to 0 plays an increasing role in enhancing the urban heat island effect.

Figure 4.41. Sky View Factor (SVF) Values at the Street Scale

The second important factor is vegetation data, which is the average vegetation coverage ratio calculated from satellite imagery to calculate the urban heat island value. Values in vegetation data also range between 0 and 1. As the values approach 1, the vegetation coverage ratio is high. As seen in Figure 4.42, the vegetation ratio in the study area has an average value of 0.07.

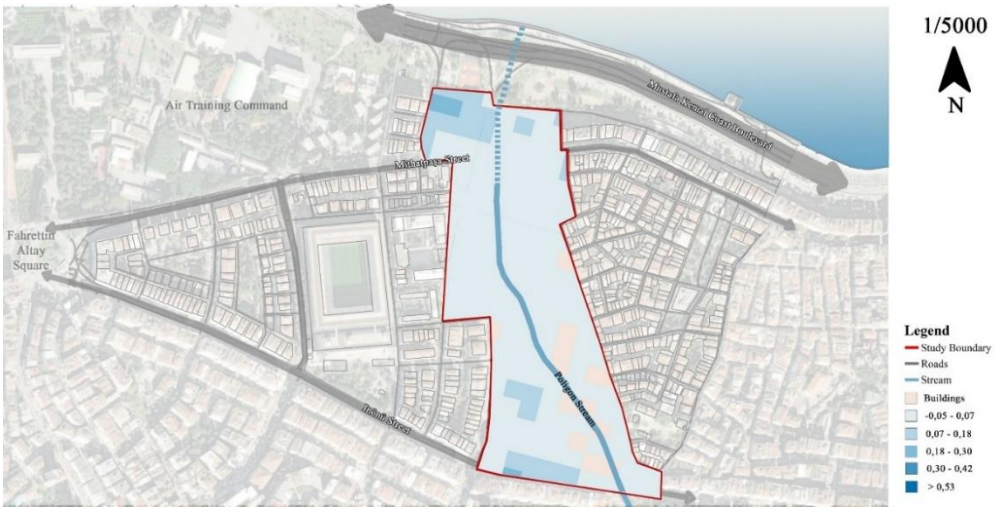

Figure 4.42. Vegetation Values at the Street Scale

The urban heat island effect equation consists of two main variables: the factor and temperature effects. The factor comprises SVF and vegetation values, ranging between 0 and 1. When both are close to 0, the factor value approaches 2. As the factor value approaches 2, the urban heat island effect will be high. As a result of the calculation, the factor value is 1.73. Since this value is close to 2, it can be clearly stated that the study area has a high urban heat island effect. While the temperature effect is calculated as 0.8, the UHImax value is calculated as 1.39. These values are shown in Table 4.5.

Table 4.5. Urban Heat Island Effect Variables at the Street Scale

Variables	**Values**
Factor	1.73
T *effect*	0.8
UHI *max*	1.39

4.5. Meteorological Data

All the data used in the study was obtained from the Güzelyalı Meteorological Station with number 17220 through the MEVBIS system. The sensors at this station measure a height of 29 meters. Initially, long-term monthly temperature, wind, and humidity data were examined. These data cover measurements made after the year 2000. The monthly averages of these data, covering 22 years, are shown in Table 4.6.

Table 4.6. Monthly Average Values of Meteorological Data
(Source: Güzelyalı Meteorological Station (MEVBIS)

Meteorological Elements	Maximum Temperature (°C)	Minimum Temperature (°C)	Average Temperature (°C)	Average Wind (m/sec)	Average Humidity (%)
January	18.52	-0.24	9.09	2.87	70.32
February	19.60	-0.26	9.21	3.16	67.56
March	23.20	1.56	11.62	2.93	65.39
April	28.40	5.88	16.07	2.90	62.71
May	32.57	10.50	20.98	2.95	59.85
June	36.45	15.91	25.99	3.17	52.58
July	38.74	19.63	28.49	3.32	50.78
August	38.39	19.52	28.03	3.13	53.64
September	35.20	14.89	23.85	2.81	57.61
October	30.53	9.12	19.00	2.63	63.40
November	24.83	3.88	13.73	2.71	68.60
December	19.87	0.94	10.27	2.91	71.78
Annual average	28.86	8.44	18.03	2.96	62.02

When examining the maximum and minimum temperature values every month, it can be stated that July has the highest average temperatures compared to other months. The summer month, where the highest temperature values were recorded, is July, with a maximum temperature of 38.74 °C. In July, the average humidity is 50.78%, and the average wind speed is measured at 3.32 m/s. Based on these data, the period for the study has been chosen as July.

Secondly, the meteorological data examined and used in the scope of the study includes hourly meteorological data measured in July 2022. The hourly data is divided into four 6-hour periods of the day. The night period covers the hours from 00:00 to 05:00, the morning period covers 06:00 to 11:00, the afternoon period covers 12:00 to 17:00, and the evening period covers 18:00 to 23:00.

When examining the average air temperature data for July, it is observed that the highest average temperature occurs during the afternoon hours at 32.8 °C. On the other hand, the lowest average air temperature is measured during the night period at 25.1 °C.

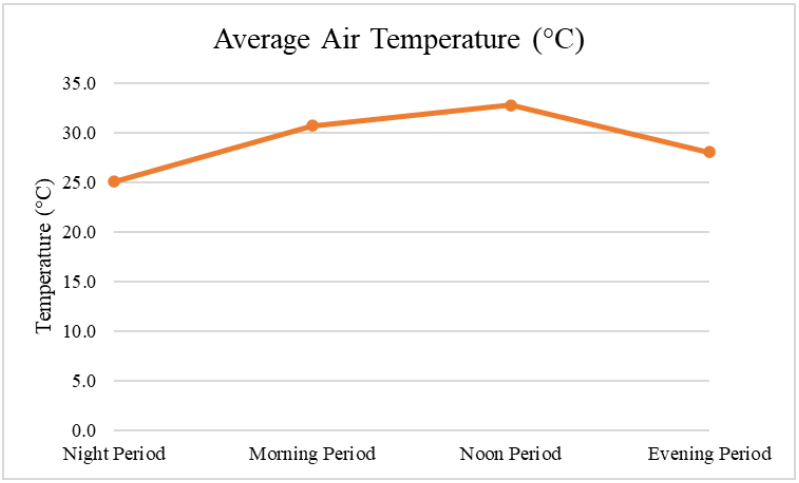

Figure 4.43. Hourly Average Air Temperature for the Month of July

(Source: Güzelyalı Meteorological Station (MEVBIS)

The average relative humidity in July was measured at the highest value of 50.6% during the night period and the period with the lowest relative humidity, which is the afternoon hours, recorded a value of 35.5%.

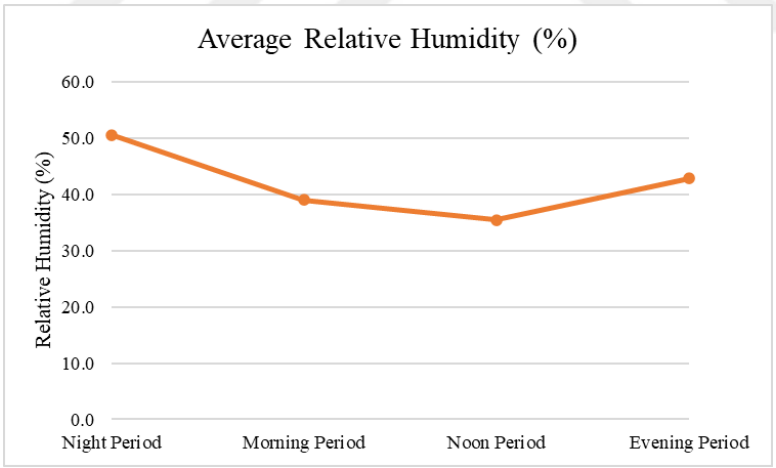

Figure 4.44. Hourly Average Relative Humidity for the Month of July

(Source: Güzelyalı Meteorological Station (MEVBIS)

The average wind speed in July was measured at its highest, 4.7 m/s, during the afternoon hours. On the other hand, the lowest average wind speed was measured at 2.5 m/s during the evening period.

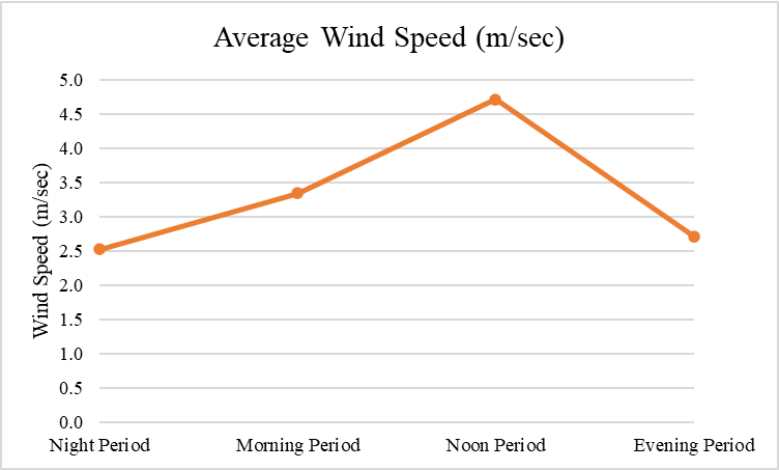

Figure 4.45. Average Wind Speed for the Month of July

(Source: Güzelyalı Meteorological Station (MEVBIS)

When examining the average global radiation measurements for July, the highest value was recorded in the morning at 853.9 watts/m². On the other hand, the lowest average global radiation value was measured during the night period at 18.2 watts/m². These measurements and evaluations were conducted between 2:00 AM and 6:00 PM.

.

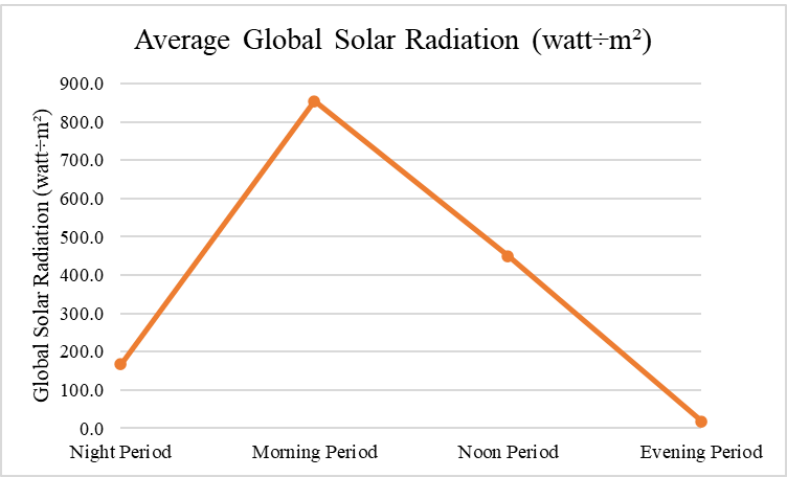

Figure 4.46. Hourly Average Global Radiation Values for the Month of July

(Source: Güzelyalı Meteorological Station (MEVBIS)

The temperature, wind speed, relative humidity, and global radiation values, segmented into four hourly periods, are presented in Table 4.7.

Table 4.7. Meteorological Data for the Month of July

(Source: Güzelyalı Meteorological Station (MEVBIS)

Period	Night Period (00:00-05:00)	Morning Period (06:00-11:00)	Noon Period (12:00-17:00)	Evening Period (18:00-23:00)
Temperature (°C)	25.1	30.7	32.8	28.1
Wind Speed (m/sec)	2.5	3.3	4.7	2.7
Relative Humidity (%)	50.6	39.0	35.5	42.8
Global Solar Radiation (watt÷m²)	166.9	853.9	449.9	18.2

4.6. Proposed Climate Sensitive Urban Design Plan

The proposed climate-sensitive design plan was developed based on regeneration of the area. Proposed design has been developed within this study without taking property ownership into consideration. The design principles obtained through the literature review have been applied in this proposed design. Climate-sensitive design principles have been adapted to the study area. Additionally, solution proposals to mitigate the urban heat island effect, obtained through content analysis, have also been incorporated. To mitigate the urban heat island effect, an urban design plan using climate-sensitive urban design principles has been developed. Design according to the wind forms the basis of this study. Additionally, increasing permeable surfaces and vegetation, and establishing connections between green spaces are crucial in terms of this design.Nature-based solutions have been integrated into the plan. A main pedestrian axis parallel to the stream and a climate research center is proposed in the study area. The detailed plan is depicted in Figure 4.47.

.

Figure 4.47. Proposed Climate-Sensitive Urban Design Plan

Firstly, the foundation of this plan is determined by the wind direction. There are two primary wind directions in the study area. The primary wind direction blows from the southeast. The vertical roads have been designed considering the wind from this direction. The horizontally planned roads are drawn according to the secondary wind from the northwest. The formation of the road network is entirely planned based on wind directions to accommodate the existing road layout. Enhancing the circulation of wind within the study area and ensuring its uninterrupted flow constitutes the primary

objectives of this plan. The draft of the road network formation is illustrated in Figure 4.48.

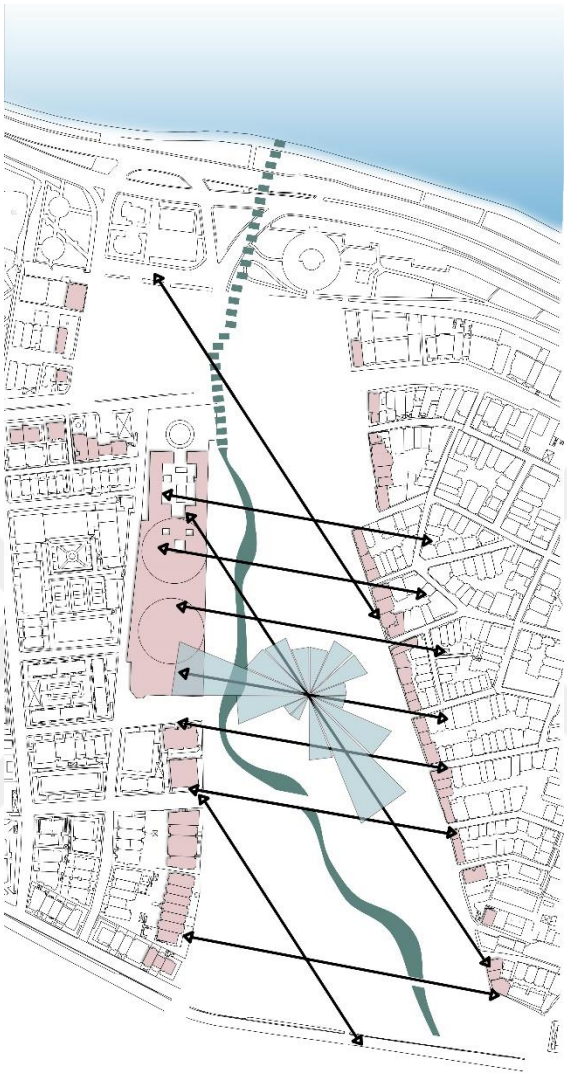

Figure 4.48. Formation of the Road Network According to the Wind Direction

Secondly, the aim is to increase green spaces. In this context, green areas are planned to be integrated with the stream. The Poligon Stream is a stream with a flood risk. Therefore, it is crucial to naturalize this stream and to increase permeable surfaces and vegetation in its surroundings. Moreover, water elements, green spaces, and trees are essential tools for reducing the urban heat island effect. Connecting green areas is intended to facilitate the transfer of rainwater to the stream. This way, it will be possible to prevent flood risks during periods of heavy rainfall.

Figure 4.49. Green Spaces and Rainwater Management

Another important goal of the plan is to integrate nature-based solutions. Naturalization of the stream, tree trenches, bioswales, east-west oriented streets, rain gardens, green walls, green roofs, and permeable surfaces are included in the study area. In this context, green walls are proposed for the art center, which has a large surface area. Green roof applications are planned for the roofs of the public spaces intended for the study area. Tree trenches have been created on the streets drawn according to the wind direction. This landscaping increases shading. The naturalization of the Poligon Stream and the increase of green surfaces around it are aimed. Regarding directing rainwater, rain gardens, and bioswales are proposed in areas with green surfaces. The pavement used in the planned main pedestrian axis in the study area is designed as a permeable surface.

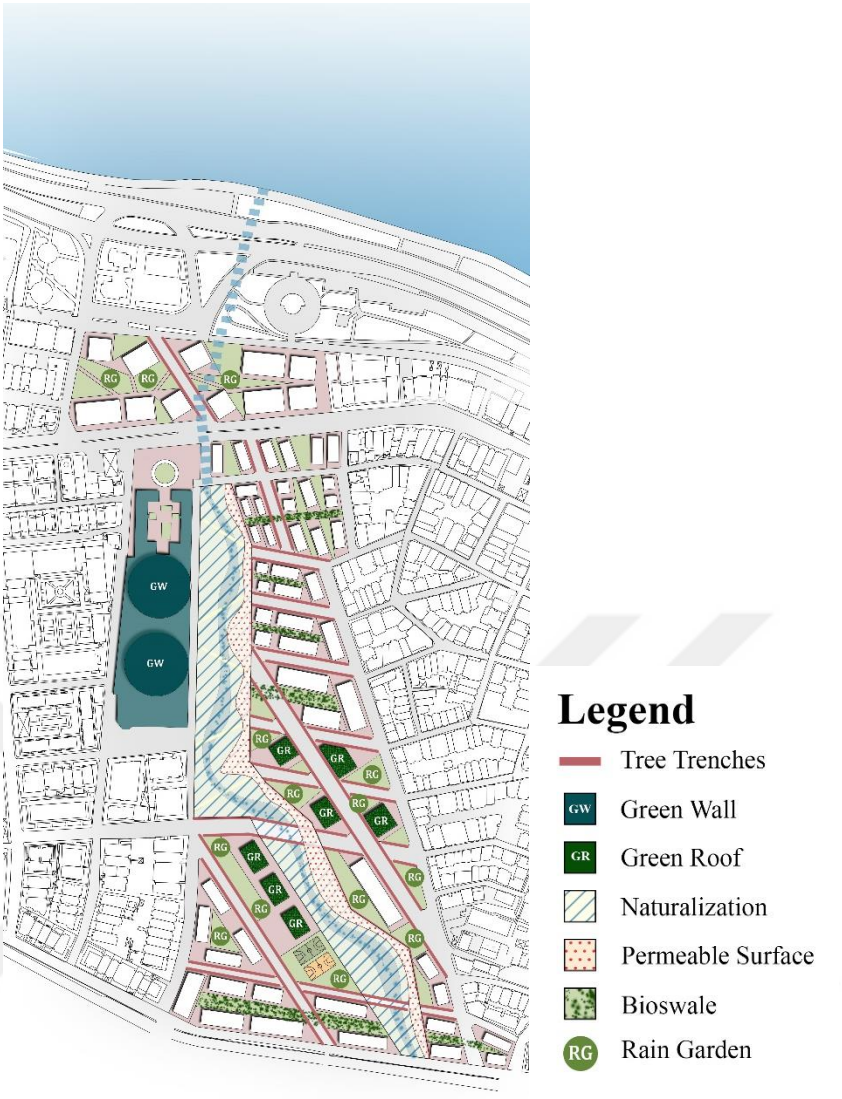

Figure 4.50. Integration of Nature-Based Solutions into The Design

The buildings around the study area are designed as two-story structures. A four-story development is proposed for the buildings on the north edge, while a three-story structure is suggested for the buildings on the west edge. An integrated plan has been attempted to be created in harmony with the surroundings. Proposing two-story buildings around the stream is a significant decision, aiming to enhance the stream's visibility and facilitate the establishment of a connection between people and water.

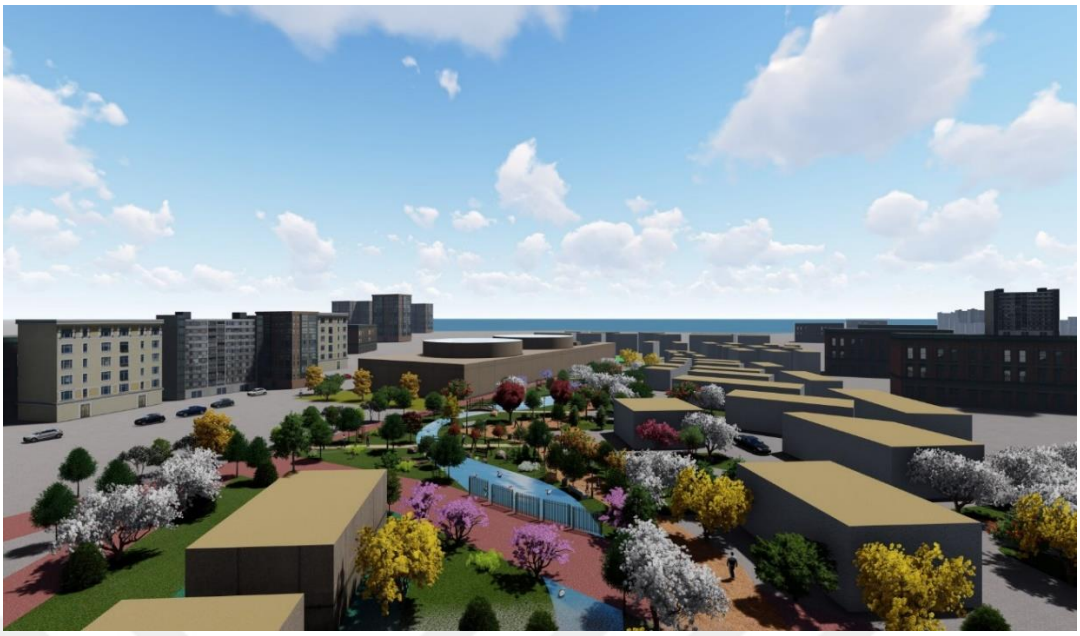

Figure 4.51. 3D View of the Proposed Urban Design Plan

In the designed plan, suggestions have been provided to enhance pedestrian comfort by proposing a pedestrian path and landscaping in continuous relation with the stream. The aim is to create a suitable environment for living organisms within the stream. Pedestrian bridges have been incorporated to facilitate crossings over the stream.

Figure 4.52. 3D Views from the Proposed Urban Design Plan

The land use decisions in the proposed plan have been calculated. Accordingly, the proportion of green areas within the entire area has been planned at 21.8%. Residential areas constitute 27.5% of the proposed plan. The proportions of other proposed uses are detailed in Table 4.8

Table 4.8. Land Use Rates in the Proposed Plan

The Proposal Situation	Area (m^2)	Area / Total Area (%)
Residential Area	37088	27.5%
Stream	5322	4.0%
Green Area	29399	21.8%
Secondary School	7707	5.7%
Mosque	1619	1.2%
Health Facility	1379	1.0%
Art Center	18005	13.4%
Climate Research Center	1450	1.1%
Other (roads, gardens, parking lot)	32731	24.3%

The built-up areas in the proposed plan make up 39.1% of the study area, impervious surfaces 59.3%, and green areas 21.8%.

Table 4.9. Proportional Distribution of Physical Parameters in the Proposed Plan

	Area(m2)	Area / Total Area (%)
Built up Area	53088	39.10%
Impermeability Rate	79818	59.3%
Green Space	29399	21.8%

4.7. Results

In conclusion, a comparison has been made between the current state and the proposed climate-sensitive urban design plan, discussing the impact of changes made to the area.

Firstly, the wind simulation has been re-conducted with the new development conditions. The results of this simulation indicate a significant increase in wind speed and its effect. The wind can now circulate without interruption and at a reduced speed in most parts of the area. The average wind speed is observed to be 3.5 m/s, showing an increase compared to the existing plan, especially around residential areas.

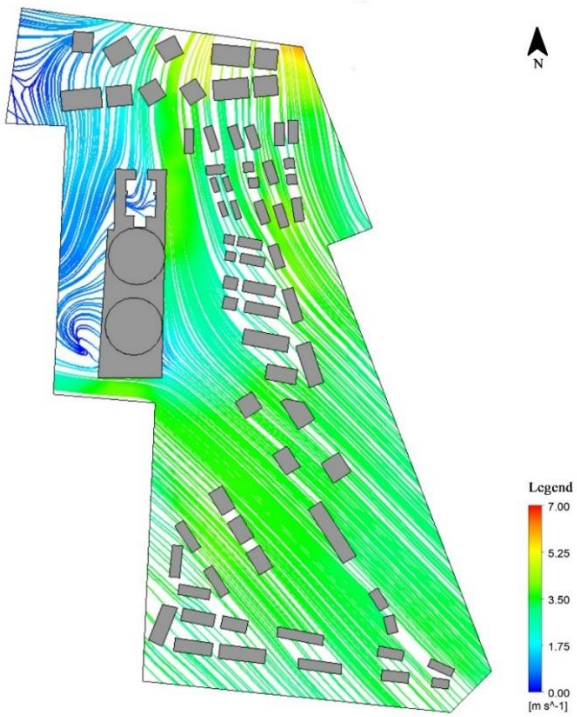

Figure 4.53. Proposed Urban Design Plan Wind Simulation

The building conditions in the proposed urban design plan are arranged to enhance pedestrian comfort during the summer months, as targeted. The three-dimensional visualization of the wind simulation is presented in Figure 4.54.

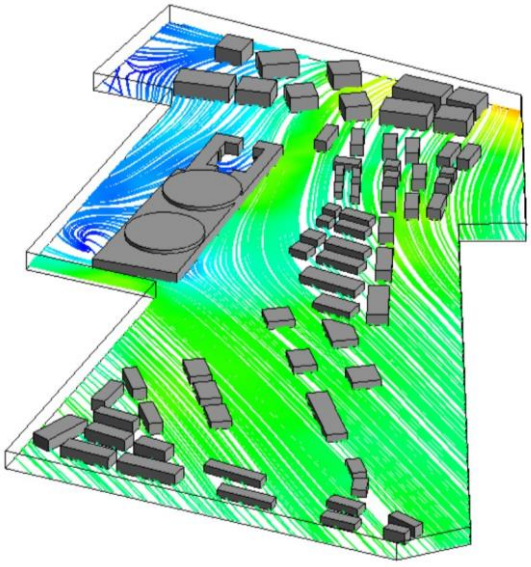

Figure 4.54. 3D Wind Simulation in the Proposed Urban Design Plan

Secondly, the proposed urban design plan includes calculating the urban heat island effect, as detailed in section 4.4.5. The maximum urban heat island effect is calculated as 1.13. The calculated urban heat island effect according to the new plan is shown in Table 4.10.

Table 4.10. Urban Heat Island Effect of the Proposed Climate-Sensitive Urban Design Plan

Variables	**Values**
Factor	1.48
T *effect*	0.76
UHI *max*	1.13

As a result, when comparing the existing conditions with the new urban design plan incorporating climate-sensitive urban design principles, it is observed that the built-up areas have decreased by 34.4%, impervious surfaces have decreased by 35.4%, the maximum urban heat island effect has decreased by 13%, and green areas have increased by 32.02%.

Table 4.11. Comparison of Existing and Proposed Plans

Variables	**Values**
Built up Area	34.40% ↓
Impermeability Rate	35.40% ↓
Green Space	32.02% ↑
Factor	14.40% ↓
T *effect*	5.00% ↓
UHI *max*	13.00% ↓

CHAPTER 5

CONCLUSION

The study focuses on the relationship between residential areas and microclimates. To understand the extent to which the built environment design is sensitive to climate, the study examines how existing urban structures can benefit from or mitigate the adverse effects of climate. A case study located around the Poligon Stream near the Güzelyalı Meteorological Station in the city center of Izmir evaluates microclimatic conditions. Considering bioclimatic design principles, the study proposes design methods to reduce the urban heat island effect in the study area.

The proposed climate-sensitive design approach in the study area aims to provide effective shading, ensure adequate ventilation, minimize heat stress for people, facilitate rapid drainage of excess rainwater, reduce the risk of flooding, ensure good natural ventilation, enhance mobility, and mitigate the urban heat island effect.

In the scope of the study, a comprehensive approach was adopted through analyses at four different scales. At the urban scale, surface temperature, NDVI analysis, and impermeability analyses were conducted. The surface temperature ranged from a minimum of 18.9°C to a maximum of 46.2°C across the city of Izmir. The analysis conducted in July mainly indicates a high-temperature impact in areas with settlements. Within the urban center, residential areas exhibit surface temperature values ranging from 37°C to 41°C. NDVI values within built-up areas were close to 0, indicating a very low vegetation ratio. Impermeability analysis revealed a significantly high impermeability rate within the urban center's built-up areas. According to the analyses, Izmir is highly vulnerable to heatwaves, extreme weather events, and heavy rainfall. Considering the anticipated increase in the impact of extreme weather events in the coming years due to climate change, solutions at the urban scale need to be developed. The implementation of nature-based solutions at the urban scale is crucial. Increasing permeable surfaces, establishing a hydraulic network of streams and streams within the city, and implementing practices such as rain gardens and bioswales in potential areas within the city contribute

to reducing the risk of flooding. Furthermore, increasing vegetation and afforestation in the built environment within the city provide benefits in terms of reducing temperature effects.

The basin within which the Poligon Stream is located has been examined at the watershed scale. The branches of the Poligon Stream extend as far as Limontepe and the Olympic Village. The Olympic Village, established in the upper basin of the Poligon Stream, has led to the formation of impermeable surfaces in this area. During periods of heavy rainfall, reduced water absorption in this area, especially in narrow stream sections, increases the risk of flooding in residential areas around the Poligon Stream. Although the presence of the Poligon Valley creates potential, there are significant issues at the watershed scale. Residential areas are directly affected by any changes occurring in the basin to which they are associated. In this context, strategies need to be developed at the watershed scale. Strategies such as naturalizing streams in water basins, conducting afforestation around streams within the basin, and implementing terracing practices in the upper basin where rainwater first falls to reduce flood risk, prevent erosion, and preserve biodiversity offer opportunities.

Within the scope of the neighborhood-scale analyses, the aim was to gather information about the immediate surroundings of the study area. At this scale, the building situation, floor heights, impermeable surfaces, green areas, and the urban heat island effect were analyzed through surface temperatures. The ratio of built-up areas at the neighborhood scale is 39%, and within these built-up areas, five-story buildings constitute a 60% share. The study area's eastern and western parts of the Poligon Stream have significantly different and distinct characteristics. The western part of the Poligon Stream has a high rate of intense construction. It features attached building arrangements and narrow roads. Due to factors such as the excessive height of buildings on the edges and the absence of garden distances between buildings, wind circulation within the area is disrupted.

The impermeability rate in this area has been calculated as 86.4%, and although this rate is very high, the green area percentage is measured at 11.8%, which is relatively low. With the influence of all these physical features, the surface temperature in this area, especially in the inner parts, exceeds 37°C. The urban heat island effect is calculated to be a minimum of 21.02°C and a maximum of 32.45°C. He evaluated these values in terms of the urban heat island effect based on the Urban Thermal Features Vulnerability Index (UTFVI) created by Zhang et al. (2006). According to the urban heat island effect index,

the segment exhibits the strongest urban heat island effect, given that it is above 0.02, placing it in the most intense category. In the coastal area to the north, where the landscape cover is strong and built-up areas are less prominent, surface temperatures are lower, and the urban heat island effect cannot be identified. When the segment to the east of the Poligon Stream is examined, the surface temperature near Mithatpaşa Avenue decreases to 34°C due to the detached buildings, higher green areas, greater diversity in vegetation, and lower residential density.

Consequently, a strong urban heat island effect is observed in this area. Developing strategies at the neighborhood scale enhances the comfort of pedestrians. Additionally, by mitigating the urban heat island effect, micro-scale local solutions contribute to preventing flood risks associated with climate change. Micro-interventions in this context should incorporate nature-based solutions. Strategies involving green roofs, green walls, rain gardens, urban gardens, city parks, flood parks, and green corridors can provide benefits.

Lastly, analyses and simulation studies were conducted at the street scale. These simulations are crucial for gaining insights into the current situation. Wind and thermal comfort simulations were developed after analyzing the existing conditions and surface characteristics (albedo effect) at the street scale. When examining the existing conditions, the ratio of built-up areas is calculated as 60.1%, the impermeability rate is 91.7%, and the ratio of green areas is 6.2%. The albedo effect takes on a low value on asphalt surfaces, while it reaches the highest value on green surfaces. An increase in this value signifies an increase in reflective capacity. Therefore, dark-colored surfaces contribute to enhancing the urban heat island effect. Two different simulations were utilized, and the data used in these simulations formed the basis for calculating the urban heat island effect at this scale. In the wind simulation, it was observed that the impact of the wind coming from the southeast, the primary wind direction, is minimal in the current built-up conditions, and the wind speed decreases due to the built-up environment. In the thermal comfort analysis, the lowest comfort value was calculated as 32°C and the highest comfort value was 38°C. When evaluated according to the PET index, a significant portion of the area is under extreme heat stress. The Sky View Factor (SVF) calculated during the thermal comfort analysis and the vegetation analysis calculated during the surface temperature analysis were used to calculate the urban heat island effect. Meteorological data were obtained from measurements taken at the Güzelyalı Meteorological Station. As a result of these calculations, the urban heat island effect in the study area was measured as 1.39. The

urban heat island effect reaches its maximum as this value approaches 2. Subsequently, drawing upon the results of detailed street-scale analyses, a proposal for a climate-sensitive urban design plan was formulated. The fundamental aspect of this plan is the establishment of wind directions, with the primary goal of facilitating the maximum circulation of winds coming from the southeast and northwest within the area.

Accordingly, a road network was developed. The Poligon Stream was naturalized, creating a green belt around it. A main pedestrian axis was designed to parallel the Poligon Stream. Green roofs were proposed for public buildings, and the art center's expansive walls were suggested to incorporate green wall installations. A green system has been devised around residential areas, incorporating bioswales and rain gardens to redirect rainwater to the Poligon Stream. Streets designed according to wind patterns feature tree trenches to achieve shading and rainwater retention. The building conditions in this design were re-run in a simulation program, resulting in increased natural ventilation, and the wind was directed to minimize interruptions. With this design proposal, the built-up area was reduced by 34.4%, impermeable surfaces were decreased by 35.4%, and green space was increased by 32.02%. As a result of all these interventions, the urban heat island effect was reduced by 13%.

After determining the boundary of the study area in the proposed climate-sensitive design project, the design area was developed based on regeneration of the area, and all design decisions have been implemented accordingly. Proposed design has been developed within this study without taking property ownership into consideration. Different design alternatives can also be developed while preserving the existing texture on the site or without reducing the density in the region. Apart from the approach adopted in this study, different design alternatives can be applied in the study area. The design alternative is to adapt climate-sensitive design principles for each parcel and building block on a parcel basis, while preserving the existing texture on the land. With this approach, design suggestions for buildings, gardens and existing road structures can be developed. Suggestions can be made on building orientations, shading, integrating nature-based solutions into suitable areas without damaging the existing texture, increasing wind circulation, and ensuring pedestrian comfort. The design alternative has limitations and challenges. Developing solutions for these limitations is also among the issues that should be taken into consideration in future studies.

For urban design to offer a more comfortable city life, a planning approach that aligns with local climate conditions must be embraced in urban development areas. Climatic parameters should be integrated into urban design projects. Additionally, specific climate-sensitive design principles tailored to the site should be established instead of using average criteria. This study can be considered an initial research and simulation experiment to review site-specific climate-sensitive urban design principles and assess the impact of proposed design criteria on urban spaces. In future studies, the methodology developed in this research can be expanded and modified regarding factors to be investigated and the duration. Specifically, field measurements for meteorological data can be collected longer. In addition to the computer-aided programs in this study, more precise analyses and simulations for microclimate studies in cities can be conducted using the ENVI-met software.

REFERENCES

Othman, A.I, A. R. Abdin, A. A. Amin, and A. H. Mahmoud. 2020. "A Bioclimatic Design Approach For The Urban Open Space Design At Business Parks." *Journal Of Engineering And Applied Science* 1883-1901.

Akyürek, Özer. 2020. "Termal Uzaktan Algılama Görüntüleri İle Yüzey Sıcaklıklarının Belirlenmesi: Kocaeli Örneği." *Journal Of Natural Hazards And Environment* 377-390. https://doi.org/10.21324/dacd.667594

Djukic, Aleksandra, Milena Vukmirovic, Srdjan Stankovic. 2016. "Principles Of Climate Sensitive Urban Design Analysis In Identification Of Suitable Urban Design Proposals. Case Study: Central Zone Of Leskovac Competition." *Energy And Buildings* 23-35. https://doi.org/10.1016/j.enbuild.2015.03.057

Delmas, Aymeric, Michael Donn, Virginie Grosdemouge, Marjorie Musy,François Garde. 2018. "Towards Context & Climate Sensitive Urban Design: An Integrated Simulation And Parametric Design Approach." *4th International Conference On Building Energy & Environment.* Melbourne, Australia: Hal.

Baik, Young-Hee Ryu And Jong-Jin. 2011. "Quantitative Analysis Of Factors Contributing To Urban Heat Island Intensity." *Journal Of Applied Meteorology And Climatology* 844-854. https://doi.org/10.1175/JAMC-D-11-098.1

Canan, Fatih. 69-80. "Kent Geometrisine Bağlı Olarak Kentsel Isı Adası Etkisinin Belirlenmesi: Konya Örneği." *Çukurova Üniversitesi Mühendislik Mimarlık Fakültesi Dergisi* 2017. https://doi.org/10.21605/cukurovaummfd.357202

Gerçek, Deniz, Neslihan Türkmenoğlu Bayraktar. 2014. "Kentsel Isi Adasi Etkisinin Uzaktan Algilama İle Tespiti Ve Değerlendirilmesi: İzmit Kenti Örneği." *V. Uzaktan Algılama Ve Coğrafi Bilgi Sistemleri Sempozyumu.* İstanbul.

Serghides, Despina Kyprianou, Stella Dimitriou,Oanna Kyprianou, And Costas Papanicolas. 2019. "The Bioclimatic Approach In Developing Smart Urban Isles For Sustainable Cities." *Renewablr Energy Environment Sustainable.* https://doi.org/10.1051/rees/2018006

Dursun, Doğan, Merve Yavaş,Sevgi Yilmaz. 2020. "Microclimate Assessment Of Design Proposals For Public Space In Cold Climate Zone: Case Of Yakutiye Square." *Megaron* 321-331.

Johansson, Erik, Moohammed Wasim Yahia. N.D. *Towards A Climate-Sensitive Urban Design: Tbe N Eed To Modify Currentplanning Regulations.* Sweden: Lund University.

Lindberg, Fredrik, C.S.B. Grimmond, Andrew Gabey, Bei Huang, Christoph W. Kent, Ting Sun, Natalie E. Theeuwes, Leena Jarvi, Helen C. Ward, I. Capel-Timms, Yuanyong Chang, Per Jonsson, Niklas Krave, Dongwei Liu, D. Meyer, K. Frans G. Olofson, Jianguo Tan,. 2018. "Urban Multi-Scale Environmental Predictor (Umep): An Integrated Tool For City-Based Climate Services." *Environmental Modelling & Software* 70-87. https://doi.org/10.1016/j.envsoft.2017.09.020

Swaid, H., M. Bar-El,M. E. Hoffman. 1993. "A Bioclimatic Design Methodology For Urban Outdoor Spaces." *Theoretical And Applied Climatalogy* 49-61.

Hepcan, Çiğdem Coşkun. 2022. "Doğa Temelli Çözümler Ve Dirençlilik." *Çevre, Şehir Ve İklim Dergisi* 19-40.

Karagöz, Damla. 2016. *An Assessment Of Energy Efficient And Climate Sensitive Urban Design Principles: Design Proposals For Residential City Blocks In Temperate Arid Andhot Humid Regions.* Ankara: Middle East Technical University.

Karakounos, Ioannis, Argyro Dimoudi, And Stamatis Zoras. 2018. "The Influence Of Bioclimatic Urban Redevelopment On Outdoor Thermal Comfort." *Energy And Buildings.* https://doi.org/10.1016/j.enbuild.2017.11.035

Mihajlović, Ljiljana Stošić, Marija Mihajlović,Svetlana Trajković. 2017. "Bioclimatic Urban Design – General, Ecological And Economic Aspect." *Journal Of Process Management.* doi:10.5937/jouproman5-14304

Katzschner, Lutz, Ulrike Bosch,Mathias Röttgen. N.D. *A Methodology For Bioclimatic Microscale Mapping Of Open Spaces.* Kassel, Germany: University Of Kassel.

Bolat, Mehmet, Mehmet Şahin. 2016. "The Calculation Of The Surface Temperature With Noaa/Avhrr Satellite Data." *International Conference On Natural Science And Engineering(* 953-964.

Yavaş, Merve, Sevgi Yılmaz. 2020. "İklim Duyarlı Kentsel Tasarım İlkeleri: Erzurum Kenti Örneği." *Planlama* 294–312. doi: 10.14744/planlama.2020.04934

Taleghani, Mohammad, Laura Kleerekoper, Martin Tenpierik, Andy Van Den Dobbelsteen. 2014. "Outdoor Thermal Comfort Within Five Different Urban Forms In The Netherlands." *Building And Environment* 1-14. https://doi.org/10.1016/j.buildenv.2014.03.014

Dirksen, M., R.J. Ronda, N.E. Theeuwes, G.A. Pagani. 2019. "Sky View Factor Calculations And Its Application In Urban Heat Island." *Urban Climate.* https://doi.org/10.1016/j.uclim.2019.100498

Nikolopoulou, Dr. Marialena. 2004. "Designing Open Space In The Urban Environment; A Bioclimatic Approach." Greece.

Nuruzzaman, Md. 2015. "Urban Heat Island: Causes, Effects And Mitigation Measures - A Review ." *International Journal Of Environmental Monitoring And Analysis* 67-73. DOI: 10.11648/j.ijema.20150302.15

Peker, Ender. 2021. "Bir Şehircilik Problemi: Değişen İklimde Termal Konforu Sağlamak." *Planlama* 108–119. DOI: 10.14744/planlama.2020.92679

Kurniati, Rina, Wakhidah Kurniawati,Diah Intan Kusumo Dewi, Annisa Sarasadi,Endah Kartika Syahri. 2020. "Comfortable Pedestrian Ways With a Climate Sensitive Urban Design Approach in The Old City Semarang." *E3S Web of Conferences.* https://doi.org/10.1051/e3sconf/202020206041

Sanborn, Emma. 2017. *Integrating Climate Sensitive Design Principles In Municipal Processes:A Case Study Of Edmonton's Winter Patios.* Luleå University Of Technology.

Gök, Seyran Büşra, Furkan Öztürk,Süleyman Toy. 2021. "Sağlıklı Kentlerde Kamusal Mekânların İklime Duyarlı Tasarlanması." *Şehir Sağlığı Dergisi* 56-67.

Toy, Süleyman, Dilara Büşra Kayip,Savaş Çağlak. 2019. "Eskişehir'de (Biyo)İklime Duyarlı Kentsel Tasarım Örneği." *Güfbed* 353-361.

Toy, Süleyman, Sevgi Yilmaz,Hasan Yilmaz. 2007. "Determination Of Bioclimatic Comfort In Three Different Land Uses In The City Of Erzurum, Turkey." *Building And Environment* 1315–1318. https://doi.org/10.1016/j.buildenv.2005.10.031

Tağil, Şermin, Kemal Ersayin. 2015. "Balikesir İlinde Diş Ortam Termal Konfor Değerlendirmesi." *Uluslararası Sosyal Araştırmalar Dergisi* 747-755.

Thessaloniki, The Municipality Of. 2017. *Bioclimatic Upgrade Of Public Spaces.* Thessaloniki: Adapting To Climate Change.

Yüksel, Ülkü Duman, Oğuz Yilmaz. 2008. "Ankara Kentinde Kentsel Isi Adasi Etkisinin Yaz Aylarinda Uzaktan Algilama Ve Meteorolojik Gözlemlere Dayali Olarak Saptanmasi Ve Değerlendirilmesi." *Gazi Üniv. Müh. Mim. Fak. Der* 937-952.

Back, Yannick, Peter Marcus Bach,Alrun Jasper-Tönnies,Wolfgang Rauch,Manfred Kleidorfer. 2021. "A Rapid Fine-Scale Approach To Modelling Urban Bioclimatic Conditions." *Science Of The Total Environment* 1-15. https://doi.org/10.1016/j.scitotenv.2020.143732

Şentürk, Yasemin, Kemal Mert Çubukçu. 2022. "Investigating Cooling Capacity Of Urban Cool Areas, Case Of İzmir." *Çevre, Şehir Ve İklim Dergisi* 107-126.

Yavas, Dogan Dursun And Merve. 2015. "Climate-Sensitive Urban Design In Cold Climate Zone: The City Of Erzurum, Türkiye." *International Review For Spatial Planning And Sustainable Development* 17-38.

Zhang, Xi, Gert-Jan Steeneveld, Dian Zhou, Chengjiang Duan, Albert A.M. Holtslag. 2019. "A Diagnostic Equation For The Maximum Urban Heat Island Effect Of A Typical Chinese City: A Case Study For Xi'an." *Building And Environment* 39-50. https://doi.org/10.1016/j.buildenv.2019.05.004

URL 1: 'Twenty-First Century Development', Eko-Vikki, accessed date November 5, 2023, https://www.21stcenturydevelopment.org/case-studies/eco-viikki/

URL 2: 'Visit Dublin', St. Stephen's Green, accessed date November 5, 2023, https://www.visitdublin.com/st-stephen-s-green

URL 3: 'Ireland Guide', St. Stephen's Green Park, accessed date November 5, 2023, https://www.irlandarehberi.com/st-stephens-green-park.html

URL 4: 'Urban Ecology Australia Inc', Christie Walk, accessed date November 5, 2023, https://www.urbanecology.org.au/eco-cities/christie-walk/

URL 5: 'World Habitat Award', Christie Walk Eco City Project, accessed date November 5, 2023, https://world-habitat.org/world-habitat-awards/winners-and-finalists/christie-walk-ecocity-project/

URL 6: ‘In Habitat’, Christie Walk is an Eco Urban Village in Australia, accessed date November 5, 2023, https://inhabitat.com/christie-walk-is-an-eco-urban-village-in-australia/new-6-59/.

URL 7: Energy Transition the Global Energiwende’, Will Freiburg go even greener? accessed date November 5, 2023, https://energytransition.org/2018/09/green-city-freiburg/

URL 8: ‘CZA’, Ex-Isotta Fraschini Area Urban Reform, accessed date November 5, 2023, https://www.zucchiarchitetti.com/projects/urban-design/ex-isotta-fraschini-area-urban-reform/

URL 9: ‘WLA’, Climate Islands, Barcelona Spain, SCOP, accessed date November 5, 2023, https://worldlandscapearchitect.com/climate-islands-barcelona-spain-scob/?v=ebe021079e5a

URL 10: ‘Atelye70 Planners and Architect’, Gebze Eco City, accessed date November 5, 2023, https://atelye70.com/project/gebze_eco_city/

URL 11: ‘Arkitera’, 5 Ocak Parkı ve Yakın Çevresi Kentsel Tasarım Yarışması, accessed date November 5, 2023, https://www.arkitera.com/proje/1-odul-5-ocak-parki-ve-yakin-cevresi-kentsel-tasarim-yarismasi/

URL 12: ‘Akıllı Şehirler Portalı’, Bursa İklim Sokağı, accessed date November 5, 2023, https://www.akillisehirler.gov.tr/proje-envanteri/bursa-iklim-sokagi/

URL 13: ‘Arkiv’, Sasalı İklim Duyarlı Tarım Eğitim ve Araştırma Enstitüsü, accessed date November 5, 2023, https://www.arkiv.com.tr/proje/sasali-iklim-duyarli-tarim-egitim-ve-arastirma-enstitusu/10986

URL 14: ‘AFAD’, Türkiye Deprem ve Tehlike Haritaları, accessed date November 5, 2023, https://tdth.afad.gov.tr/TDTH/main.xhtml

URL 15: ‘iklimBU’, Albedo Nedir?, accessed date November 5, 2023, http://climatechange.boun.edu.tr/albedo-nedir/

URL 16: ‘Beton ve Çimento’, Albedo Etkisi : Beton ve Asfalt, accessed date November 5, 2023, https://www.betonvecimento.com/beton-2/albedo

URL 17: ‘UMEP’, Thermal Comfort, accessed date November 5, 2023,https://umepdocs.readthedocs.io/projects/tutorial/en/latest/Tutorials/IntroductionToSolweig.html

URL 18: ‘EARTHDATA’, accessed date November 5, 2023, https://search.asf.alaska.edu/#/

URL 19: ‘Open Topography’, ALOS World 3D, accessed date November 5, 2023, https://portal.opentopography.org/raster?opentopoID=OTALOS.112016.4326.2

URL 20: ‘UMEP’, Urban Geometry: Sky View Factor Calculator, accessed date November 5, 2023, https://umep-docs.readthedocs.io/en/latest/pre-processor/Urban%20Geometry%20Sky%20View%20Factor%20Calculator.html

APPENDIX

T.C.
ÇEVRE,ŞEHİRCİLİK VE İKLİM DEĞİŞİKLİĞİ BAKANLIĞI
Meteoroloji Genel Müdürlüğü

Yıl/Ay: 2022/7 İstasyon Adı/No: İZMİR BÖLGE/17220

Saatlik Sıcaklık (°C)

Gün/Saat	0	1	2	3	4	5	6	7	8	9	10	11	12	13	14	15	16	17	18	19	20	21	22	23
1	24.8	25.5	25.3	24.9	26.3	27.1	28.2	30.4	31.2	32.7	34.2	35.1	36.1	36.2	35.7	35.0	34.0	32.8	31.0	30.0	29.3	29.1	28.8	28.4
2	28.0	26.9	27.3	26.8	27.5	29.1	29.9	30.6	31.3	33.2	34.2	36.1	37.4	37.0	36.5	34.7	33.5	32.7	31.3	30.6	30.4	29.0	28.5	28.3
3	27.5	27.2	26.9	26.7	27.5	29.0	29.7	31.8	33.4	33.6	34.9	36.0	37.0	37.1	36.3	35.5	34.0	32.3	31.3	29.6	28.8	28.1	26.9	26.3
4	24.3	23.5	24.6	22.9	22.6	24.7	26.1	28.3	30.5	32.0	33.5	32.1	33.0	33.4	33.9	34.2	33.3	32.5	31.3	30.1	29.3	28.7	27.8	27.1
5	26.4	25.2	23.9	23.3	23.1	24.5	26.4	28.4	31.1	31.8	33.0	31.8	32.5	33.2	33.8	33.6	32.8	31.7	30.4	29.5	28.6	28.3	26.8	26.0
6	24.9	24.2	23.5	22.7	22.9	25.3	26.8	27.3	28.3	29.5	29.0	29.8	30.0	30.1	30.2	30.3	29.9	28.9	28.6	28.4	27.9	26.9	26.2	25.5
7	24.2	23.5	22.9	23.2	23.7	25.0	27.6	28.3	31.1	32.7	31.6	32.3	31.0	31.3	31.0	30.0	28.3	27.0	27.3	26.9	27.1	27.3	26.1	26.3
8	25.5	25.0	24.6	24.1	24.0	24.9	27.0	28.3	29.2	30.2	31.1	30.8	31.6	31.2	30.9	30.7	30.5	29.4	28.8	28.0	27.9	26.2	25.7	25.0
9	24.6	24.7	23.7	23.4	24.1	25.9	26.1	26.0	27.2	26.7	28.4	29.3	29.7	28.3	28.2	28.2	27.3	26.4	25.0	24.1	24.1	24.3	24.6	23.5
10	24.0	23.7	22.4	22.3	23.0	23.3	25.1	27.3	30.1	29.6	31.4	30.9	31.8	31.9	30.3	29.7	28.9	27.8	26.6	26.0	25.2	23.9	23.5	23.2
11	23.3	22.5	22.1	22.0	22.7	24.1	26.6	28.0	29.4	30.9	31.5	31.3	32.1	30.4	29.6	29.0	28.6	27.9	26.9	26.4	26.5	25.6	24.9	24.1
12	23.3	23.8	23.1	22.7	23.4	24.4	25.8	28.5	28.6	29.8	30.7	31.1	31.0	31.0	31.4	28.8	28.0	26.5	26.5	25.9	26.7	25.0	23.7	24.1
13	23.9	23.3	22.6	22.6	23.4	24.9	26.9	29.0	30.9	32.1	32.7	33.4	30.7	30.7	32.0	31.6	29.6	28.0	26.9	26.4	26.2	25.8	25.3	25.1
14	24.9	24.5	24.1	24.1	24.2	25.3	26.2	27.9	30.0	31.4	32.6	33.9	35.3	35.8	35.9	35.0	33.2	31.6	30.2	29.4	28.6	28.0	28.0	27.1
15	26.5	25.6	25.3	24.1	24.2	25.0	26.3	27.5	28.9	29.6	31.2	31.6	31.6	32.3	32.5	32.9	33.0	31.3	29.8	28.5	28.4	27.7	27.8	27.6
16	27.0	25.9	25.0	24.6	24.6	25.9	28.6	31.8	32.4	33.6	33.9	34.8	35.7	36.1	36.2	36.0	33.7	32.1	30.7	30.6	30.3	29.7	29.4	27.5
17	27.0	26.2	25.7	25.0	24.7	26.0	27.4	30.7	33.1	35.3	37.2	37.3	36.8	37.6	35.9	34.8	33.7	32.2	31.7	31.2	30.4	29.1	28.0	27.7
18	27.3	26.6	26.1	25.2	25.9	28.4	29.9	30.8	31.7	33.0	33.8	34.3	34.5	34.5	34.1	33.1	32.1	30.5	29.3	28.4	27.2	26.5	26.2	25.4
19	24.8	23.9	23.6	23.6	23.8	24.6	26.2	27.5	29.0	29.5	31.2	32.4	33.2	34.0	33.5	32.2	31.3	29.3	28.1	27.6	27.0	26.1	25.8	25.3
20	25.0	24.7	24.4	24.0	24.0	25.4	26.5	28.0	28.5	30.2	31.0	30.9	33.0	34.1	33.1	32.7	31.6	29.7	28.4	27.9	27.1	26.5	25.9	25.3
21	25.1	24.8	24.1	23.6	23.9	25.8	25.4	27.6	28.8	29.2	31.1	32.1	34.6	35.8	35.7	35.3	33.6	32.2	31.5	31.3	30.6	30.0	29.3	28.7
22	28.3	26.7	27.5	26.9	26.8	27.0	29.5	31.6	32.2	34.0	35.3	36.6	36.2	36.4	35.8	35.2	33.7	32.1	30.8	29.7	30.1	30.0	29.3	29.0
23	28.0	26.3	25.9	26.8	26.3	28.1	29.9	30.7	31.6	33.6	35.0	35.8	36.7	37.0	37.0	35.7	34.4	32.4	31.3	30.4	29.8	28.7	28.2	27.7
24	26.5	25.9	26.0	25.3	25.4	27.1	28.8	31.6	33.4	35.0	35.2	34.7	35.4	38.6	38.0	37.4	35.8	33.9	32.9	32.2	32.3	29.7	29.4	29.3
25	27.8	26.4	25.0	25.1	25.1	28.0	29.3	30.6	32.8	34.2	35.7	34.2	35.2	35.4	34.4	34.4	33.6	31.9	31.2	31.0	30.3	30.3	30.1	29.3
26	28.9	27.9	27.8	26.6	26.6	27.0	27.5	29.5	32.1	32.4	31.8	31.9	34.3	33.7	33.4	32.6	32.1	31.0	30.6	29.9	27.5	26.6	28.0	26.5
27	26.2	24.9	24.3	23.4	24.7	28.6	27.8	28.2	30.7	32.4	32.5	34.5	33.9	34.7	34.6	34.5	33.8	33.0	32.0	29.5	28.1	27.1	26.5	25.9
28	25.0	24.3	23.5	23.2	24.0	26.1	27.0	29.9	29.8	32.6	33.0	32.3	32.6	34.1	34.4	33.9	34.3	32.0	31.5	30.4	29.8	28.2	27.8	26.7
29	25.8	25.7	25.3	24.8	25.3	25.6	26.9	28.8	30.6	30.0	30.3	31.1	31.8	32.0	32.2	32.4	32.2	31.5	31.1	29.2	28.7	28.1	27.9	26.5
30	25.4	25.7	24.9	24.5	24.9	25.6	27.1	27.9	30.4	32.0	31.8	31.5	32.3	32.5	31.1	32.5	32.1	30.8	30.5	29.8	28.0	27.4	26.2	25.4
31	24.8	25.3	25.1	24.3	24.3	25.4	26.8	28.7	29.8	31.0	29.9	31.1	31.8	32.2	31.2	31.7	30.8	30.0	29.0	28.2	28.7	28.5	28.3	27.8

Figure A.1. Air Temperature Data Obtained from Güzelyalı Meteorology Station

T.C.
ÇEVRE,ŞEHİRCİLİK VE İKLİM DEĞİŞİKLİĞİ BAKANLIĞI
Meteoroloji Genel Müdürlüğü

Yıl/Ay: 2022/7 İstasyon Adı/No: İZMİR BÖLGE/17220

Saatlik Nispi Nem (%)

Gün/Saat	0	1	2	3	4	5	6	7	8	9	10	11	12	13	14	15	16	17	18	19	20	21	22	23
1	57.0	59.0	60.0	67.0	62.0	66.0	57.0	47.0	45.0	39.0	32.0	32.0	32.0	28.0	31.0	30.0	31.0	32.0	37.0	42.0	42.0	42.0	43.0	43.0
2	43.0	49.0	45.0	45.0	48.0	50.0	49.0	46.0	40.0	36.0	33.0	28.0	25.0	30.0	28.0	35.0	42.0	43.0	44.0	46.0	44.0	47.0	47.0	46.0
3	47.0	50.0	48.0	47.0	46.0	44.0	41.0	40.0	34.0	35.0	28.0	25.0	24.0	26.0	26.0	32.0	33.0	38.0	41.0	38.0	37.0	38.0	41.0	40.0
4	46.0	48.0	45.0	48.0	55.0	55.0	49.0	44.0	36.0	32.0	28.0	35.0	38.0	35.0	35.0	34.0	34.0	37.0	37.0	38.0	35.0	35.0	34.0	37.0
5	43.0	50.0	52.0	58.0	56.0	54.0	49.0	43.0	39.0	36.0	32.0	37.0	35.0	35.0	34.0	32.0	35.0	35.0	37.0	36.0	38.0	35.0	39.0	42.0
6	43.0	46.0	49.0	52.0	54.0	49.0	43.0	45.0	41.0	42.0	49.0	51.0	46.0	46.0	43.0	45.0	46.0	53.0	53.0	53.0	40.0	48.0	49.0	52.0
7	59.0	61.0	63.0	63.0	61.0	58.0	51.0	48.0	44.0	38.0	42.0	39.0	46.0	45.0	45.0	45.0	61.0	64.0	63.0	60.0	57.0	48.0	47.0	48.0
8	54.0	60.0	65.0	68.0	71.0	69.0	61.0	53.0	47.0	49.0	47.0	51.0	43.0	50.0	48.0	47.0	41.0	46.0	51.0	58.0	54.0	53.0	57.0	59.0
9	62.0	70.0	73.0	73.0	77.0	73.0	71.0	68.0	61.0	68.0	58.0	47.0	49.0	52.0	57.0	54.0	52.0	57.0	68.0	70.0	77.0	72.0	70.0	72.0
10	67.0	62.0	70.0	75.0	70.0	71.0	68.0	53.0	46.0	47.0	41.0	44.0	39.0	37.0	39.0	41.0	44.0	43.0	48.0	50.0	52.0	55.0	60.0	63.0
11	61.0	64.0	64.0	64.0	62.0	58.0	49.0	41.0	33.0	29.0	27.0	39.0	35.0	38.0	46.0	48.0	48.0	48.0	52.0	57.0	49.0	49.0	48.0	51.0
12	52.0	50.0	51.0	56.0	58.0	54.0	54.0	44.0	43.0	40.0	40.0	42.0	37.0	35.0	34.0	48.0	57.0	54.0	48.0	55.0	40.0	40.0	42.0	50.0
13	51.0	51.0	53.0	56.0	53.0	46.0	37.0	34.0	31.0	26.0	28.0	27.0	33.0	32.0	32.0	29.0	31.0	35.0	35.0	38.0	41.0	35.0	33.0	35.0
14	40.0	41.0	44.0	42.0	44.0	44.0	42.0	42.0	40.0	36.0	32.0	30.0	29.0	27.0	25.0	32.0	34.0	35.0	39.0	38.0	39.0	41.0	36.0	46.0
15	40.0	52.0	49.0	51.0	55.0	55.0	53.0	46.0	41.0	41.0	39.0	43.0	38.0	38.0	37.0	34.0	39.0	39.0	41.0	46.0	43.0	40.0	37.0	33.0
16	34.0	40.0	40.0	40.0	41.0	41.0	39.0	25.0	24.0	27.0	23.0	31.0	23.0	22.0	22.0	24.0	31.0	30.0	41.0	34.0	28.0	30.0	28.0	37.0
17	39.0	39.0	43.0	41.0	46.0	46.0	46.0	32.0	22.0	14.0	18.0	19.0	24.0	27.0	30.0	33.0	34.0	35.0	36.0	34.0	35.0	39.0	44.0	45.0
18	41.0	41.0	44.0	47.0	47.0	43.0	38.0	35.0	30.0	29.0	30.0	27.0	28.0	29.0	30.0	33.0	33.0	36.0	37.0	35.0	41.0	43.0	40.0	41.0
19	41.0	49.0	47.0	43.0	41.0	38.0	37.0	35.0	32.0	31.0	28.0	27.0	26.0	27.0	31.0	35.0	35.0	39.0	42.0	42.0	46.0	47.0	53.0	48.0
20	49.0	50.0	51.0	51.0	54.0	56.0	49.0	49.0	43.0	39.0	38.0	44.0	40.0	36.0	36.0	36.0	38.0	43.0	43.0	41.0	44.0	41.0	44.0	40.0
21	37.0	38.0	37.0	43.0	41.0	38.0	45.0	33.0	32.0	32.0	33.0	33.0	23.0	16.0	19.0	21.0	29.0	31.0	31.0	27.0	29.0	31.0	34.0	36.0
22	37.0	39.0	47.0	38.0	34.0	40.0	34.0	24.0	24.0	21.0	20.0	22.0	22.0	22.0	28.0	27.0	29.0	30.0	34.0	33.0	27.0	23.0	25.0	25.0
23	24.0	35.0	30.0	30.0	35.0	32.0	29.0	29.0	28.0	24.0	22.0	18.0	23.0	18.0	21.0	25.0	26.0	29.0	29.0	29.0	29.0	29.0	32.0	35.0
24	33.0	31.0	35.0	35.0	37.0	42.0	34.0	25.0	17.0	15.0	15.0	29.0	26.0	18.0	17.0	19.0	21.0	28.0	30.0	28.0	25.0	29.0	31.0	29.0
25	32.0	32.0	37.0	37.0	37.0	37.0	37.0	33.0	28.0	24.0	24.0	28.0	26.0	29.0	30.0	36.0	37.0	40.0	37.0	32.0	35.0	35.0	32.0	39.0
26	38.0	43.0	43.0	45.0	47.0	50.0	49.0	42.0	35.0	38.0	41.0	37.0	33.0	34.0	32.0	31.0	29.0	35.0	33.0	32.0	36.0	40.0	38.0	41.0
27	44.0	45.0	49.0	52.0	50.0	42.0	49.0	42.0	36.0	33.0	34.0	30.0	27.0	23.0	24.0	23.0	24.0	24.0	25.0	28.0	32.0	34.0	42.0	41.0
28	45.0	48.0	50.0	50.0	50.0	55.0	50.0	45.0	44.0	40.0	37.0	36.0	37.0	34.0	31.0	31.0	29.0	32.0	34.0	36.0	40.0	44.0	48.0	49.0
29	54.0	56.0	57.0	60.0	61.0	59.0	58.0	54.0	48.0	47.0	52.0	47.0	44.0	44.0	44.0	39.0	40.0	41.0	43.0	47.0	52.0	52.0	54.0	57.0
30	60.0	65.0	68.0	69.0	67.0	65.0	63.0	58.0	50.0	44.0	45.0	49.0	48.0	43.0	42.0	42.0	42.0	42.0	43.0	45.0	56.0	61.0	59.0	63.0
31	65.0	70.0	71.0	73.0	77.0	73.0	66.0	61.0	55.0	52.0	58.0	53.0	49.0	50.0	54.0	51.0	52.0	53.0	60.0	63.0	59.0	56.0	56.0	62.0

Figure A.2. Relative Humidity Data Obtained from Güzelyalı Meteorology Station

T.C.
ÇEVRE,ŞEHİRCİLİK VE İKLİM DEĞİŞİKLİĞİ BAKANLIĞI
Meteoroloji Genel Müdürlüğü

Yıl/Ay: 2022/7 İstasyon Adı/No: İZMİR BÖLGE/17220

Saatlik Rüzgar Yönü ve Hızı (m÷sn)

Gün/Saat	0	1	2	3	4	5	6	7	8	9	10	11	12	13	14	15	16	17	18	19	20	21	22	23
1	1.1	3.1	0.2	2.1	2.3	1.3	1.1	1.4	1.9	2.1	1.9	2.3	2.7	3.2	4.8	4.9	4.7	3.8	2.8	2.7	1.6	1.4	3.1	5.3
2	2.9	1.6	2.2	3.4	3.2	2.5	1.7	1.9	1.4	2.4	2.2	2.2	2.2	2.3	3.5	4.5	3.9	2.9	1.9	4.4	3.6	2.4	1	3.4
3	3.3	5.5	4.8	5.4	3.8	3.2	1.7	2.3	3.4	3.4	4	3.4	3.7	2.9	3.9	3	3.3	2.8	1.2	2.4	1.9	2.2	1	1.2
4	3.3	2.1	1.6	2.1	3.3	1.9	2	2.4	2.4	2.4	2	4.1	5.9	5.3	5.4	4.6	3.7	1.6	1.2	1.7	3.7	2.8	4.1	4.4
5	2.9	1.3	1.1	2.8	2.3	2.5	2.3	2	2.4	2.6	2.8	4.7	5.8	5.7	5.3	4.9	4.2	4.1	3.5	2.8	1.5	1.6	0.5	1
6	1	3.1	3.7	4.1	3.8	2	1.2	1.8	3.9	4.4	5.9	6.8	6.5	6.3	6.2	5.2	5	4.2	4.1	2.7	2.9	3.5	3.1	3.5
7	3.7	3.7	3.6	3.2	4.1	4	3.4	4.3	4.2	3.7	5.9	6	5.8	5.8	5.8	6.4	5.4	5.2	4.6	4.5	3.3	2	2.1	2.7
8	3	2.8	3.1	2.6	3.2	2.6	2.3	2.2	2.3	3.5	3.8	5.7	5.6	5.8	5.5	5.2	5	4.5	4.1	3.5	2.3	1	1.5	1.3
9	1.4	2	1.5	1.1	1	2.1	2	3.6	4.6	5.5	3.8	3.5	3.6	4.9	5.1	4.8	4.4	3.7	3.3	3.1	3.1	2.4	2.1	3
10	2.3	1.7	3.3	2.8	3.3	4.1	3.7	3.4	2.9	4.3	4.9	5.1	4.4	5.9	5.1	5.7	6.6	5.3	5.2	4.8	4.5	3.5	2.1	2.9
11	2.4	2.3	2.2	2.3	2.7	2.1	1.9	1.7	1.7	1.6	1.8	3.9	4.9	5.5	5.7	5	5	4.1	4.1	4.1	2.6	1.3	0.5	1
12	1.7	2.4	2.5	3.3	2.7	3.3	3.7	2.6	3.5	3.7	4.6	5.4	5.8	5.7	5.4	4.7	5	4.4	4	4	3.4	2.1	0.5	1.6
13	1.9	1.9	2.9	3.2	2.8	2	2.4	4.3	3.8	4.3	4.6	5.2	5.8	6.6	5.9	5.4	5.9	6.6	5.7	3.7	3.2	3.3	2.6	2.9
14	2.9	3.8	4.4	6.2	6.7	4.8	5.5	5.1	4.2	3.8	3.7	3.6	3.6	2.6	2.4	2.5	3.8	3.2	1.7	1.5	1.5	1	4.6	2.5
15	4.4	1.7	0.8	0.8	1.8	2.2	2.7	3.6	4.3	4.6	4.5	5.2	5.6	5.8	5.8	5	4.4	3.2	2.1	2	2.9	3.8	4.6	4.8
16	4.1	2.1	1.5	2.8	4.1	4.3	3.5	3.1	3.7	4	4.3	4.5	3.2	3	2.7	2.8	5.1	4.2	2	3	5	4.1	4.6	3.1
17	1.9	1.4	1	1.5	1	1.9	2.7	2.6	2.4	1.8	2.9	4.2	4.4	5	5.6	6.7	5.7	3.4	2.5	3.8	2	2.5	2.1	1.7
18	1.4	3.3	3.1	2.7	1.9	1.5	1.8	1.5	1.7	2.9	3.9	3.6	4.2	4.4	5.3	5.2	5.1	4.5	2.7	2.5	4.1	4.2	4.1	4.8
19	5.6	3.8	1.9	1.6	1.8	4.7	4.4	4.9	2.7	2.5	2.2	2.3	2.7	2.7	4.4	4.3	4.5	3	2.3	1.7	3.7	5.4	2.1	4.5
20	3.6	4.6	4.5	4.6	3.6	2.8	4.2	2.5	2	2.2	2.6	3.9	4	3.4	5	5.4	4.5	3.6	2.4	2.1	3.1	4.8	7.2	3.8
21	4.4	4.4	4.8	5.6	6.3	4.4	2.4	1.7	2.1	3.5	4.3	3.6	2.2	1.7	2.8	4.1	4	4.8	2	2.5	4.8	5.1	4.6	2.9
22	2.4	1.2	2	4.1	3	2.6	1.7	2.6	1.8	4	4.5	3.8	4.2	4.3	4.5	5.2	5.7	5.4	4	1.7	2.4	5.1	4.1	2.8
23	4.3	3.5	1.4	2.2	2.4	1.9	3.6	2.3	1.9	2.9	4.6	4.9	4.4	4	3.3	4.5	6.2	3.6	3.1	2.7	1.4	1.1	1	1.1
24	1.1	1.3	1.2	1.3	1.2	2.3	2.4	1.6	1.7	1.7	2.2	4.3	4.7	3.5	5	6.2	6	4.3	4.3	3.6	1.6	1.2	0.5	1.2
25	1.6	1.8	1.4	1.1	0.7	2.3	2.9	3.8	4.3	4.4	3.8	4.4	5.5	5.1	5.3	4.3	4.1	4.3	4.4	3.2	3	1.6	3.6	2.1
26	2.3	0.8	1.2	0.7	1.3	1.9	3.8	3.6	2.7	4.1	4.9	5.6	5.1	5.5	5.6	6.5	5.7	5.5	4	2.4	1	1	1.5	1.1
27	1.5	0.9	1.8	1.1	1.5	0.8	2.4	3	3.6	3.4	3.9	3.6	5	6.1	5.6	5.1	4.9	4.1	2.3	0.6	0.8	1.3	0.5	0.4
28	0.7	0.8	0.9	1	1	1.5	2.3	1.4	2.9	3.2	3.7	4.5	4.7	5.3	4.9	4.9	4.8	4.4	3.6	3.3	2	1	0.5	1.2
29	0.5	1	0.9	1.9	2.7	2.6	4	3.2	3.3	4.9	5.8	5.7	6.1	6.3	5.6	5.5	5.1	4.4	3.3	3.1	2	0.8	1.5	2.4
30	0.9	2.3	3.2	3.3	2.2	2.2	2.7	3.6	3.4	3.2	4.1	5	6.3	5.9	5.8	5.1	5	4.4	3.5	2.7	3.2	1.4	0	0.8
31	0.9	1.5	3	3.2	2.9	2.5	2.2	2.3	3.2	3	5.7	5.7	6	6.1	6	5.7	5.1	5.2	4.6	4.3	2.9	2.7	1.5	2.2

Figure A.3. Wind Speed data obtained from Güzelyalı Meteorology Station

T.C.
ÇEVRE,ŞEHİRCİLİK VE İKLİM DEĞİŞİKLİĞİ BAKANLIĞI
Meteoroloji Genel Müdürlüğü

Yıl/Ay: 2022/7 İstasyon Adı/No: İZMİR BÖLGE/17220

Saatlik Küresel Güneş Radyasyonu (wattsaat-m²)

Gün/Saat	0	1	2	3	4	5	6	7	8	9	10	11	12	13	14	15	16	17	18	19	20	21	22	23
1			19.6	70.3	220.6	412.3	604.5	767.4	890.0	970.7	993.6	962.7	871.9	734.9	560.5	370.6	176.8	40.9	18.4					
2			20.0	69.8	219.7	409.8	595.5	758.0	883.9	965.6	995.5	960.1	874.2	671.7	543.9	349.4	163.3	38.0	18.8					
3			20.7	71.5	227.6	421.1	616.0	785.0	897.2	998.0	1017.7	985.1	894.1	754.3	566.6	374.2	175.3	36.9	17.1					
4			18.8	71.3	229.9	433.2	627.9	797.6	922.4	952.4	1025.4	992.3	906.6	767.7	582.2	377.7	180.6	38.6	17.8					
5			19.7	68.5	223.3	423.3	616.2	786.5	915.2	995.5	1018.0	983.5	893.8	756.5	573.8	376.9	176.9	41.1	18.2					
6			19.8	66.8	215.8	413.7	605.4	775.8	899.8	980.0	1004.0	970.2	880.6	746.1	572.0	372.2	172.6	39.2	18.8					
7			19.4	66.8	217.5	410.8	598.6	764.2	891.7	962.3	994.8	964.2	882.9	744.8	569.2	361.9	161.1	38.0	18.4					
8			17.7	59.1	202.4	369.7	588.0	753.9	878.4	946.4	970.2	949.5	870.2	733.8	556.2	359.4	164.9	37.4	19.0					
9			17.9	62.5	224.3	368.6	567.0	743.9	869.3	867.2	1027.6	897.8	867.0	738.0	559.0	348.6	157.1	36.7	18.8					
10			19.6	64.0	194.9	362.8	579.8	725.0	697.5	910.0	800.9	833.3	793.3	747.6	431.4	375.6	174.2	38.7	19.0					
11			19.1	63.8	215.9	412.8	603.8	767.2	896.4	973.2	995.2	965.4	877.5	724.6	546.0	349.4	157.8	37.6	18.9					
12			19.0	60.4	206.6	403.0	591.7	758.3	887.8	965.1	992.3	962.5	883.1	753.7	569.6	362.7	165.4	38.9	18.5					
13			18.5	61.1	211.9	402.7	580.5	711.8	890.0	981.8	1011.9	979.0	892.7	758.2	576.1	357.8	131.3	39.5	18.1					
14			19.4	59.1	198.7	391.0	578.8	733.1	867.3	953.2	979.9	948.5	865.6	731.6	553.1	348.2	153.4	34.9	17.9					
15			17.8	59.3	205.0	404.5	599.7	770.9	896.0	974.3	1000.5	965.6	877.8	740.2	561.7	365.4	167.9	37.4	17.5					
16			18.3	60.3	214.3	415.7	610.1	788.3	917.0	991.6	1021.3	988.6	901.1	764.0	577.0	367.5	168.2	37.6	17.8					
17			17.9	57.0	206.3	412.7	608.8	777.4	902.0	975.8	993.0	955.6	871.8	736.4	563.7	360.3	163.3	34.5	18.8					
18			18.7	54.6	196.7	392.4	580.6	752.6	889.0	978.5	1006.6	976.0	882.5	742.2	560.2	350.1	151.6	32.7	18.1					
19			17.9	55.1	202.7	404.5	599.6	765.4	895.0	980.0	1011.5	977.2	885.8	747.4	566.1	357.9	156.7	33.2	17.9					
20			19.2	54.1	191.8	389.7	577.7	750.6	881.3	965.4	986.3	952.9	865.3	706.5	561.5	354.1	155.0	33.1	18.0					
21			18.8	53.8	195.5	390.5	589.9	763.8	903.1	991.8	1013.3	980.0	894.1	756.0	563.4	346.7	149.3	31.9	17.7					
22			16.7	54.5	199.2	394.1	597.7	771.1	903.8	984.1	1001.1	967.5	880.8	736.0	561.4	356.0	159.4	32.3	17.0					
23			17.6	52.7	195.6	397.6	592.0	766.4	906.1	997.8	1020.3	980.6	893.7	750.6	549.6	353.4	159.9	31.8	16.9					
24			17.0	46.9	170.0	390.1	586.0	761.7	898.2	988.6	1004.5	967.4	880.3	740.7	562.2	349.2	151.3	30.8	18.0					
25			18.3	48.0	175.2	361.3	553.5	727.3	861.1	943.0	965.9	925.2	832.3	697.9	514.6	307.1	120.8	29.1	19.0					
26			17.8	45.0	170.0	359.9	556.0	730.3	865.2	953.1	981.6	950.6	864.1	730.1	549.5	340.7	146.2	30.9	18.3					
27			17.8	45.3	176.1	369.3	568.2	740.8	872.7	956.4	982.2	954.3	873.8	740.1	553.1	337.9	145.1	28.6	16.4					
28			18.5	43.7	168.8	358.1	552.8	722.2	853.6	936.2	965.6	931.1	842.8	706.1	523.4	311.4	128.0	27.7	18.7					
29			18.4	42.9	166.4	360.1	483.3	680.0	774.3	915.4	950.9	920.1	838.1	697.8	518.8	308.8	124.4	27.2	18.8					
30			18.9	43.0	167.7	359.1	552.2	727.1	856.8	942.7	975.5	943.4	861.4	727.7	538.7	319.4	128.7	27.7	18.1					
31			18.6	42.5	171.6	365.8	561.5	729.6	855.8	940.1	961.3	927.6	838.6	706.2	526.4	305.9	118.4	26.3	19.2					

Figure A.4. Global Solar Radiation Data Obtained from Güzelyalı Meteorology Station